

TECHNISCHE UNIVERSITÄT MÜNCHEN

Lehrstuhl für Entwicklungsgenetik

Generation of autologous and allorestricted cytotoxic
T cell clones directed against Ewing Tumor antigens

Stefan Pirson

Vollständiger Abdruck der von der Fakultät Wissenschaftszentrum
Weihenstephan für Ernährung, Landnutzung und Umwelt der Technischen
Universität München zur Erlangung des akademischen Grades eines

Doktors der Naturwissenschaften

genehmigten Dissertation.

Vorsitzender: Univ.-Prof. Dr. S. Scherer

Prüfer der Dissertation:

1. Univ.-Prof. Dr. W. Wurst

2. Univ.-Prof. Dr. St. Burdach

Die Dissertation wurde am 18.05.2009 bei der Technischen Universität
München eingereicht und durch die Fakultät Wissenschaftszentrum
Weihenstephan für Ernährung, Landnutzung und Umwelt am 02.12.2009
angenommen.

Table of Contents

1	Introduction.....	1
1.1	Ewing Family Tumor (EFT).....	1
1.1.1	History.....	2
1.1.2	Incidence and symptomatology.....	3
1.1.3	Diagnosis.....	3
1.1.4	Prognostic factors.....	4
1.1.5	Treatment.....	5
1.2	Immunotherapy.....	7
1.2.1	Dendritic Cells.....	8
1.2.2	T cell therapy.....	10
1.3	Aim of the study.....	11
2	Materials.....	13
2.1	Instruments and Equipment.....	13
2.2	Commonly used materials.....	14
2.3	Chemicals and biological reagents.....	15
2.4	Kits.....	17
2.5	Cell Culture media and solutions.....	17
2.6	Cells.....	19
2.7	ELISpot Reagents.....	20
2.7.1	Antibodies.....	20
2.7.2	Enzymes, Buffers, Plates.....	20
2.8	Flow cytometry reagents.....	20
2.8.1	Reagents.....	20
2.8.2	Antibodies.....	21
2.9	Peptides.....	22
2.10	Plasmids.....	23
2.11	List of manufacturers.....	27
3	Methods.....	29

Table of Contents

3.1	Cell culture	29
3.1.1	Cell counting.....	29
3.1.2	Cryopreservation of cells	30
3.1.3	Thawing of cryopreserved cells	30
3.1.4	Culture of adherent tumor cell lines	30
3.1.5	Culture of suspension tumor cell lines	31
3.2	Isolation of peripheral blood mononuclear cells	31
3.2.1	Isolation of PBMC from blood donor unit (500ml)	31
3.2.2	Isolation of PBMC from whole blood.....	32
3.3	Isolation of CD14 ⁺ cells	32
3.4	Isolation of CD8 ⁺ cells	32
3.5	Generation of Dendritic cells	33
3.6	Lipofection.....	34
3.7	Flow cytometry	35
3.8	Cell sorting with Pentamer-staining.....	35
3.9	RNA isolation	36
3.10	cDNA synthesis.....	37
3.11	Real-time PCR.....	38
3.12	Minipreparation of plasmid DNA	39
3.13	Restriction analysis	40
3.14	DNA agarose gel electrophoresis	40
3.15	Maxipreparation of plasmid DNA	40
3.16	In vitro Priming.....	41
3.17	Limiting Dilution.....	41
3.18	ELISpot	42
3.19	CTL expansion.....	44
3.20	In silico prediction of peptide epitopes	44
3.21	HLA-A*0201 / peptide-binding assay	45
3.22	V β analysis of TCR repertoire.....	46
3.23	Generation of EBV-immortalized B cells (LCLs)	48
3.24	Up-regulation of HLA expression in EFT cell lines by IFN γ	49
3.25	Peptide titration assay.....	50

3.26	Statistical analysis	50
4	Results.....	51
4.1	mRNA Chip.....	51
4.1.1	CHM1	51
4.1.2	GPR64	51
4.1.3	EZH2.....	51
4.1.4	STEAP	52
4.1.5	ITM2A	52
4.1.6	LIPI.....	52
4.2	Real-Time PCR.....	54
4.2.1	CHM1	54
4.2.2	GPR64	54
4.2.3	EZH2.....	54
4.2.4	STEAP	54
4.2.5	ITM2A	54
4.2.6	LIPI.....	54
4.3	HLA-A*0201 status of EFT cell lines.....	56
4.3.1	A673.....	57
4.3.2	TC-71	57
4.3.3	SBSR-AKS.....	57
4.4	Peptide-binding assay	58
4.4.1	CHM1	61
4.4.2	GPR64	61
4.4.3	EZH2.....	61
4.4.4	STEAP and EWS-FLI1	61
4.4.5	ITM2A	62
4.4.6	LIPI.....	62
4.4.7	Detailed peptide-binding assay	62

Table of Contents

4.5	CD14 selection.....	63
4.6	Dendritic cells.....	64
4.7	CD8 selection.....	66
4.8	Autologous <i>in vitro</i> priming.....	68
4.8.1	CHM1	68
4.8.2	GPR64.....	72
4.8.3	EZH2	74
4.8.4	STEAP	76
4.8.5	ITM2A.....	78
4.8.6	LIPI.....	78
4.8.7	Summary of the autologous <i>in vitro</i> priming.....	79
4.9	Allogeneic <i>in vitro</i> priming	80
4.9.1	CHM1	80
4.9.2	EZH2	90
5	Discussion.....	99
5.1	Autologous <i>in vitro</i> priming.....	100
5.2	Allogeneic <i>in vitro</i> priming	102
5.2.1	EZH2-666	104
5.2.2	CHM1-319	105
5.2.3	Comparison of autologous and allogeneic approach.....	107
6	Summary.....	110
7	Zusammenfassung.....	111
8	Acknowledgements	113
9	References.....	115
10	Abbreviations.....	126

1 Introduction

1.1 Ewing Family Tumor (EFT)

The EFT is an aggressive osteolytic bone tumor. It is the second most common malignant pediatric bone tumor after osteosarcoma. One characteristic of the EFT is its propensity for dissemination. Microscopically, EFT cells are uniformly bland, undifferentiated, small round cells. This allows only a classification into the heterogeneous group of pediatric small round-cell tumors, consisting of neuroblastoma, lymphoma, rhabdomyosarcoma and EFTs, among others (1). Rapid identification of the tumor entity is crucial to influence therapy, as each of these pediatric tumors calls for a different therapeutic approach. With the identification of a specific balanced $t(11;22)(q24;q12)$ chromosome translocation in 1984 (2, 3), and the discovery of the EWS/ETS gene fusion by Delattre *et al.* in 1992 (4) the fast and accurate diagnosis of the EFT became possible by detecting the presence of this translocation in the tumor cells by molecular diagnostic tools like polymerase chain reaction (PCR) and Fluorescence *in situ* hybridization (FISH). Tumors that are sharing the same $t(11;22)$ chromosomal translocation are a diverse group, not limited to the phenotypic traits of the Ewing tumor. In 1985 Schmidt *et al.* (5) studied another group of tumors, malignant peripheral neuroectodermal tumors (MPNTs) which closely resembled Ewing tumors histologically. This diverse group consists of primitive peripheral neuroectodermal tumors (PNETs) occurring outside the central nervous system, which have been designated by many different names, historically (6). Depending on their location and extent of neural differentiation they were called peripheral neuroepithelioma, Askin tumor or peripheral primitive neuroectodermal tumor (pPNET). The identification of the EWS/ETS fusion gene forced the new definition of so called Ewing family of tumors (EFTs) which included the classical Ewing Tumors, MPNTs and the Askin Tumor of the thoracic wall. These tumors are considered to be tumor phenotypes along a gradient of limited neuroglial maturation that arise from the same stem cell (7).

1.1.1 History

James Ewing was born in Pittsburgh, Pennsylvania, USA in 1866. His father was of Irish-Scottish heritage and was an attorney and judge. His mother was a teacher from Stockbridge, Massachusetts, USA of German-American descent. James Ewing was the second son (8).

As a 14-year-old high-school student, James Ewing had an accident while ice skating. The sustained leg injury resulted in chronic osteomyelitis with a draining sinus, and a hip joint ankylosis. He was bedridden for several months after the accident. Finally, his family consulted the most prominent surgeon of the time, Samuel W. Gross in Philadelphia, who, in accord with other surgeons, proposed a leg amputation. The teenaged Ewing overheard this discussion, which understandably made a terrifying lifelong impression on him. The amputation was avoided and the injury was treated conventionally. Ewing recovered but suffered from a permanent limp and chronic pain all his life.

In 1899, Ewing became Cornell University Medical College's first professor of pathology, a position he held for 33 years. In 1913, he became the first Director of Pathology at Memorial Hospital. In 1921, Ewing encountered a 14-year-old girl with a large tumor of the ulna (9). The patient was treated with X-ray irradiation only, although amputation was recommended by the involved surgeons. This mirrored Ewing's own experience at the same age of facing the traumatic loss of a limb by amputation and showed his willingness to avoid this procedure by exploring other treatment possibilities. The irradiation resulted in the complete disappearance of gross tumor and a remarkable restoration of the ulnar shaft, however the girl died of the disease a year or two later. The extraordinary sensitivity of the tumor to X-rays observed in other similar cases was a phenotypic trait Ewing identified for this peculiar type of bone sarcoma. Defining a tumor by its microscopic appearance as well as by a specific response to radiation treatment was a novel concept. He popularized and designated it as a "diffuse endothelioma of the bone " and later as an "endothelial myeloma" (10). To this day this tumor bears his name.

James Ewing died in 1943, considered by his peers the outstanding tumor pathologist of his generation (11).

1.1.2 Incidence and symptomatology

Ten percent of primary malignant bone tumors in children are identified as EFTs. The tumors occur most commonly in the second decade of life, and approximately 80 percent of those with EFT are younger than twenty years old. Age at diagnosis of EFT patients ranges from five months to 83 years but it is uncommon that EFTs occur in patients older than thirty years or in the very young (12).

Slightly more male patients are diagnosed with EFT than female patients (3:2) but an easily observable difference exists when comparing racial backgrounds of the patients. More than 95 percent of EFT patients are white (13). The incidence is fewer than two percent of cases reported in the black population. EFT cases have been reported Asian countries such as India, Japan and Vietnam, but seem to be distinctly uncommon in China. The incidence of the tumors in Germany is 3.1 cases per million children under 15 years of age.

The most common symptoms of EFT are pain and swelling, often occurring after a pathological fracture. Fever, weight loss, and other systemic symptoms often lead to differential diagnosis, especially osteomyelitis. EFTs can originate in any bone in the body or even in extraosseous sites. Patients also can present with symptoms from a metastatic site rather than the primary site. A delay between the onset of symptoms and diagnosis is common for this tumor entity. This may be caused by intermittent pain at the site of the tumor, or by a mass that is not palpable until it is fairly large in some locations. Common sites of metastatic spread of EFTs are lung, bone, and bone marrow, with approximately 25 percent of patients presenting with metastatic disease at time of diagnosis (12).

1.1.3 Diagnosis

Most EFTs (about 85 percent) present as destructive lesions. They can be associated with any bone but about 15 percent of patients show only soft tissue masses without apparent bone involvement. Microscopically and histopathologically, no accurate diagnosis can be performed. Tumor markers like level of serum lactate dehydrogenase (LDH) (14) or CD99 (15) can give hints but are not specific enough for an exact identification. In 1984, the

diagnostic accuracy of EFTs was vastly improved by discovery of a t(11;22) chromosomal translocation (2) which can be ascertained with molecular diagnostic tools. The translocation results in the expression of an aberrant hybrid protein in which the N-terminal part of the EWS protein is linked to the DNA-binding domain (ets domain) of ets transcription factors (4). This hybrid protein may alter the transcriptional regulation of target genes. EWS-FLI1 characterizes about 85 percent of histopathologically defined CD99⁺ EFTs. In another ten percent of tumors, a gene fusion between EWS and the closest relative of FLI1, ERG, is found. The protein resulting from the fusion of EWS with ERG is similar to the typical EWS-FLI1 protein as the N-terminal portion of EWS is also linked to the ETS domain of ERG (16). Rare EFT cases carry one of three alternative rearrangements of the EWS gene with either E1AF, FEV or ETV1 (7).

The presence of these fusion genes turned out to be the defining criterion for the EFTs (1).

1.1.4 Prognostic factors

Survival rate for patients with EFTs vary with several parameters. The overall five-year disease-free survival rate for localized EFT treated with surgery, radiation, and multiagent chemotherapy is 65 to 76 percent (17, 18). Most important prognostic factors are site of the primary tumor, presence of metastases, and tumor size. Tumor sites located in the pelvis, skull or spine negatively affect event free survival (EFS). The overall survival rate drops to less than 30 percent in patients with metastatic EFT (19). The location of the metastases is an important prognostic factor as well. Patients with lung metastases alone have better EFS than those who have bone metastases or bone marrow metastases. Patients with bone metastases have survival rates less than ten percent (20), independent of absence or presence of lung metastases. Patients with primary tumors of a size larger than 100 cm³ have to expect a lessened time of EFS. Another factor is the age of the patient at time of diagnosis. Patients older than 15 years will have shorter EFS, generally. Poor response to chemotherapy and / or radiation and a high level of serum LDH at diagnosis are also linked to a shorter EFS time (14, 21, 22). A positive

influence on EFS is achieved by radical surgery (23). Extent of neuroectodermal differentiation seems not to have any prognostic significance (24). The type of EWS-FLI1 fusion transcript may also play some role in the outcome of patients with EFT. The most common fusion type is called type 1 and consists of exon 7 of EWS fused to exon 6 of FLI1. Evidence so far suggests that patients who have the fusion type 1 have a better outcome compared to patients with other EWS-FLI1 fusion types (25).

1.1.5 Treatment

The ultimate goal of treatment is to cure the disease without severe side effects and amputation of afflicted limbs. A treatment consisting of radiation therapy and surgery when necessary was established, started by James Ewing. But more than 90 percent of patients died from metastatic disease. In 1973, systemic chemotherapy was added to the treatment approach. This resulted in a significant improvement of EFS rates (26). Currently, the treatment for EFTs is a combination of chemotherapy, radiation therapy, and surgery. The primary tumor site is treated by radiation and surgery, microscopic disease is targeted by systemic chemotherapy.

Several studies led to the collaborative children's oncology groups (COG) initiating randomized, controlled trials. In 1981, the cooperative Ewing's sarcoma study (CESS-81) was initiated with initial 18-weeks-chemotherapy consisting of vincristine, actinomycin D, cyclophosphamide and adriamycin (VACA) followed by either radical surgery with complete resection of the involved bone or incomplete resection followed by radiation or radiotherapy only (23). These studies led to the identification of several prognostic parameters, as described in 1.1.4.

For patients with poor prognosis special intensified treatment protocols have been adopted. Several studies found intensified chemotherapy to be not effective in positively influencing the EFS of the patients (17, 27), intensified radiotherapy, however, was shown to contribute to improvement of EFS.

High-dose chemotherapy (HDC) used for patients with metastatic EFT in a phase II study of a Children's Oncology Group (COG) in 2001 resulted in a two-year EFS of 20 percent. Patients with bone and bone marrow metastases did

not benefit from total body irradiation (TBI) and / or HDC with autologous stem cell rescue (ASCR) (28). Similar results were reported in 2001 in a Memorial Sloan Kettering study (29).

Patients with pulmonary metastases were treated with whole lung irradiation (WLI) in conjunction with standard therapy in a study of a European Intergroup Cooperative Ewing's Sarcoma Study (EICESS). The reported EFS of 40 percent was superior to a result obtained for patients who were treated with standard therapy alone. This evidence again supports that local control of lung metastases with WLI may be important to keep the metastatic disease in check (30). Patients with lung and bone metastases who were treated with WLI and HDC with ASCR had a 28 percent EFS at four years, whereas this same group of patients had universally fatal outcomes when treated with conventional therapy alone. A survival advantage did exist for patients who underwent HDC for bone and bone marrow metastases or WLI for lung metastases. This suggests that focal or myeloablative treatments for sites of metastases may be essential (31).

As published in 2000, Burdach *et al.* performed either allogeneic or autologous transplants following HDC in patients with primary metastatic or relapsed disease at two transplant centers in Europe. The results of this study do not show that for patients with advanced EFT the EFS had improved in allogeneic graft compared to autologous graft recipients. According to the results there is no difference in relapse rate between both patient groups and thus no evidence of an existing graft *versus* tumor (GvT) effect in patients (32). In 2003, Burdach *et al.* published the results of a study with patients with most advanced EFTs where the five-year EFS was increased up to 29 percent with one regimen compared to 22 percent with another protocol (33).

Some case studies have examined the utility of allogeneic stem cell transplantation in the treatment of advanced disease. In 2005, Koscielniak *et al.* reported a prolonged disease-free interval (3.5 years) following allogeneic transplant using a haploidentical donor in a teenager with relapsed metastatic EFT. Their results suggest that there may be a GvT effect in EFT (34). Methods to maximize the benefit of GvT while simultaneously lowering the toxic effects of graft *versus* host disease (GvHD) are therefore highly desirable.

1.2 Immunotherapy

To stimulate antitumor immunity two fundamentally different strategies have been tested in humans over the past five decades: therapeutic vaccination and passive immunization (35). Passive immunization is also referred to as adoptive T cell therapy or immunotherapy. Autologous or allogeneic T cells are given to the patients by transfusion. Analysis of tumor progress and persistence in immunodeficient mice and humans (36) led to evidence of the ability of T cells to control the tumor. Inhibitory effects of transplanted autologous leukocytes were shown in the 1960s by the work of Southam *et al.*. The growth of transplanted autologous tumor cells was stunted by co-transfer with autologous leukocytes in about half of the patients (37). These leukocytes were present in many patients. While not able to control the established advanced cancer they were able to inhibit the growth on new sites and could be used as potential candidates for adoptive immunotherapy.

The first step of adoptive immunotherapy is the identification of tumor-specific antigens (TSAs) that are expressed only in tumor cells or tumor-associated antigens (TAAs) that are over-expressed in tumor cells relative to normal tissue. Tumor-specific cytotoxic T cells (CTLs) need to be isolated and characterized from either healthy donors or patients with cancer (38). CTLs specific for TSAs allow specific targeting of tumor cells without side effects. CTLs specific for TAAs however may also attack normal healthy target tissue expressing the antigen (39). The immune system may recognize TAAs as self-antigens and limit the T cell immune response through mechanisms of central and peripheral tolerance, including clonal deletion and anergy (40, 41). During maturation T cells with high affinity for self-antigens may be deleted in the thymus, so the isolated TAA-specific T cells may only possess low-affinity T cell receptors (TCRs) and be less effective at killing tumor cells (42). When proteins are not expressed in normal tissues, then T cells specific for epitopes derived from TSAs are immunologically naïve and rare. These factors limit the number of specific T cells that can be isolated from patient peripheral blood and affect the ability of specific T cells to expand *in vitro* following stimulation with cognate antigen. Researchers have tried to circumvent these practical limitations by different strategies. DNA of rare, tumor-reactive T cells detected in patients was

isolated, and the genes for the α and β chain of the TCR was cloned and transferred into recipient T cells. These genetically modified T cells acquired the antigen specificity and reactivity of the parent clone as shown by *in vitro* experiments (43). Another strategy uses T cells with chimeric T cell receptors. This receptor is a fusion of the antigen-specific recognition domain of a specific antitumor antibody with the intracellular T cell receptor signaling chains. CTLs modified to express such receptors are specifically activated on contact with the antigen, without the need for antigen presentation on major histocompatibility complex (MHC) molecules. T cells with chimeric T cell receptors have been used successfully to treat human ovarian cancer cells in immunodeficient mice (44). Others tried to enhance antitumor efficacy by modifying the T cells to secrete cytokines that stunt tumor growth, like tumor necrosis factor, or interleukins that stimulate T cell proliferation and thus improve the persistence of the T cells in the patient (45).

Another approach is to use dendritic cells (DCs) to generate specific CTLs *in vitro*. This approach theoretically has the advantage of being able to obtain CTLs specific for any naturally processed antigen. It does not depend on harvesting previously existing specific CTLs circulating in the patient's body which - if they exist at all- would be very rare and possibly ineffective since the patient's immune system is already compromised by central and peripheral tolerance.

1.2.1 Dendritic Cells

DCs represent a heterogeneous cell population, residing in most peripheral tissues, particularly at sites of interface with the environment, e.g. mucous membranes and skin. At these sites they represent one to two percent of the total cell number (46). In the absence of ongoing inflammatory and immune responses, immature DCs patrol the blood, peripheral tissues, lymph and lymphoid organs. In peripheral tissues, DCs capture self and non-self antigens via specific receptors such as DC-SIGN, and various mechanisms, such as phagocytosis, receptor-mediated endocytosis and macropinocytosis. Internalized antigens are then processed into proteolytic peptides, and these peptides are loaded onto MHC class I and class II molecules. To efficiently

present antigens the immature DCs must receive signals to enter maturation. Those signals are often referred to as "danger signals" and are sent by pathogens or pathogen-induced tissue damage. "Danger signals" are generated when receptors on DCs recognize an encounter with bacteria, viruses, fungi or their respective products, cytokines or molecules derived from autologous cells like tumor cell lysate and heat-shock proteins.

DCs are effective antigen presenting cells and express the molecules needed to activate naïve T cells and stimulate T cell immunity in high levels. Those include MHC molecules, co-stimulatory molecules, and adhesion molecules. It is now possible to generate large numbers of functional DCs from a patient's CD14⁺ peripheral blood monocytes (47) or CD34⁺ hematopoietic stem cells *ex vivo*. This methodological improvement led to considerable interest in the use of dendritic cell vaccines as a means to induce antitumor immunity. DCs loaded with tumor antigens in the form of peptide fragments, whole antigens, or tumor cell lysate are beginning to enter clinical trials, with some encouraging results. Patients with metastatic melanoma were injected with DCs loaded with several tumor-specific peptides or tumor lysate, and with a chemical adjuvant to boost the immune response. Three in 16 patients had complete responses and two had partial responses (48). Metastatic renal cell carcinoma has been a target for vaccination with a hybrid cell vaccine consisting of autologous tumor cells fused to DCs. Despite the poor prognosis for such patients, objective clinical responses, including four complete remissions, were seen in 41 percent of patients (49). Ongoing clinical trials are using dendritic cells in renal cell carcinoma, prostate cancer, and melanoma. In 2001, a Phase I trial of tumor lysate-pulsed DCs in the therapy of several different pediatric solid tumors was completed. Two patients with PNET and two patients with ET were included (50). Patients were vaccinated with autologous DCs pulsed with tumor lysate. The DC vaccine was able to generate specific T cell reactivity and mediated regression of established metastatic tumors in heavily pretreated patients without significant toxicity.

1.2.2 T cell therapy

Adoptive transfer of antigen-specific T cells as treatment of opportunistic disease and some virus associated malignancies has led to encouraging results (51-54). Patients with non-viral cancers so far did not benefit as much from this therapeutic approach, as these cancers use many and varied techniques to escape the immune system. These techniques include evasion by down-regulation of target antigens and MHC molecules, recruitment of regulatory T helper cells to the tumor site, and secretion of inhibitory cytokines (38).

In the case of melanoma, improved CTL cell culture technology (55) has permitted the first clinical tests of adoptive transfer of CTLs, and the approach seems to result in substantial activity in patients. Patients with refractory metastatic melanoma were treated with CTLs derived from peripheral blood lymphocytes (PBLs) and eight of the 20 patients had minor, mixed, or stable antitumor immune responses (56). One patient who was infused with autologous CD8⁺ T cells specific for a melanoma-specific antigen (the MART-1 protein) showed T cell infiltration into both the skin and tumor tissue (57). The infused T cell population was capable of destroying normal melanocytes and tumor cells. The tumor however reacted with immune evasion and the outgrowth of a MART-1–negative tumor was observed (57). An independent trial confirmed these findings. Engrafted CTLs were detectable by specific tetramer-staining up to two weeks after transfer in all patients with a maximal frequency of two percent of the total CD8⁺ T cells (58). Clinical antitumor responses were only observed in three of eleven patients, however, and immune escape by selective loss of MART-1-expression in lymph node metastases occurred (58). Morgan *et al.* engineered autologous T cells of melanoma patients by retroviral transfer of the genes for the α and β chain of the anti-MART-1 TCR (59). The genes were derived from a MART-1—specific tumor infiltrating lymphocyte (TIL) of a melanoma patient in nearly full regression after the adoptive transfer of TILs as published by Dudley *et al.* in 2002 (60). Two patients in 14 injected with the genetically engineered autologous T cells showed a sustained objective regression of their metastatic melanoma.

Long-term regression of metastasized renal cell carcinoma and melanoma has been reported after treatment with interleukin 2 (IL-2), although the mechanism is unclear. The stimulatory effect of IL-2 on T cells is believed to be the cause for these remissions (61). TILs were isolated from patients' tumor samples and expanded *ex vivo* using IL-2. Those expanded T cells were then injected into the patient and induced remission. The combination of the treatment with IL-2 and infusion of expanded TILs, however, did not result in a significant improvement of EFS when compared with the patients who were treated with IL-2 alone (62).

When patients are treated with allogeneic donor T cells two side effects can be observed. One is called GvHD. Donor T cells recognize the patient's healthy tissue as foreign and attack it. The other effect is called GvL or GvT (see 1.1.5). The donor T cells recognize the patients' remaining tumor cells and attack them. In the case of chronic myeloid leukemia patients who relapsed after allogeneic transplantation were infused with allogeneic T cells derived from the same donor. This led to clinical responses in 60 to 80 percent of the patients. Other reports show the same GvT effect with patients with renal cell carcinoma (63). Novel approaches to increase the desired GvT effect while simultaneously decreasing the GvHD are needed and tried. One strategy is to separate T cells which are specific for tumor tissue from T cells which recognize healthy tissue (64).

1.3 Aim of the study

The goal of this work was to identify new CTL epitopes specific for EFTs and to generate CTLs capable of recognizing cells presenting this epitope and which are effective in killing them specifically *in vitro*. This goal was to be achieved by priming naïve T cells with DCs loaded with peptides representing CTL epitope candidates. As mentioned above the first step of this approach is to find suitable targets. A pool of targets was provided by the work of Staeger *et al.* from our group published in Cancer Research in 2004 (65). The published chip data had to be verified *in vitro* and most promising candidate targets had to be selected. EWS-FLI1 would be a perfect candidate as it is specific for EFT, but no HLA class I binding epitopes in the fusion region were found (66).

The first approach was *in vitro* priming (IVP) in an autologous context, where naïve T cells and DCs were derived from the same healthy donor. After successfully establishing the methods and evaluating the results the next step was to generate specific CTLs by an allogeneic approach, where the DCs represented the patient, and the T cells the donor. Mismatch by design was HLA-A*0201 status, with the DCs being HLA-A*0201 positive. This situation tries to emulate the case where an EFT patient is transplanted with allogeneic bone marrow with the possibility of giving the generated EFT-specific CTLs at a later time point similar to Donor-Lymphocyte-Infusions (DLI) common in treatments of leukemia. Specific CTLs would maximize the GvT effect while possibly eliminating the GvHD effect common to DLI comprised of a bulk lymphocyte population.

2 Materials

2.1 Instruments and Equipment

Type of device		Manufacturer
Bacteria shaker	Certomat BS-T	Sartorius
Ice machine	AF 100	Scotsman
Balance	EW 300-LM	Kern
Balance (analytical)	770	Kern
Cell Separation System	BD IMag™	BD Biosciences
Cell Separation System	MidiMACS™ Separator	Miltenyi Biotec
Cell counting chamber	Neubauer	Brand
Centrifuge	Multifuge 3 S-R	Heraeus
Centrifuge	Biofuge fresco	Heraeus
Controlled-freezing box		Nalgene
Electrophoresis chamber		BioRAD
ELISpot reader	AID iSpot Reader Unit	AID GmbH
Flow cytometer	FACSCalibur™	Becton Dickinson
Freezer (-80 °C)	Hera freeze	Heraeus
Freezer (-20 °C)	cool vario	Siemens
Fridge (+4 °C)	cool vario	Siemens
Gel documentation	Gene Genius	Syngene
Incubator	Hera cell 150	Heraeus
Liquid Nitrogen Tank	L-240 K series	Taylor-Wharton
Multichannel pipette	(10 -100 µl)	Eppendorf
Heating block	Thermomixer Comfort	Eppendorf
Micropipettes	(0.5-10 µl, 10-100 µl, 20-200 µl, 100-1000 µl)	Eppendorf
Microscope		Optech
Microscope (fluorescence)	Eclipse TS100	Nikon
Microscope		Leica
Microwave oven		Siemens, AEG

Materials

Pipetting assistant	Easypet	Eppendorf
Spectrophotometer	GeneQuant II	Amersham Biosciences
Sterile Bench		Heraeus
Water bath		GFL
Electroporator	Gene Pulser Xcell™	BioRad
Real Time PCR	7300 Real-Time PCR	Applied Biosystems
Vortexer	Vortex-Genie 2	Scientific Industries
Water purification system	TKA GenPure	TKA GmbH

2.2 Commonly used materials

Cryovials	Nunc
Filters for cells, Cell Strainer	Falcon
Filters for solutions (0.2 µm and 0.45 µm)	Sartorius
Flasks for cell culture (75 cm ² and 175 cm ²)	TPP
Flasks for cell culture (75 cm ² and 175 cm ²)	Falcon
Gloves (nitrile, latex)	Sempermed
Parafilm	Pechiney Plastic Packaging
Pasteur pipettes	Peske OHG
Petri dishes	Falcon
Pipettes (2, 5, 10 and 25 ml)	Falcon
Pipette tips (10, 200 and 1000 µl)	MβP
Pipette tips (10, 200 and 1000 µl with a filter)	Biozym
Plates for cell culture (6-well, 24-well and 96-well)	TPP
Scalpels (Nr. 12, 15, 20)	Feather
Tubes for cell culture (polystyrene, 15 ml)	Falcon
Tubes for cell culture (polypropylene, 15 ml and 50 ml)	Falcon
Tubes for molecular biology, Safelock (1.5 ml and 2 ml)	Eppendorf
Tubes for FACS™ (5 ml)	Falcon

2.3 Chemicals and biological reagents

Agar	Sigma
Agarose	Invitrogen
AIM V medium	Invitrogen
Ampicillin	Merck
β -Mercaptoethanol	Sigma
β_2 -Microglobuline	Sigma
Blue Juice Gel Loading Buffer	Invitrogen
Chloroform	Merck
CD8 ⁺ T Cell Isolation Kit II	Miltenyi Biotec
Cyclosporin A	Sigma
DEPC (diethyl pyrocarbonate)	Sigma
DMEM medium	Invitrogen
DMSO (dimethyl sulfoxide)	Merck
Dimethylformamide	ROTH
Erythrocyte Lysis Buffer	Pharmacy Klinikum rechts der Isar
Ethidium bromide	BioRad
Ethanol	Merck
FACS™ Flow	Becton Dickinson
FACS™ Rinse	Becton Dickinson
FACS™ Clean	Becton Dickinson
Ficoll-Paque	GE Healthcare
FBS (fetal bovine serum)	Biochrom
Gentamicin	Biochrom
Glycerol	Merck
GM-CSF (Leukine sargramostim)	Bayer HealthCare Pharmaceuticals
Human CD14 Magnetic Particles - DM	BD Biosciences
Human male AB serum	Lonza
IL-1 β (interleukin 1 β)	R&D Systems
IL-2 (interleukin 2)	R&D Systems
IL-4 (interleukin 4)	R&D Systems
IL-6 (interleukin 6)	R&D Systems
IL-7 (interleukin 7)	R&D Systems

Materials

IL-12 (interleukin 12)	Pan Biotech GmbH
IL-15 (interleukin 15)	R&D Systems
Isopropanol	Sigma
LB Broth Base	Invitrogen
Lipofectamine™	Invitrogen
L-glutamine	Invitrogen
MACS® BSA Stock Solution	Miltenyi Biotec GmbH
autoMACS™ Rinsing Solution	Miltenyi Biotec GmbH
Na-pyruvate	Invitrogen
100 × non-essential amino acids	Invitrogen
One Shot TOP10F´ competent cells	Invitrogen
OptiMEM I medium	Invitrogen
PBS 10 × (phosphate buffered saline)	Invitrogen
pCMV-Tag4A vector	Stratagene
Peptone	Invitrogen
Penicillin / streptomycin	Invitrogen
PGE ₂ (prostaglandin E2)	Cayman Chemical Company
pmaxGFP vector	Lonza
Propidium iodide	Sigma
<i>Pst</i> I restriction enzyme	Roche
Ready-Load 1 Kb DNA Ladder	Invitrogen
RNase A (ribonuclease A)	Roche
RPMI 1640 medium	Invitrogen
Sodium chloride	Merck
<i>Spe</i> I restriction enzyme	New England BioLabs
TAE (tris acetate EDTA) buffer	Invitrogen
TBE (tris borate EDTA) buffer	Ambion
Trypan blue	Sigma
Trypsin / EDTA	Invitrogen
Tween 20	Sigma
TNF α (tumor necrosis factor α)	R&D Systems
<i>Xba</i> I restriction enzyme	Fermentas
X-vivo 15 medium	Biowhittaker

2.4 Kits

RNeasy® Mini Kit	Qiagen
NucleoSpin® Plasmid Kit	Macherey-Nagel
JETstar 2.0 Maxiprep Kit	Genomed.
QIAEX II Gel Extraction Kit	Qiagen
IOTest® Beta Mark Kit	Beckman Coulter
TaqMan® Gene Expression Assays	Applied Biosystems

2.5 Cell Culture media and solutions

Standard medium:

RPMI 1640
10 % Fetal calf serum (FCS)
2 mM L-glutamine (200 mM)
100 U / ml Pen / Strep (10^4 U / ml)

LCL medium:

RPMI 1640
10 % FCS
2mM L-glutamine (200 mM)
1 mM Na-pyruvate (100 mM)
1 x non-essential amino acids (100 x)
0.1 % Gentamicin (50 mg / ml)

T cell medium:

AIM V
5 % human serum
2 mM L-glutamine (200 mM)
0.1 % Gentamicin (50 mg / ml)

Trypsin / EDTA 1 x:

45 ml PBS
5 ml Trypsin-EDTA (10 x)

Freezing Medium:

FCS 90 %
DMSO 10 %

CTL Freezing Medium:

Human serum 90 %
DMSO 10 %

Dendritic cell medium:

X-Vivo 15
1 % human serum

Lipofection medium:

OptiMEM

LB medium:

10 g peptone
5 g Yeast extract
10 g sodium chloride
ad 1 l distilled water

LB agar medium:

10 g LB Broth Base
7.5 g Agar
ad 500 ml distilled water

DNA electrophoresis gel:

200 ml TAE buffer
1.5 g agarose = 1.5 %
3 µl ethidium bromide

DNA electrophoresis running buffer:

180 ml distilled water

20 ml TAE buffer (10 x) = 1 x

2.6 Cells**Table 1: Cell lines and sources**

Name	Description	Source
697	cALL cell line (HLA-A*0201 ⁺)	DSMZ (67)
(MHH)-cALL2	cALL cell line (HLA-A*0201 ⁻)	DSMZ (68)
A673	EFT cell line (HLA-A*0201 ⁺)	ATCC (69)
Cado-ES1	EFT cell line (HLA-A*0201 ⁻)	DSMZ (70)
CHP126	Neuroblastoma cell line	DSMZ (71)
Cos-7	The cell line Cos-7 (ATCC CRL 1651) is a derivative of the simian kidney cell line CV1 (ATCC CCL70) transformed with a mutant of simian virus 40 (SV40)	H. Bernhard (72)
DCs	differentiated from monocytes of a healthy HLA-A*0201-positive blood donor	generated in the laboratory
LCLs	EBV-immortalized B cells	generated in the laboratory
MHH-ES1	EFT cell line	DSMZ (73)
MHH-NB11	Neuroblastoma cell line	DSMZ (74)
Nalm6	cALL cell line (HLA-A*0201 ⁺)	DSMZ (75)
RD-ES	EFT cell line (HLA-A*0201 ⁻), not published	DSMZ
SBSR-AKS	EFT cell line (HLA-A*0201 ⁻)	generated in the laboratory(76)
SH-SY5Y	Neuroblastoma cell line	DSMZ (77)
SK-ES1	EFT cell line	DSMZ (78)
SK-N-MC	EFT cell line (HLA-A*0201 ⁻), Established as neuroblastoma cell line, erroneously	DSMZ (77)
T2	hybrid of a T and a B lymphoblastoid cell line; TAP-deficient	J. Mautner (79)
TC-71	EFT cell line (HLA-A*0201 ⁺)	DSMZ (80)

2.7 ELISpot Reagents

2.7.1 Antibodies

anti-h-Perforin mAbs Pf-80 / 164, purified	Mabtech
anti-h-Perforin mAb Pf-344, biotinylated	Mabtech
anti-h-Granzyme B mAb GB10, purified	Mabtech
anti-h-Granzyme B mAb GB11, biotinylated	Mabtech
anti-h-IFN- γ mAb 1-D1K, purified	Mabtech
anti-h-IFN- γ mAb 7-B6-1, biotinylated	Mabtech

2.7.2 Enzymes, Buffers, Plates

MultiScreen-HA Filter Plate, 0.45 μ m, clear, sterile (Millipore)

Streptavidin-Horse Radish Peroxidase (Mabtech)

Wash Buffer: 1 \times PBS / 0.05 % Tween

Antibody Buffer: 1 \times PBS / 0.5 % BSA

Acetate Buffer: 37.5 ml H₂O dest. + 3.75 ml 0.2 N acetic acid + 8.8 ml 0.2 N sodium acetate

3-Amino-9-ethyl-carbazole (AEC) tablets (Sigma)

AEC solution: 1 AEC tablet in 2.5 ml Dimethylformamide (DMF) + 47.5 acetate buffer

Developing solution / plate: 10 ml AEC solution + 30 μ l 30 % H₂O₂

Positive control: 5 μ g / ml anti-CD3 antibody (OKT3) in T cell medium

2.8 Flow cytometry reagents

2.8.1 Reagents

Staining buffer: 0.1 % sodium azide, 0.1 % BSA in PBS

Fixing solution: 1 % paraformaldehyde in PBS

2.8.2 Antibodies

Table 2: Antibodies used in flow cytometry

Specificity	Clone	Fluorophor	Manufacturer
CD8	RPA-T8	FITC / PE / APC	BD Biosciences
CD27	M-T271	FITC	BD Biosciences
CD28	CD28.2	FITC	BD Biosciences
CD3	HIT3a	FITC / APC	BD Biosciences
CD4	RPA-T4	FITC / PE	BD Biosciences
CD45RA	HI100	PE	BD Biosciences
CD56	B159	PE	BD Biosciences
CD62L	Dreg 56	APC	BD Biosciences
CD83	HB15e	APC	BD Biosciences
CD86	2331 (FUN-1)	FITC	BD Biosciences
HLA-A2	BB7.2	FITC	BD Biosciences
HLA class I	G46-2.6	APC	BD Biosciences
HLA class II	L243	PE	BD Biosciences
Propidium Iodide	-	-	Sigma
CCR7	2H4	PE	BD Biosciences
CCR5	2D7	APC	BD Biosciences
CD127 (II7R)	40131	APC	R&D

2.9 Peptides

Peptides were ordered and synthesized by Thermo Scientific.

(<http://www.thermohybid.de/cgi-bin/start.app>)

Table 3: *In silico* predicted peptides and their scores

Gene	HLA-Allele	Sequence	Position (first N-terminal aa)	NetCTL1.2	SYFPEITHI	BIMAS
CHM1	A*0201	RLLGVGAVV	38	0.92	24	105.51
	A*0201	KLQDGSMEI	84	1.35	24	149.71
	A*0201	FLSSKVLEL	184	1.49	29	226.01
	A*0201	VIMPCSWWV	319	1.33	22	2481.34
EZH2	A*0201	FMVEDETVL	120	1.27	21	119.00
	A*0201	YMCSFLFNL	666	1.49	25	3.60
EWS-FLI1	A*0201	GQQNPSYDSV	-	0.46	13	5.18
GPR64	A*0201	GTLTGVLSSL	107	0.85	26	2.53
	A*0201	TLSETYFIM	129	0.97	16	72.66
	A*0201	FIMCATAEA	135	1.29	20	11.63
ITM2A	A*0201	GLSFILAGL	59	1.14	27	49.13
	A*0201	YLMPLNNTSI	161	1.52	26	177.57
Influenza (FLU)	A*0201	GILGFVFTL	-	1.29	30	550.93
LIPI	A*0201	WLQNFVRIL	113	0.78	25	70.43
	A*0201	LLNEEDMNV	121	1.00	25	485.00
	A*0201	SIFSGIQFI	262	1.13	25	67.14
	A*0201	TMMDGSFSF	370	1.52	14	4.74
	A*0201	KLLNQLGMI	379	0.90	25	40.40
STEAP	A*0201	FLYTLLEEV	86	1.35	29	470.95

2.10 Plasmids

pmaxGFP:

The pmaxGFP plasmid (3.49 kb) was provided in the Nucleofector kit (Amaxa Biosciences, Cologne, Germany, now purchased by Lonza). In pmaxGFP, maxGFP expression is driven by a cytomegalovirus (CMV) promoter (for more details, see <http://www.amaxa.com>; (81))

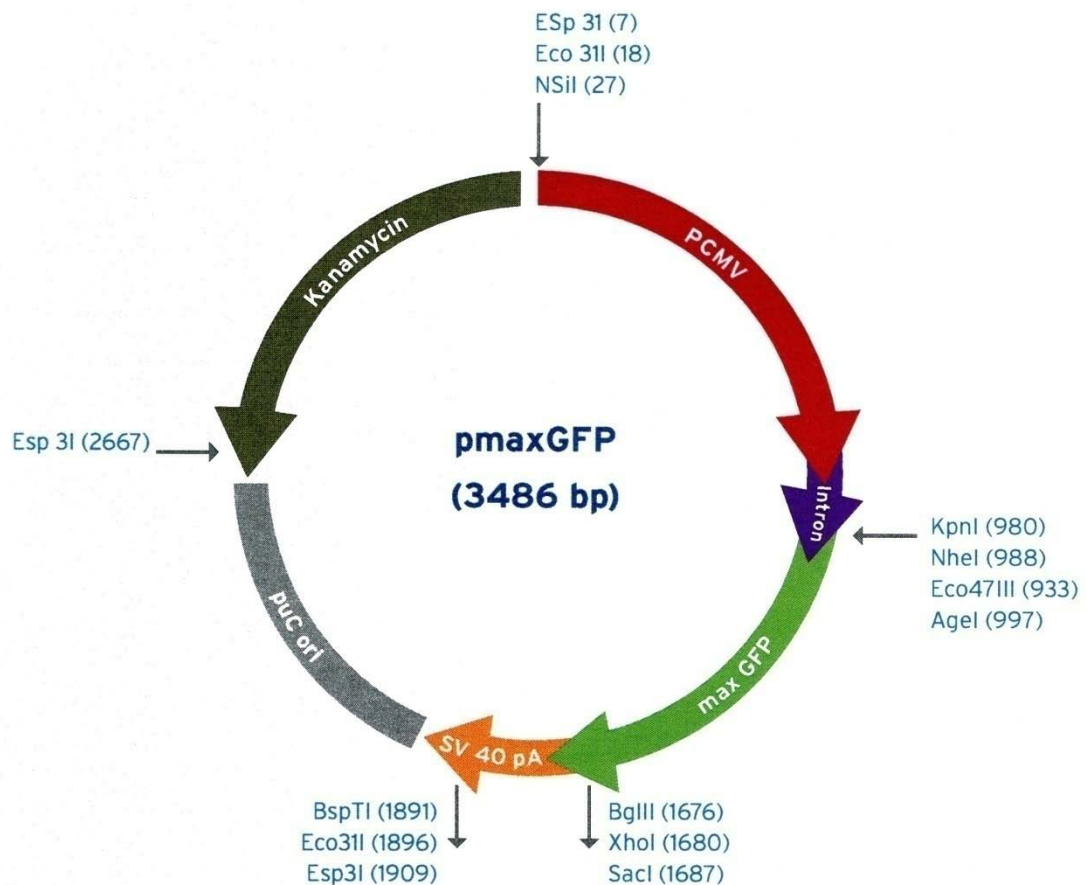


Figure 1: Vector map of pmaxGFP

pCDN3.1 / Zeo(-) / HLA-A2:

This vector was a gift from the laboratory of Prof. Dr. Helga Bernhard, Department of Hematology / Oncology, Klinikum rechts der Isar, Technische Universität München, 81664 Munich, Germany.

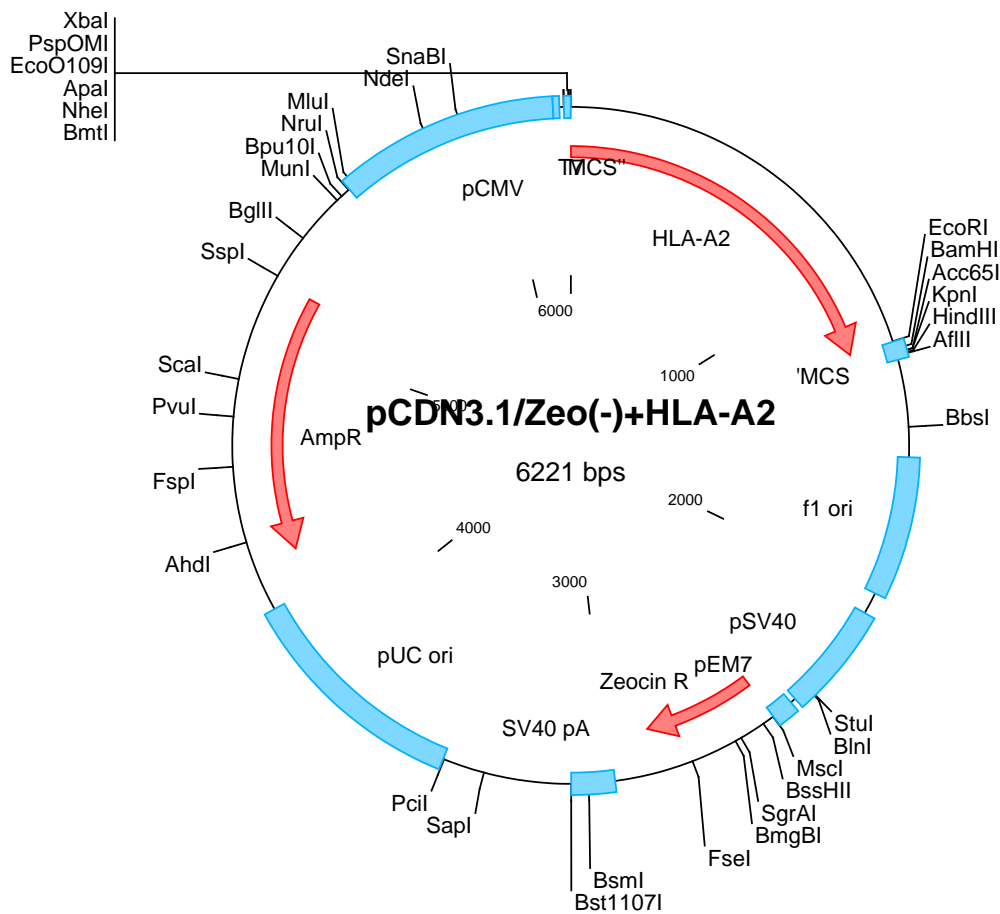


Figure 3: Vector map of the HLA-A2 expression vector

pCMV-Sport6-EZH2:

This vector was purchased from ImaGenes (formerly RZPD) GmbH, Berlin, Germany (ImaGenes clone ID IRATp970F1210D).

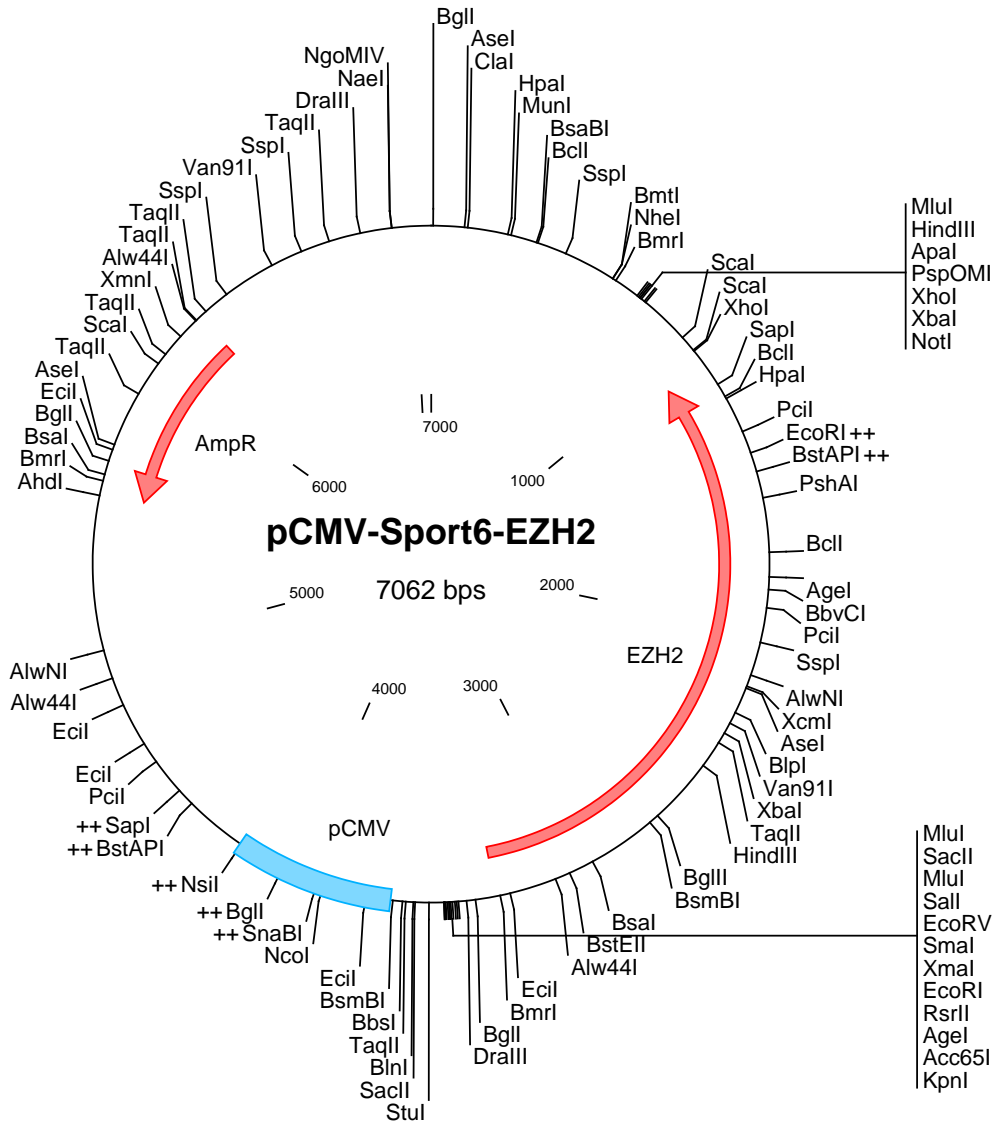


Figure 4: Vector map of pCMV-Sport6-EZH2

2.11 List of manufacturers

AEG	Nürnberg, Germany
AID GmbH	Straßberg, Germany
Ambion	Austin, Texas, USA
Amersham Biosciences	Piscataway, New Jersey, USA
ATCC	Rockyville, Maryland, USA
B. Braun Biotech Int.	Melsungen, Germany
Bayer HealthCare Pharmaceuticals	Leverkusen, Germany
BD Biosciences	Heidelberg, Germany
Beckman Coulter	Palo Alto, California, USA
Becton Dickinson	Jersey City, New Jersey, USA
Biochrom	Berlin, Germany
BioRad	Richmond, California, USA
Biowhittaker	East Rutherford, New Jersey, USA
Biozym	Hess. Olendorf, Germany
Cayman Chemical Company	Ann Arbor, Michigan, USA
DSMZ	Braunschweig, Germany
Eppendorf	Hamburg, Germany
Falcon	Oxnard, California, USA
Fermentas	St. Leon-Rot, Germany
GE Healthcare	Uppsala, Sweden
Genomed	St. Louis, Missouri, USA
Greiner	Nürtingen, Germany
Heraeus	Hanau, Germany
ImaGenes GmbH	Berlin, Germany
Invitrogen	Karlsruhe, Germany
Leica	Wetzlar, Germany
Lonza	Basel, Switzerland
Mabtech	Nacka Strand, Sweden
Macherey-Nagel	Düren, Germany
Merck	Darmstadt, Germany
Millipore	Billerica, Massachusetts, USA
Miltenyi Biotec GmbH	Bergisch Gladbach, Germany

Materials

Molecular BioProducts, MβP	San Diego, California, USA
Nalgene	Rochester, New York, USA
New England BioLabs	Frankfurt am Main, Germany
Nunc	Naperville, USA
Pan Biotech GmbH	Aidingen, Germany
Pechiney Plastic Packaging	Menasha, Wisconsin, USA
Peske OHG	München, Germany
ProlImmune	Oxford, UK
Promega	Madison, Wisconsin, USA
Qiagen	Chatsworth, California, USA
R&D Systems	Minneapolis, Minnesota, USA
Roche	Mannheim, Germany
(Carl) ROTH	Karlsruhe, Germany
Sartorius	Göttingen, Germany
Schleicher und Schüll	Dassel, Germany
Scientific Industries	Bohemia, New York, USA
Semperit	Wien, Austria
Sigma	St. Louis, Missouri, USA
Stratagene	Cedar Creek, Texas, USA
Syngene	Cambridge, UK
TKA GmbH	Niederelbert, Germany
TPP	Trasadingen, Switzerland
Thermo Fisher Scientific	Ulm, Germany
Zeiss	Jena, Germany

3 Methods

3.1 Cell culture

3.1.1 Cell counting

The cell count and viability was assessed by trypan blue exclusion. Live cells or tissues with intact cell membranes are not colored. The cell suspension was diluted 1:2 with trypan blue by adding 10 μl of the cell suspension to 10 μl of trypan blue. Suspensions should be diluted enough so that the cells or other particles do not overlap each other on the grid, and should be uniformly distributed to a maximum cell number of 200 cells per 16 small squares. Using an inverted microscope, the number of viable (unstained) cells in the four corner squares was counted. Either the cells touching the top and left of the ruled squares or those touching the bottom and right were counted, but not both. Formulas used to calculate cell concentrations and total cell numbers are shown in Tab.4.

Table 4: Determining the cell number by counting in a Neubauer hemocytometer

$$\frac{\text{cell concentration}}{\text{ml}} = \text{average number of cells counted per square} \times \text{CF} \times \text{DF}$$

$$\text{CF: chamber factor} = \frac{1}{\text{volume of chamber counted}} \times \text{ml}$$

The volume of one big square of an improved Neubauer hemocytometer is 0.1 μl .

The chamber factor is 10^4 .

$$\text{DF: dilution factor} = \frac{\text{final volume}}{\text{initial volume}}$$

$$\text{total number of cells} = \text{cell concentration} \times \text{volume of cell suspension}$$

3.1.2 Cryopreservation of cells

Tumor cell lines and T cell cultures were frozen at concentrations between 1×10^6 and 1×10^7 / ml in 1 ml volumes respectively. Peripheral blood mononuclear cells (PBMCs) were frozen at 5×10^7 / ml in 1 ml volumes. Pelleted cells were first resuspended in an appropriate volume of FCS or human serum (for T cells). The same volume of pre-cooled 20 % DMSO was then gradually added to the cell suspension. After thorough mixing, 1 ml aliquots of the cell suspension were transferred into pre-cooled cryovials. The cryovials were placed into controlled freezing boxes and stored at -80 °C overnight. The following day, the cryovials were transferred into the liquid nitrogen freezer for long-term storage at -196 °C. Pulsed mature dendritic cells were stored in human serum (male AB) containing 10 % DMSO and 5 % glucose (82).

3.1.3 Thawing of cryopreserved cells

The thawing medium used was the corresponding medium. The cryovials were retrieved from the liquid nitrogen freezer and thawed rapidly in a water bath at 37 °C. As soon as only small ice crystals were seen floating inside the cryovial, the contents of a vial were transferred into a 15 ml Falcon tube containing 1 ml of medium. The tube was immediately centrifuged at 1500 rpm for 5 minutes. Pelleted cells were then resuspended in the corresponding culture medium pre-warmed to 37 °C.

3.1.4 Culture of adherent tumor cell lines

A673, SBSR-AKS, TC-71, and Cos-7 tumor cell lines were cultured in the standard tumor medium. Volume of the medium in a middle-sized culture flask (75 cm² adherence surface) was 10 ml. Volume of the medium in a large-sized flask (175 cm² adherence surface) was 25 ml. Approximately every 3 - 4 days cells grew to confluence. At that time point, their medium was exchanged and they were split 1:2 to 1:10, depending on the growth rate of individual cell lines. The medium was removed; cells were washed once with warm PBS and then incubated with up to 10 ml trypsin / EDTA at room temperature. Degree of

detachment was controlled microscopically. Detached cells were resuspended in fresh standard tumor medium and distributed in new culture flasks.

3.1.5 Culture of suspension tumor cell lines

K562, LCL and T2 tumor cell lines were cultured in the corresponding medium. Volume of the medium was 30 ml in a middle-sized culture flask. Approximately every 4 days, half of the cell suspension was removed and the same volume of fresh medium was added.

3.2 Isolation of peripheral blood mononuclear cells

3.2.1 Isolation of PBMC from blood donor unit (500ml)

500 ml whole blood of a healthy donor was freshly centrifuged to obtain a concentrate of white cells and platelets. The concentrate usually had a volume of 20 - 30 ml and contained about 5×10^8 to 1×10^9 PBMC. The concentrate was provided by the DRK-Blutspendedienst Baden-Württemberg-Hessen in Ulm and shipped to our laboratory within 24 hours.

The concentrate was carefully transferred from the blood unit bag to 50 ml conical tubes, and then diluted 1:3 with PBS. The diluted concentrate was layered on top of Ficoll-Paque in a ratio of 2:3, e.g. 30 ml of diluted blood onto 20 ml Ficoll-Paque.

To not disturb the interface and cause the layers to mix, pipetting had to be done slowly and carefully. The tubes were centrifuged at $400 \times g$ for 30 minutes at room temperature without brake. The plasma above the lymphocyte layer (buffy coat) was removed using a pipette, leaving approximately one centimeter of plasma layer above the buffy coat. The buffy coat was then aspirated with a Pasteur pipette and collected in a new tube. PBS was added to a final volume of 45 ml. A centrifugation step at $209 \times g$ for ten minutes was done to remove the platelets. The supernatant was carefully decanted, the pellet resuspended in the residual liquid. Lysis of erythrocytes was done by adding Erythrocyte-Lysis-Buffer and incubating for approximately five minutes. The lysis was stopped by adding PBS to a final volume of 45 ml and a subsequent

centrifugation at 1500 rpm for five minutes. The pellet was resuspended after decanting and washed with PBS twice.

After that the pellet was resuspended in 10 ml PBS, an aliquot diluted 1:100 and counted to determine the cell number in a hemocytometer.

3.2.2 Isolation of PBMC from whole blood

This method is the same as 3.2.1 with the exception of the first diluting step. Whole blood was diluted 1:2 instead of 1:3.

3.3 Isolation of CD14⁺ cells

CD14⁺ cells were isolated with the BD Anti-Human CD14 Magnetic Particles set using the BD IMagnet™. Labeling and cell separation were performed according to the manufacturer's instructions. Briefly, PBMC isolated from a HLA-A*0201⁺ healthy blood donor were counted and washed with an excess volume of BD IMag™ Buffer, the supernatant completely removed. The BD IMag™ Anti-Human CD14 Magnetic Particles were vortexed thoroughly, and 50 µl of particles for every 10⁷ total cells were added, mixed and incubated at room temperature for 30 minutes. After incubation the labeling volume was brought up to 2 × 10⁷ cells / ml with 1 × BD IMag™ buffer, the tube immediately placed on the BD IMagnet™ and incubated for 8 - 10 minutes. With the tube still on the magnet the supernatant containing the CD14⁻ fraction was aspirated. The tube was then removed from the magnet, the pellet resuspended with buffer and the magnetic separation was repeated twice. The remaining pellet represented the CD14⁺ fraction and was used to generate dendritic cells (see 3.5). A small portion was analyzed by flow cytometry.

3.4 Isolation of CD8⁺ cells

Untouched CD8⁺ T cells were isolated from human HLA-A*0201⁻ PBMCs using the CD8⁺ T Cell Isolation Kit, an LS Column, and a MidiMACS™ Separator. Labeling and cell separation were performed according to the manufacturer's instructions. Briefly, PBMCs were counted and washed with MACS Separation

Buffer. The buffer was obtained by diluting the MACS® BSA Stock Solution which consists of phosphate-buffered saline supplemented with 10 % bovine serum albumin 1:20 with the autoMACS™ Rinsing Solution. After washing, the pellet was resuspended with 40 µl buffer per 10^7 total cells. 10 µl CD8⁺ T cell Biotin-Antibody Cocktail was added per 10^7 total cells. The cells were mixed and incubated at 4 °C for ten minutes. After incubation 30 µl of buffer and 10 µl of CD8⁺ T cell MicroBead Cocktail were added per 10^7 total cells, followed by another incubation period of 15 minutes at 4 °C. The cells were washed with buffer and resuspended in buffer to a final concentration of 2×10^8 cells / ml. To obtain a single cell suspension and to remove possible cell debris and cell clumps the cells were passed through a 40 µm cell strainer before magnetic separation. A MS column (MACS) was rinsed with 500 µl buffer. The cell suspension was then pipetted into the prepared column, which was attached to the MidiMACS™ Separator. The column was washed three times with buffer. The total effluent containing the unlabelled CD8⁺ cells was collected, the cells counted and used in *in vitro* priming experiments.

3.5 Generation of Dendritic cells

PBMC of one healthy HLA-A*0201⁺ blood donor provided by the DRK-Blutspendedienst Baden-Württemberg-Hessen in Ulm were isolated as described. Monocytes were enriched by immuno-magnetic CD14 selection. CD14⁺ monocytes were cultured in X-Vivo15 / 1 % AB serum with 1000 IU / ml IL-4 and 800 IU / ml GM-CSF at a concentration of 3×10^5 / ml with 25 to 30 ml per 75 cm² cell culture flask at 37 °C and 5 % CO₂. On the third day cytokines were replaced.

On the 6th day of culture DC maturation was induced by adding a cytokine cocktail consisting of 10 ng / ml TNFα, 10 ng / ml IL-1β, 1000 IU / ml IL-6 and 1 µg / ml PGE₂. On culture day 8 and 9 cells displayed a mature phenotype as evidenced by light microscopy. The immune phenotype was analyzed by flow cytometry. Dendritic cells were considered mature when positive for CD86, CD83 and HLA-DR.

Mature DCs were pulsed with peptides (30 μmol / ml) and 20 μg / ml β_2 -microglobuline and used for T cell priming immediately or frozen and stored in liquid nitrogen for subsequent experiments.

3.6 Lipofection

Lipofection is a highly effective method of transfecting genetic material into cells. Reagents used in lipofection consist of cationic lipid and neutral lipid components. The positively charged group of the cationic lipid component binds to the negatively charged DNA. This interaction results in the formation of bundle-like RNA-lipid complexes. The hydrophilic negative charge of the nucleic acid is neutralized inside the complex. Entry of the complex into the cytoplasm occurs either via endocytosis or fusion with the plasma membrane. The role of the neutral lipid component is endosomal disruption through which the complex is released into the cytoplasm. The reagent used for lipofection in this thesis was LipofectamineTM.

Before transfection cells were plated into 6-well plates at a concentration resulting in 80 - 90 percent confluence the day of transfection. Three μg of DNA (gene of interest or reporter gene GFP) were diluted with 250 μl OptiMEM and mixed gently. In another tube 7.5 μl LipofectamineTM were diluted with 250 μl OptiMEM and incubated for five minutes at room temperature. Diluted DNAs and diluted LipofectamineTM reagent was combined by mixing gently and incubated for 20 minutes at room temperature to allow DNA-liposome complexes to form. While complexes were forming the medium on the cells was replaced with cell culture medium without antibiotics. For each transfection in a well of a 6-well-plate 500 μl medium containing the complexes was added drop-wise onto the cells and incubated at 37 $^{\circ}\text{C}$ in a CO_2 incubator. Every experiment included a control lipofection with the pmaxGFP plasmid. The transfection efficiency by percent of fluorescence was evaluated microscopically and by flow cytometry 24 hours after start of transfection.

3.7 Flow cytometry

Per staining sample 2 - 5 × 10⁵ cells were allocated, washed in staining buffer and resuspended in 40 µl buffer. Unspecific binding sites were blocked for 20 minutes on ice shielded from light with 100 µg / ml human IgG (10 µl), afterwards the cells were washed with staining buffer and resuspended in 100 µl buffer per sample. Five µl of antibody was given to the samples. One sample was left unstained. This sample was used for setting up the correct forward scatter (FSC) and sideward scatter (SSC) for the cell population. One sample was stained with the isotypes for every used fluorophore. This sample was used for setting up the correct parameters for detecting fluorescence. The samples were incubated on ice shielded from light for 30 minutes, washed twice with staining buffer and resuspended in 200 µl PBS whenever the samples were processed in the cytometer right away. When the samples were to be stored for longer than two hours before measurement, the samples were fixated by resuspending in 200 µl PBS / 1 % paraformaldehyde.

3.8 Cell sorting with Pentamer-staining

Two weeks after starting the *in vitro* priming all T cells were pooled, counted and washed. To remove potential protein aggregates that contribute to non-specific staining the Pentamer was spinned in a chilled microcentrifuge at 14.000 × g for three minutes, then chilled on ice, shielded from light. 2 - 5 × 10⁵ T cells per staining condition were allocated. Cells were washed with wash buffer (0.1 % sodium azide, 0.1 % BSA in PBS) and resuspended in 50 µl buffer volume. Tubes had to be kept chilled on ice for all subsequent steps, except where otherwise indicated. 10 µl of labeled Pentamer or 2 µl of unlabeled Pentamer were added to the cells that were about to be sorted. Volumes of buffer and Pentamer were scaled up according to cell number of the sample. The samples were incubated at room temperature for 10 minutes, shielded from light. After incubation the samples were washed and resuspended in 100 µl buffer.

Table 5: Staining scheme for cell sorting

Sample	FITC	PE	No of cells
unstained	-	-	$2 - 5 \times 10^5$
Isotypes	IgG ₁	IgG ₁	$2 - 5 \times 10^5$
Compensation 1	CD8	-	$2 - 5 \times 10^5$
Compensation 2	-	CD8	$2 - 5 \times 10^5$
Cells to sort	F × CD8	F × Pentamer	$F \times (2 - 5 \times 10^5)$

Secondary antibodies (Tab. 5) were added, 5 µl per sample, mixed by pipetting and incubated on ice for 20 minutes, shielded from light. After incubation the samples were washed twice and resuspended in 200 µl PBS. To exclude dead cells, Propidium iodide (PI; stock concentration: 50 µg / ml) was added to the samples immediately before sorting (work concentration: 1 µg / ml).

Cell sorting was executed by the Flow Cytometry Sorting Facility on a BD FACS Aria in the laboratory of Prof. Dr. Dirk Busch of the Technische Universität München.

3.9 RNA isolation

Total cellular RNA was isolated from tumor cells using the RNeasy® Mini Kit. The isolation procedure was performed with up to 10^7 cells per column according to manufacturer's instructions. Cellular plasma membranes and organelles were first disrupted by vortexing cells with a buffer containing guanidine isothiocyanate. The lysate was passed at least five times through a blunt 20-gauge needle (0.9 mm diameter) fitted to an RNase-free syringe to reach a homogeneous lysate. The lysate was mixed with an ethanol containing buffer and transferred onto an RNeasy® column. Ethanol provided conditions which promoted selective binding of RNA to a silica-gel membrane during centrifugation of the solution through the column. Washing buffers were then used to eliminate contaminants while RNA remained attached to the membrane inside the column. Finally, DEPC-treated water was used to elute the RNA from the column. Isolated and purified RNA was stored at -80 °C.

3.10 cDNA synthesis

Reverse Transcription (RT reaction) is a process in which single-stranded RNA is reverse transcribed into complementary DNA (cDNA) by using total cellular RNA or poly(A) RNA, a reverse transcriptase enzyme, in this case SuperScript® II, a primer, dNTPs and an RNase inhibitor. The resulting cDNA can be used in RT-PCR reaction. RT reaction is also called first strand cDNA synthesis. As primers for RT reaction oligo (dT) primers were used.

- 1) RNA was first incubated with a primer at 70 °C to denature RNA secondary structure and then quickly chilled on ice to let the primer anneal to the RNA.

Volume / sample: 20 µl

Oligo(dT)	1 µl
RNA	1 µg
DEPC-H ₂ O	to 12 µl

- 2) Other components of RT were added to the reaction including dNTPs, redox agent Dithiothreitol (DTT) to prevent disulfide binding and RT buffer.

5 × first strand buffer	4 µl
0.1 M DTT	2 µl
10mM dNTP Mix	1 µl

The mixture was incubated at 42 °C for two minutes, then 1 µl SuperScript® II enzyme was added.

- 3) The RT reaction was extended at 42 °C for 50 minutes.
- 4) To inactivate the enzyme the reaction was heated to 70 °C and incubated for 15 minutes.

3.11 Real-time PCR

Differential gene expression of cDNA was verified by real-time RT-PCR. Total RNA was reverse transcribed using the Superscript First-Strand Synthesis System with oligo-dT primers, according to the manufacturer's instructions. Quantitative real-time PCR was performed by use of TaqMan® Universal PCR Master Mix and fluorescence detection with an AB 7300 Real-Time PCR System. Gene-specific primers and probes were obtained as TaqMan® Gene Expression Assays from Applied Biosystems which consisted of a FAM™ dye-labeled TaqMan® MGB probe and two unlabeled PCR primers. 1.25 µl of these primer assays were added to the TaqMan® Universal PCR Master Mix (12.5 µl) with cDNA (0.5 µl; synthesized as described in 3.10) at adjusted to a final volume of 25 µl with water. The final concentration of primers and probe were 900 and 250 nM respectively. For EWS-FLI1 detection the following primers were designed:

sense 5'-TAGTTACCCACCCAAACTGGAT-3'
 antisense 5'-GGGCCGTTGCTCTGTATTCTTAC-3'
 probe 5'-FAM-CAGCTACGGGCAGCAGAACCCTTCTT-TAMRA -3'

Inventoried TaqMan® Gene Expression Assays were used for other genes (Tab. 6):

Table 6: List of TaqMan® primer assays

Gene	Assay ID
GPR64	Hs00971391_g1
CHM1	Hs00170877_m1
EZH2	Hs00544830_m1
STEAP	Hs00185180_m1
ITM2A	Hs01011360_g1
LIPI	Hs01017703_m1
GAPDH	Hs99999905_m1

For all assays the same program was used (Tab. 7):

Table 7: Temperature profile and repetitions of real time PCR in 7300 Real-Time PCR System

Stage 1	Stage 2	Stage 3	
Repetition: 1	Repetition: 1	Repetition: 40	
50.0 °C	95.0 °C	95.0 °C	60.0 °C
2:00 min	10:00 min	0:15 min	1:00 min

3.12 Minipreparation of plasmid DNA

Isolation of plasmid DNA from *Escherichia coli* was performed with the NucleoSpin® Plasmid Kit from Macherey-Nagel according to manufacturer's instructions.

Briefly, a single colony from a freshly streaked bacterial plate was picked and used to inoculate 5 ml of LB medium supplemented with an appropriate antibiotic. The culture was incubated overnight with shaking. Bacteria were harvested and centrifuged at 11.000 × g for 30 seconds at 4 °C to pellet the bacterial cells, the supernatant was discarded. The pellet was resuspended in 250 µl of resuspension buffer supplemented with RNase A. After vigorous vortexing 250 µl lysis buffer containing sodium hydroxide was added and mixed gently by inverting the tube. After five minutes of incubation at room temperature 300 µl neutralization buffer containing guanidine hydrochloride was added and the tube was mixed by inverting the tube. The suspension was then centrifuged at 11.000 × g in a microcentrifuge for 10 minutes at 4 °C. The supernatant was loaded into a NucleoSpin® column which was placed in a 2 ml collection tube and centrifuged at 11.000 × g for one minute at room temperature. The flow-through was discarded. The NucleoSpin® column was washed with 500 µl of preheated (50 °C) wash buffer containing guanidine hydrochloride and isopropanol, centrifuged as before and the flow-through discarded. The plasmid DNA bound to the silica membrane in the NucleoSpin® column was then eluted with 50 µl elution buffer. The flow-through containing the plasmid DNA was collected in a tube, the concentration measured via spectrophotometry, and the plasmid was analyzed by restriction enzymes.

Bacterial stocks containing correct plasmids were stored with 15 % glycerin. Those stocks were used to inoculate LB medium for Maxi prep (see 3.15).

3.13 Restriction analysis

To determine if the correct plasmid was obtained by the cloning strategy, plasmid DNA was analyzed by digesting it with restriction enzymes. The pattern of DNA fragments of different size present after agarose gel electrophoresis was compared to the pattern expected of the correct plasmid.

3.14 DNA agarose gel electrophoresis

Separation of DNA fragments was performed in 1.5 % agarose gel at 5 - 10 V / cm.

3 g agarose was dissolved in 200 ml TAE buffer, mixed, heated and after that 2 µl ethidium bromide was added before casting the gel.

The solution containing the DNA was loaded into the slots of the gel in a volume of 24 µl. At least 0.5 µg of DNA - diluted with H₂O if necessary - was used. 4 µl of 6 × Blue Juice Gel Loading Buffer was added. A 1 Kb DNA ladder was included as a size standard in electrophoresis. For extraction of DNA fragments from agarose gels, the desired fragments were cut from the gel after electrophoresis and purified using the QIAEX II Gel Extraction Kit according to manufacturer's instructions.

3.15 Maxipreparation of plasmid DNA

Isolation of plasmid DNA from *E. coli* was performed with the JETstar 2.0 Maxiprep Kit from Genomed according to manufacturer's instructions.

The isolation method was very similar to the miniprep method (see 3.12), only differing in scope. This method was used to obtain a large amount of known correct plasmid DNA.

3.16 *In vitro* Priming

Mature HLA-A*0201⁺ DCs were loaded with HLA-A*0201-binding Ewing Tumor-specific peptides. The DCs were pulsed with peptide at a concentration of 30 μ M for four hours and mixed every 20 minutes. DCs were washed three times to remove unbound peptide and were then irradiated with 35 Gy.

CD8⁺ T cells from an HLA-A*0201⁻ donor were stimulated with allogeneic HLA-A*0201⁺ DCs in 200 μ l of T cell medium (AIM-V, 20 % human serum, 2 mM L-glutamine, 50 μ g / ml Gentamicin) in a stimulator to responder rate of 1:20 (5 \times 10³ DCs / well : 10⁵ CD8⁺ T cells / well) in 96-well round-bottom plates. In the case of autologous *in vitro* priming stored autologous PBMC were primed. For priming, the T cells (PBMC) and DCs were co-cultured with 10 ng / ml IL-12 and 1000 U / ml IL-6 and restimulated with the same number of loaded DCs in the presence of 5 ng / ml IL-7 and 100 U / ml IL-2 after one week.

The proliferating T cells were pooled, counted and stained with CD8-FITC / Pentamer-PE for cell sorting. Specific T cells (double positive for CD8 and Pentamer-PE) were sorted and cloned by limiting dilution (see 3.17).

In the case of autologous *in vitro* priming T cells were not pooled but every well was screened by ELISpot for specific IFN γ release comparing interaction with T2 cells loaded with relevant and irrelevant peptide.

The expansion of the CTL clones was conducted in the presence of anti-CD3 (30 ng / ml), IL-2 (50 IU / ml), IL-15 (2 ng / ml), and irradiated lymphoblastoid cell lines (LCLs; 2.5 \times 10⁷) and PBMCs as feeder cells as previously described (20).

3.17 *Limiting Dilution*

After identifying peptide-specific T cells via ELISpot screening (autologous) or cell sorting (allorestricted) those T cell bulk cultures needed to be cloned by limiting dilution. T cells were counted and resuspended at concentrations of one T cell / well, five T cells / well and ten T cells / well. For every concentration two 96-well plates (round bottom) were filled with 200 μ l T cell medium / well. The cloning was conducted in the presence of anti-CD3 (30 ng / ml), IL-2 (50 IU / ml), IL-15 (2 ng / ml), and irradiated lymphoblastoid cell lines (LCLs; 1 \times 10⁵ /

well) and PBMCs pooled from three different healthy donors (5×10^4 / well) as feeder cells. Cytokines and 100 μ l medium were replaced after one week. Expanded T cells were tested in ELISpot for specificity.

3.18 ELISpot

The procedure takes three days. On day one the ELISpot plate is coated with the capture antibody.

Table 8: Antibodies used in ELISpot

Cytokine	Capture Antibody		Detection Antibody	
	Name	Concentration	Name	Concentration
IFN γ	1-D1K	10 μ g / ml	7-B6-1, biotinylated	2 μ g / ml
Perforin	Pf-80 / 164	20 μ g / ml	Pf-344, biotinylated	4 μ g / ml
Granzyme B	GB10	10 μ g / ml	GB11, biotinylated	2 μ g / ml

The wells of the ELISpot plate were coated over night (4 °C) with 50 μ l of capture antibody solution in 1 \times PBS.

On day two the plates were washed four times with sterile PBS, 200 μ l per well, then filled with T cell medium (150 μ l / well) to block unspecific binding for 60 minutes at 37 °C.

T cells were washed and counted. Per well 1.000 T cells were allocated. Per well 20.000 target cells were allocated. If peptide-loaded T2 cells were used, they were incubated with peptide for at least two hours at 37 °C. If Ewing Tumor cells were used, they were incubated with 100 U / ml IFN γ 48 h prior to being used in the experiment.

After blocking the T cells were pipetted into the wells carefully, in 50 μ l T cell medium per well and incubated for 30 minutes at 37 °C. The target cells were washed (pulsed T2 cells were washed three times), resuspended in T cell medium (50 μ l / well) and pipetted carefully into the wells to avoid dispersing

the T cells clinging to the membrane. The plates were then incubated for 20 hours at 37 °C to allow time for cytokine release and capture.

On day three the plates were washed six times with wash buffer (PBS / 0.05 % Tween).

The detection antibody was diluted with PBS / 0.5 % BSA to a volume of 200 µl per well and pipetted on to the plate. A two hour incubation at 37 °C followed. The plates were washed six times again and the Streptavidin-Horse Radish Peroxidase was diluted with PBS / 0.5 % BSA to a volume of 200 µl per well. The plate was incubated shielded from light at room temperature for one hour. During this period the development solution was prepared. To remove possible aggregates the solution was passed through a 0.45 µM filter. The H₂O₂ was added right before usage. After incubation with the conjugated enzyme the plates were washed three times with wash buffer and three times with PBS. 100 µl developing solution was then added per well. The reaction was stopped when spots were easily detected by eye after about four to eight minutes, the plates washed, dried and read in the ELISpot reader.

When the ELISpot method was used to determine specific cytotoxicity by measuring Granzyme B, the number of T cells was titrated. The same number (20.000) of target cells was used as in the Interferon-γ and Perforin-ELISpots. The highest effector / target ratio was 10:1, which meant 200.000 T cells per well. The effector / target ratio was varied by a twofold serial dilution:

Table 9: Effector / target titration of Granzyme B ELISpot

10:1	5:1	2.5:1	1.25:1	0.625:1	0.3125:1	0.15625:1	empty
200.000	100.000	50.000	25.000	12.500	6.250	3.125	-
20.000	20.000	20.000	20.000	20.000	20.000	20.000	20.000

3.19 CTL expansion

Cloned CTLs that passed the specificity screen were expanded for 10 – 14 days and stored in aliquots of 1×10^6 / 100 μ l T cell freezing medium.

From 5×10^4 to 1×10^5 T cells were resuspended in 25 ml T cell medium in 50 ml cell culture flasks. The expansion was conducted in the presence of anti-CD3 (30 ng / ml), IL-2 (50 IU / ml), IL-15 (2 ng / ml), and irradiated lymphoblastoid cell lines (LCLs; 5×10^6 / flask) and PBMCs pooled from three different healthy donors (2.5×10^7 / flask) as feeder cells. Cytokines were added one day after start of the expansion and added every other day. Part of the medium was replaced whenever necessary.

3.20 *In silico* prediction of peptide epitopes

To find immunogenic epitopes derived from the protein sequence of the EFT-specific target genes several web-based *in silico* prediction methods were used:

1. SYFPEITHI:

<http://www.syfpeithi.de/Scripts/MHCServer.dll/EpitopePrediction.htm>

SYFPEITHI is a free web based service that provides prediction of the ligation strength of short peptides to a defined HLA type. The algorithms used are based on the book "MHC Ligands and Peptide Motifs" by Rammensee *et al.*. The probability of being processed and presented is given in order to predict T cell epitopes (83).

2. The Bioinformatics & Molecular Analysis Section (BIMAS):

http://www-bimas.cit.nih.gov/molbio/hla_bind/

The BIMAS web site provides a free web based prediction algorithm of binding probabilities of peptide octamers, nonamers and decamers to HLA class I molecules (84).

3. NetCTL 1.2:

<http://www.cbs.dtu.dk/services/NetCTL/>

NetCTL 1.2 server predicts CTL epitopes in protein sequences. Additionally to prediction of binding probability and strength of peptides to HLA molecules, this free web based service predicts probabilities of proteasomal cleavage and transport of the cleaved peptides into the endoplasmatic reticulum by TAP (85).

The scores of each predicted epitope was compared and the best scoring candidates were ordered.

3.21 HLA-A*0201 / peptide-binding assay

Peptides for the selected epitopes were ordered and tested for their binding affinity to HLA-A*0201 molecules using the human antigen processing-defective cell line T2 (86, 87).

T2 cells express a very low level of HLA-A*0201 molecules under normal culture conditions, but they express the molecules at much higher levels when allowed to bind with appropriate peptides that stabilize the HLA-A*0201 molecule. Thus, up-regulation of peptide-induced HLA-A*0201 expression in T2 cells can be regarded as an indication of an HLA-A*0201-restricted epitope (88).

T2 cells were incubated overnight for 16 hours with each peptide at concentrations of 50 μ M and 100 μ M. Good binding peptides were tested over a range of peptide concentrations from 0.1 – 100 μ M. T2 cells were washed, counted and resuspended in T cell medium to a concentration of 1×10^6 / ml. For every peptide concentration to be tested three wells of a 96-well plate were filled with 300 μ l cell suspension. For negative control two triplets were incubated without peptide, for positive control, one triplet was incubated with 50 μ M influenza peptide (GILGFVFTL), and another triplet with 100 μ M influenza peptide.

After incubation the cells were washed three times to get rid of unbound peptide and stained with an HLA-A*0201-FITC antibody for flow cytometric

determination of HLA expression which correlates with the amount of peptide bound.

Relative binding affinity (RA) was determined by dividing the value of the fluorescence intensity of the peptide at a certain concentration by the fluorescence intensity of the T2 cell line without peptide.

$$RA = \frac{\text{fluorescence intensity (median) with peptide}}{\text{fluorescence intensity (median) without peptide}}$$

A good binding epitope should have a comparable RA at 100 μ M to the positive control influenza peptide.

3.22 V β analysis of TCR repertoire

To determine the status of clonality of T cell clones the IOTest® Beta Mark Kit was used.

This kit is designed for flow cytometric determination of the TCR V β repertoire of human T lymphocytes. The kit contains eight vials. Each vial contains three monoclonal antibodies specific for three different V β families. The kit allows testing for 24 different V β specificities (see Tab. 10), which covers about 70 percent of the normal human TCR V β repertoire. One antibody is conjugated with the fluorophore FITC, a second with the fluorophore PE. A third antibody is conjugated with a balanced mix of both fluorophores. This combination reduces the amount of cells needed and the time required for obtaining the results. The staining protocol corresponds to the protocol described in 3.7.

Table 10: V β families and their respective fluorochromes used to determine clonality of T cell clones

Tube	Vβ	Fluorochrome
A	V β 5.3	PE
	V β 7.1	PE+FITC
	V β 3	FITC
B	V β 9	PE
	V β 17	PE+FITC
	V β 16	FITC
C	V β 18	PE
	V β 5.1	PE+FITC
	V β 20	FITC
D	V β 13.1	PE
	V β 13.6	PE+FITC
	V β 8	FITC
E	V β 5.2	PE
	V β 2	PE+FITC
	V β 12	FITC
F	V β 23	PE
	V β 1	PE+FITC
	V β 21.3	FITC
G	V β 11	PE
	V β 22	PE+FITC
	V β 14	FITC
H	V β 13.2	PE
	V β 4	PE+FITC
	V β 7.2	FITC

3.23 Generation of EBV-immortalized B cells (LCLs)

Lymphoblastoid cell lines (LCLs) are human B cells latently infected and immortalized by Epstein-Barr virus (EBV).

PBMC were isolated as described in 3.2. 100 μ l of cell suspension containing 1×10^6 PBMC were seeded into a well of a 96-well flat bottom plate. 100 μ l of filtered supernatant containing mini-EBV was added to each well containing PBMC.

A mini-EBV plasmid consists of less than half the EBV genome and is unable to cause virus production, but still immortalizes B cells *in vitro*. Mini-LCLs are identical to LCLs in terms of latent cycle protein expression, antigen presentation, and T-cell co-stimulation, but they do not express lytic cycle proteins of EBV and do not release viral particles (89). The supernatant was provided by Drs. Josef Mautner and Andreas Moosmann, Helmholtz-Zentrum München.

After two days approximately 150 μ l of medium was removed and substituted with fresh LCL medium. 1 μ l of Cyclosporin A (100 μ g / ml) was added per well to inhibit T cell activation. Whenever the medium turned yellow 100 μ l media was exchanged with LCL medium containing 1 μ g / ml Cyclosporin A. Within the next two weeks, most of the PBMC disintegrated while EBV-infected B cells formed clusters of irregularly shaped blasts. Once they reached density of approximately $5 \times 10^4 - 1 \times 10^5$ / well (2 – 4 weeks) they were split 1:2 into a second well of the plate and so on to expand them. LCLs stop growing when the density drops below 1×10^5 / ml, so they should never be split too harshly.

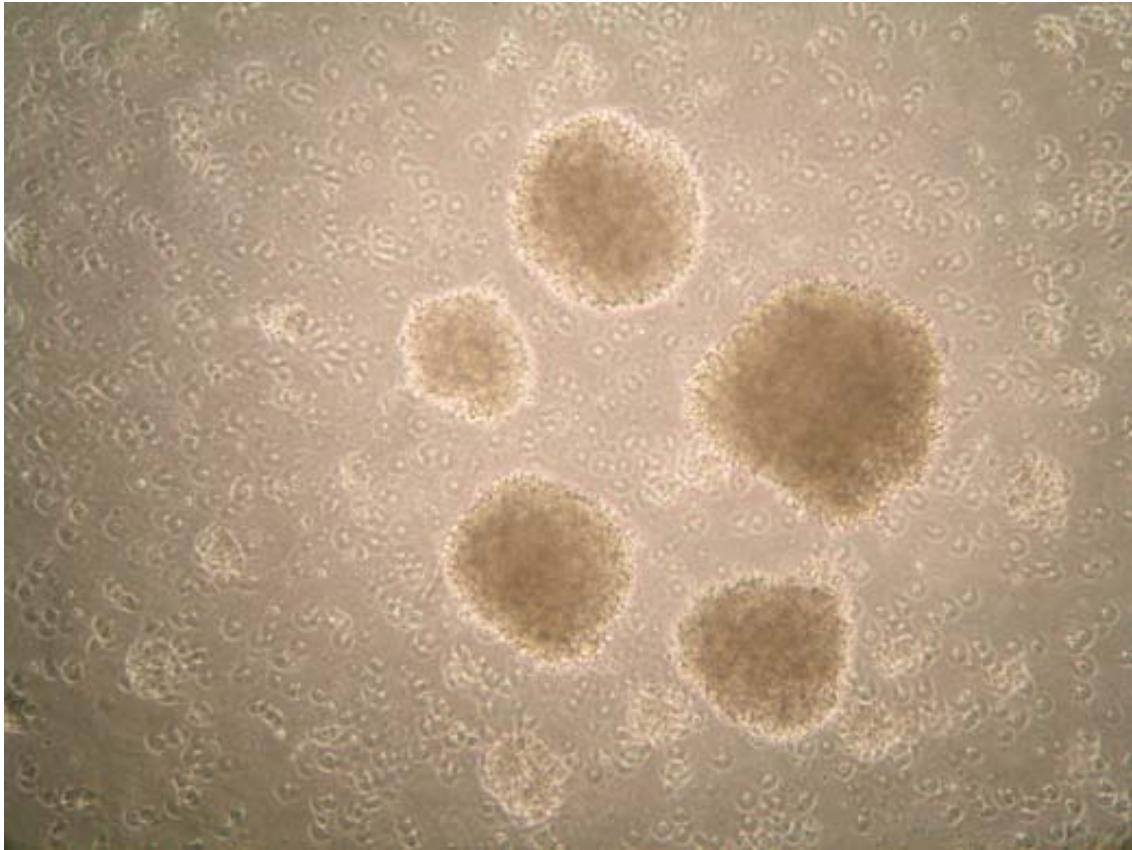


Figure 5: Growing LCL cluster; cells in suspension as seen under the microscope at 10 × magnification

Fig. 5 shows growing clusters of immortalized B cells in a well of a 96-wells round bottom plate.

3.24 Up-regulation of HLA expression in EFT cell lines by $IFN\gamma$

Human leukocyte antigen (HLA) molecules expressed on the cell surface are required for antigen presentation to T cells. HLA class I antigens are crucial for recognition of tumor cells by tumor-specific CTLs, as tumor-specific antigens are often intracellular proteins expressed in association with membrane-bound HLA class I molecules. Loss or down-regulation of HLA class I antigens therefore represents a way by which tumors can escape T cell surveillance (90). The cause of loss or down-regulation of HLA class I can be absence of β_2M , absence of TAP, large or partial deletions, point mutations or transcriptional down-regulation, among others.

If the cause for low or absent HLA class I expression is transcriptional down-regulation instead of loss of an essential gene function HLA class I expression

in cell lines can be restored (91) by adding 100 U / ml IFN γ to the culture medium for 48 hours.

3.25 Peptide titration assay

The peptide titration assay was basically an IFN γ ELISpot as described in 3.18. T2 cells were pulsed with different amounts of peptide. Peptide concentration ranged from 10^{-12} M (1 pM) to 10^{-6} M (1 μ M) and included a control of T2 cells without peptide. T2 cells were pulsed as described for two hours at 37 °C and subsequently washed three times.

3.26 Statistical analysis

Error bars represent the mean \pm standard deviation of triplicates if not stated otherwise. Statistical significance of differences was determined by independent two-sample t-test. Differences were considered statistically significant for $P < 0.05$. Statistical analyses were performed using Microsoft Excel.

4 Results

4.1 mRNA Chip

For the identification of EFT-specific markers, we used customized microarrays (EOS-Hu01) containing 35,356 oligonucleotide probe sets for the interrogation of a total of 25,194 gene clusters. In addition to 11 EFT samples, samples from 133 normal tissues were analyzed on the same microarray (EOS-Hu01). This was published by Staeger *et al.* from our group in Cancer Research in 2004 (65). As shown in Fig. 6 we selected six genes as potential EFT-specific or EFT-associated antigens.

4.1.1 CHM1

Chondromodulin I (OMIM: *605147) is a cartilage-specific glycoprotein that stimulates the growth of chondrocytes and inhibits the tube formation of endothelial cells (92).

It was found to be significantly over-expressed in EFT tissue samples and cell lines compared to samples derived from normal body tissue.

4.1.2 GPR64

G Protein-coupled Receptor 64 (OMIM: *300572) contains seven transmembrane-spanning domains typical of G protein-coupled receptors. It has an extended extracellular N terminus with similarity to highly glycosylated cell surface molecules such as mucin. The transcript is abundant in the epididymis, but not found in any other tissue examined (93).

It was found to be significantly over-expressed in EFT tissue samples and cell lines compared to samples derived from normal body tissue.

4.1.3 EZH2

Enhancer of Zeste, Drosophila, Homolog 2 (OMIM: *601573) is a member of the Polycomb-group (PcG) family. PcG family members form protein complexes, which are involved in maintaining the transcriptional repressive

state of genes over successive cell generations. EZH2 is over-expressed in many cancer types (76, 94).

EZH2 is also present in the bone marrow, testes and thymus.

4.1.4 STEAP

Six-Transmembrane Epithelial Antigen of Prostate (OMIM: *604415) is highly expressed in advanced prostate cancer. It encodes a 339-amino acid protein with six potential membrane-spanning regions flanked by hydrophilic N- and C-terminal domains. This structure suggested a potential function as a channel or transporter protein. This gene is up regulated in multiple cancer cell lines, including EFT (95).

STEAP, as previously published by Hubert *et al.* in 1999, is highly expressed in prostate tissue and also in tissue samples derived from EFT.

4.1.5 ITM2A

Integral membrane protein 2A (OMIM: *300222) was found to be expressed in human CD34⁺ hematopoietic stem / progenitor cells (96).

ITM2A was also found to be expressed in tissue samples derived from EFT and numerous other tissue samples from the normal body atlas. It is not an EFT-specific antigen, but an EFT associated antigen.

4.1.6 LIPI

Lipase I (OMIM: *609252) is expressed in EFT samples. Expression of LIPI in normal tissues was restricted to testis and thyroid. However, expression in these tissues was low compared with EFT (97).

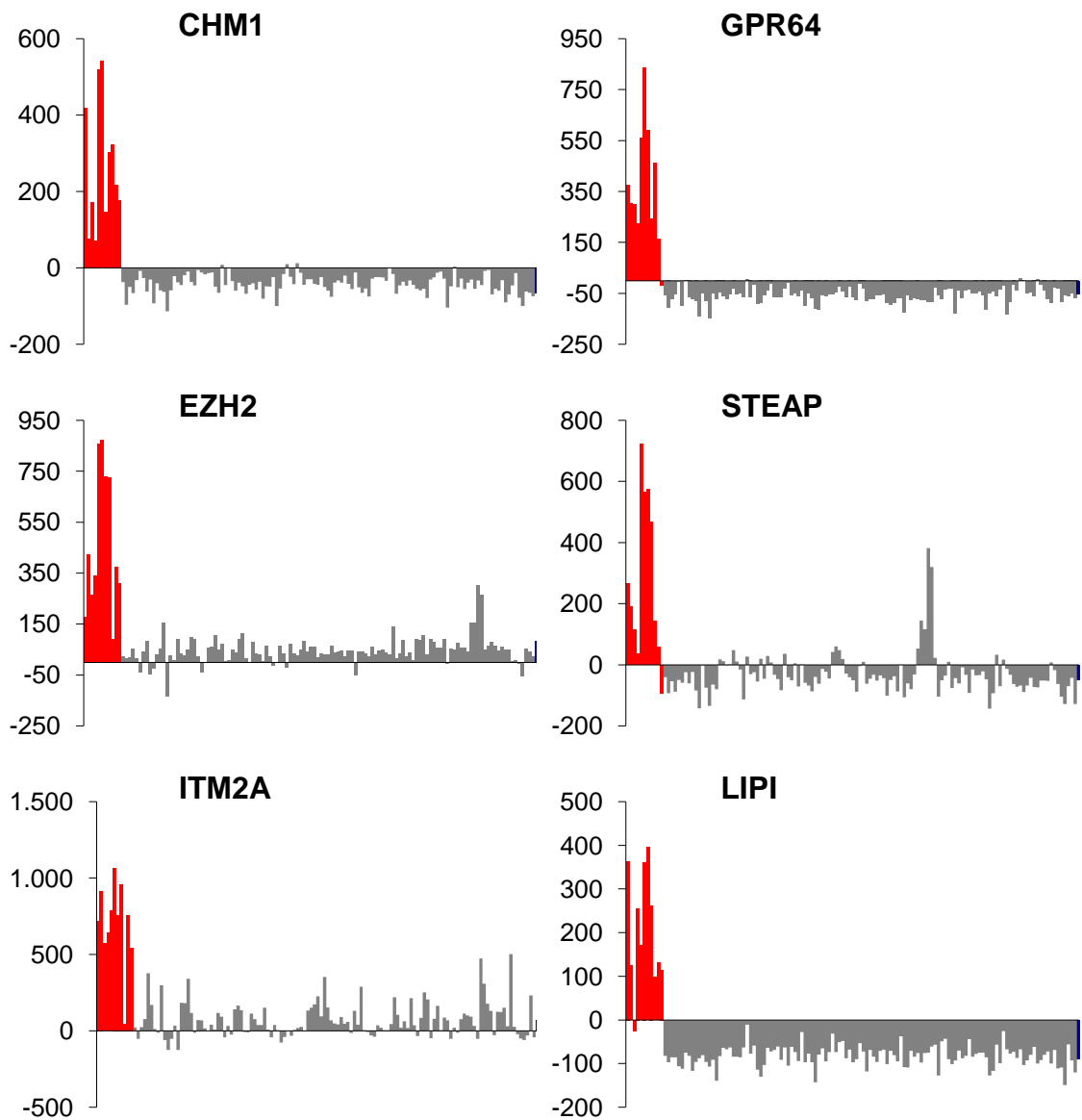


Figure 6: Gene expression on mRNA level in EFT tissue samples (red bars), normal body tissue (gray bars) and fetal tissue (blue bars); ordinate is fluorescence intensity

4.2 Real-Time PCR

To evaluate the observed expression profile of the microarray data the mRNA expression in EFT cell lines in comparison to neuroblastoma and pediatric leukemia (cALL lines) was analyzed (see Fig. 7).

4.2.1 CHM1

CHM1 is expressed in some EFT cell lines, especially in SBSR-AKS and A673. It is also present in the EFT cell line MHH-ES1 and the neuroblastoma cell line MHH-NB11.

4.2.2 GPR64

GPR64 is expressed in most EFT cell lines. It is absent in cALL cell lines and neuroblastoma cell lines.

4.2.3 EZH2

EZH2 is expressed in all EFT cell lines. It is also present in cALL cell lines and neuroblastoma cell lines, albeit at a lower level.

4.2.4 STEAP

STEAP is expressed in all EFT cell lines, albeit at different levels. It is absent in all other tested cell lines.

4.2.5 ITM2A

ITM2A is expressed in all EFT cell lines, albeit at different levels. It is absent in all other tested cell lines.

4.2.6 LIPI

LIPI is expressed in all EFT cell lines. It is absent in all other tested cell lines.

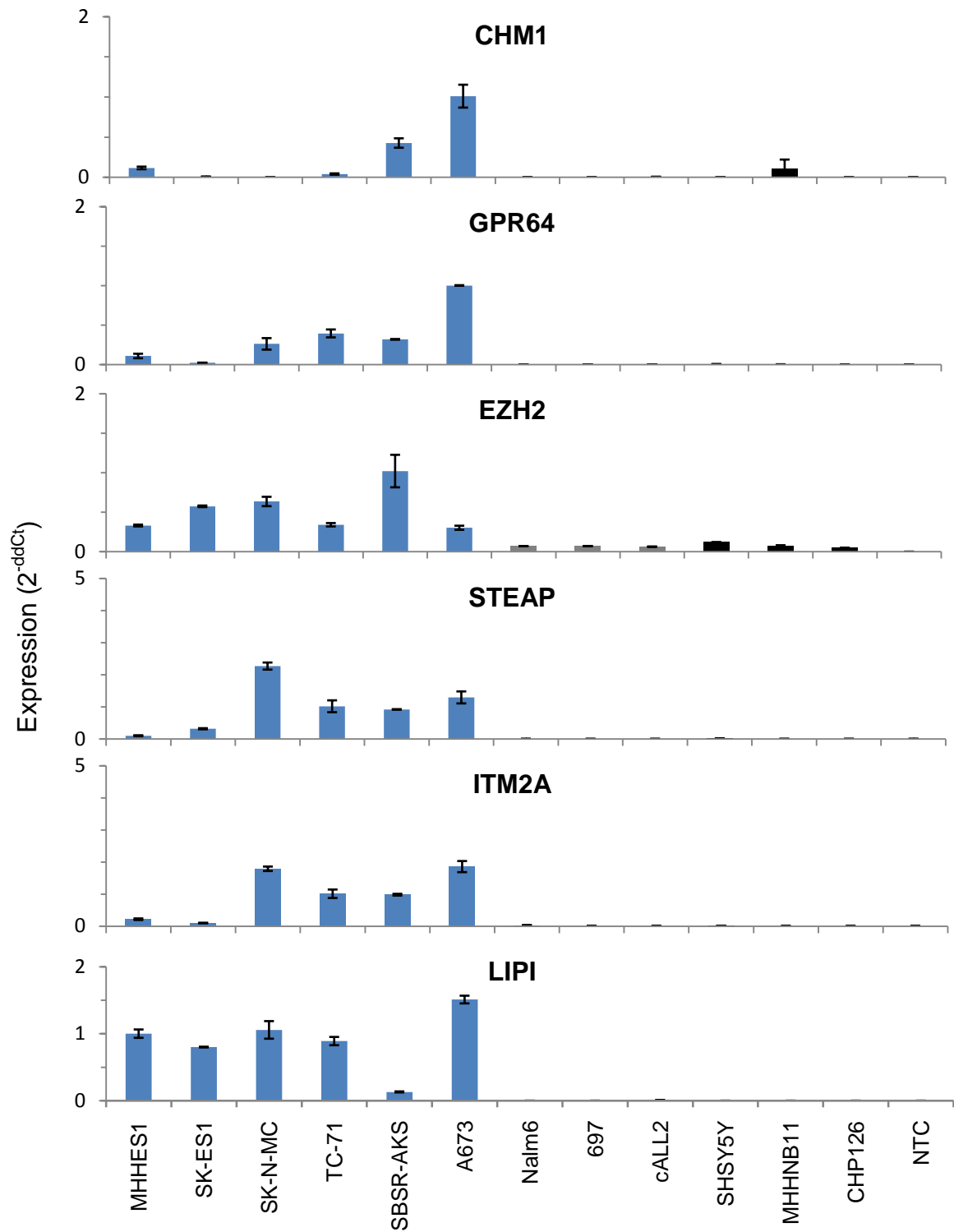


Figure 7: mRNA expression of target in genes in tumor cell lines: EFT cell lines (blue bars); cALL (gray bars); neuroblastoma (black bars); NTC: non template control (water); note the predominant expression in EFT lines.

We were trying to find EFT cell lines which expressed the antigens at a high level specifically and chose SBSR-AKS, TC-71 and A673 for subsequent experiments.

4.3 HLA-A*0201 status of EFT cell lines

Since this work focuses on HLA-A*0201-binding peptide epitopes the HLA-A*0201 status of EFT lines was evaluated by flow cytometry (Fig. 8).

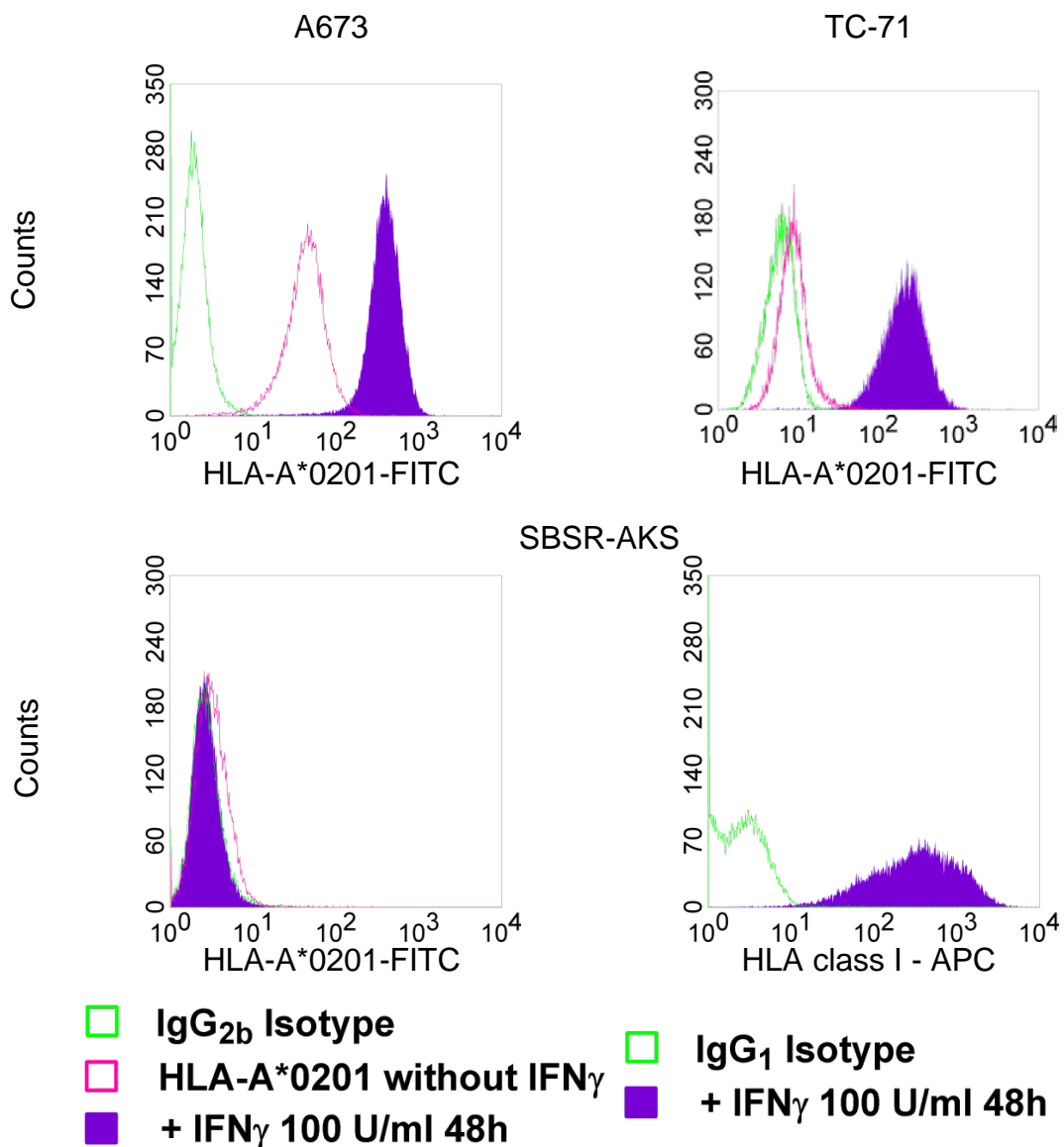


Figure 8: HLA-A*0201 status of the EFT cell lines A673, TC-71 and SBSR-AKS; cell lines were incubated with IFN_γ for 48 hours prior to analysis to up-regulate HLA expression

4.3.1 A673

The EFT cell line A673 was tested by flow cytometry for HLA-A*0201 expression without IFN γ and after 48 hours of culturing the cell line in the presence of 100 U / ml IFN γ .

A673 is expressing HLA-A*0201. The expression can be up-regulated by adding 100 U / ml IFN γ to the cell culture 48 hours prior to using the cell line in assays.

4.3.2 TC-71

The EFT cell line TC-71 was tested by flow cytometry for HLA-A*0201 expression without IFN γ and after 48 hours of culturing the cell line in the presence of 100 U / ml IFN γ .

TC-71 is expressing HLA-A*0201. The expression needs to be up-regulated by adding 100 U / ml IFN γ to the cell culture 48 hours prior to using the cell line in assays.

4.3.3 SBSR-AKS

The EFT cell line SBSR-AKS was tested by flow cytometry for HLA-A*0201 expression without IFN γ and after 48 hours of culturing the cell line in the presence of 100 U / ml IFN γ .

SBSR-AKS is not expressing HLA-A*0201. The expression cannot be up-regulated by adding 100 U / ml IFN γ to the cell culture 48 hours prior to using the cell line in assays. To show the efficacy of up-regulation of HLA class I expression in this cell line, it was tested for HLA class I expression, additionally. HLA class I is up-regulated by adding IFN γ to the cell culture. This confirms that the EFT cell line SBSR-AKS is not expressing HLA-A*0201.

4.4 Peptide-binding assay

HLA-A*0201-specific peptides were selected by *in silico* prediction (see 2.9, Tab. 3). To confirm good binders of selected peptides they were pulsed onto T2 cells and compared to influenza peptide (GILGFVFTL) as a positive control for this assay (see 3.21). The influenza peptide was used at high concentrations to ensure saturation.

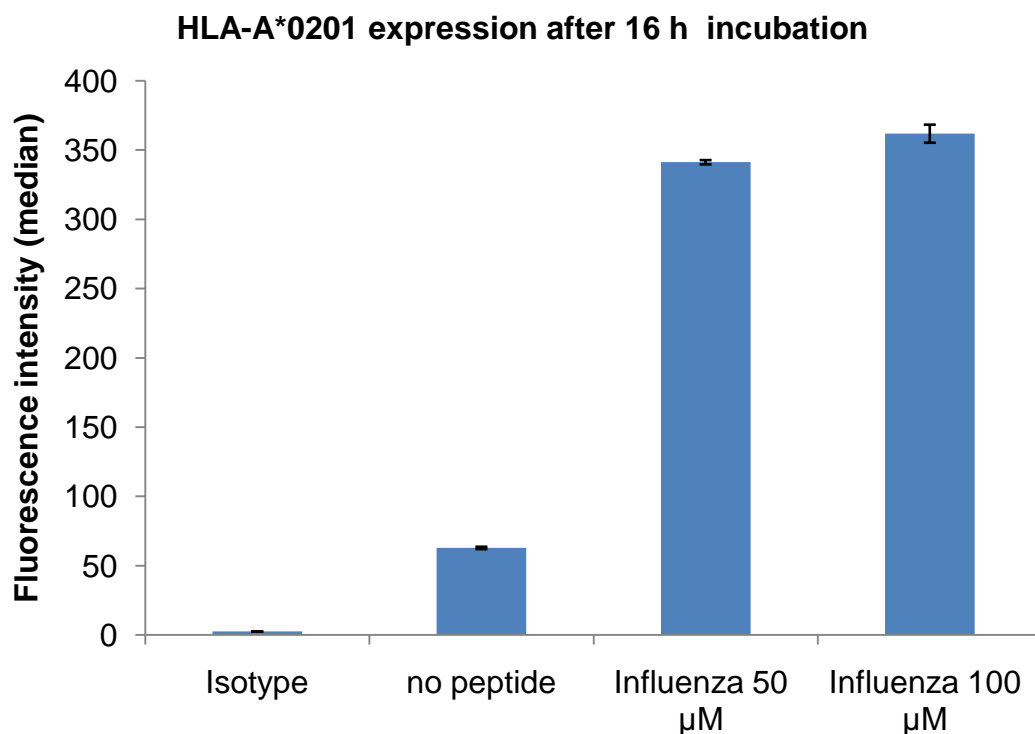


Figure 9: Fluorescence intensity representing binding affinity of influenza peptide

The RA was calculated as described in 3.21. T2 cells express a low level of HLA-A*0201 even without pulsed peptide.

Table 11: RA of influenza peptide positive control

Concentration [µM]	Fluorescence intensity (median)	RA
0	62.93	1
50	341.36	5.42
100	361.96	5.75

The binding affinities of the other peptides was compared to the RA of the influenza peptide at 100 μ M and shown in percentages (Fig. 10).

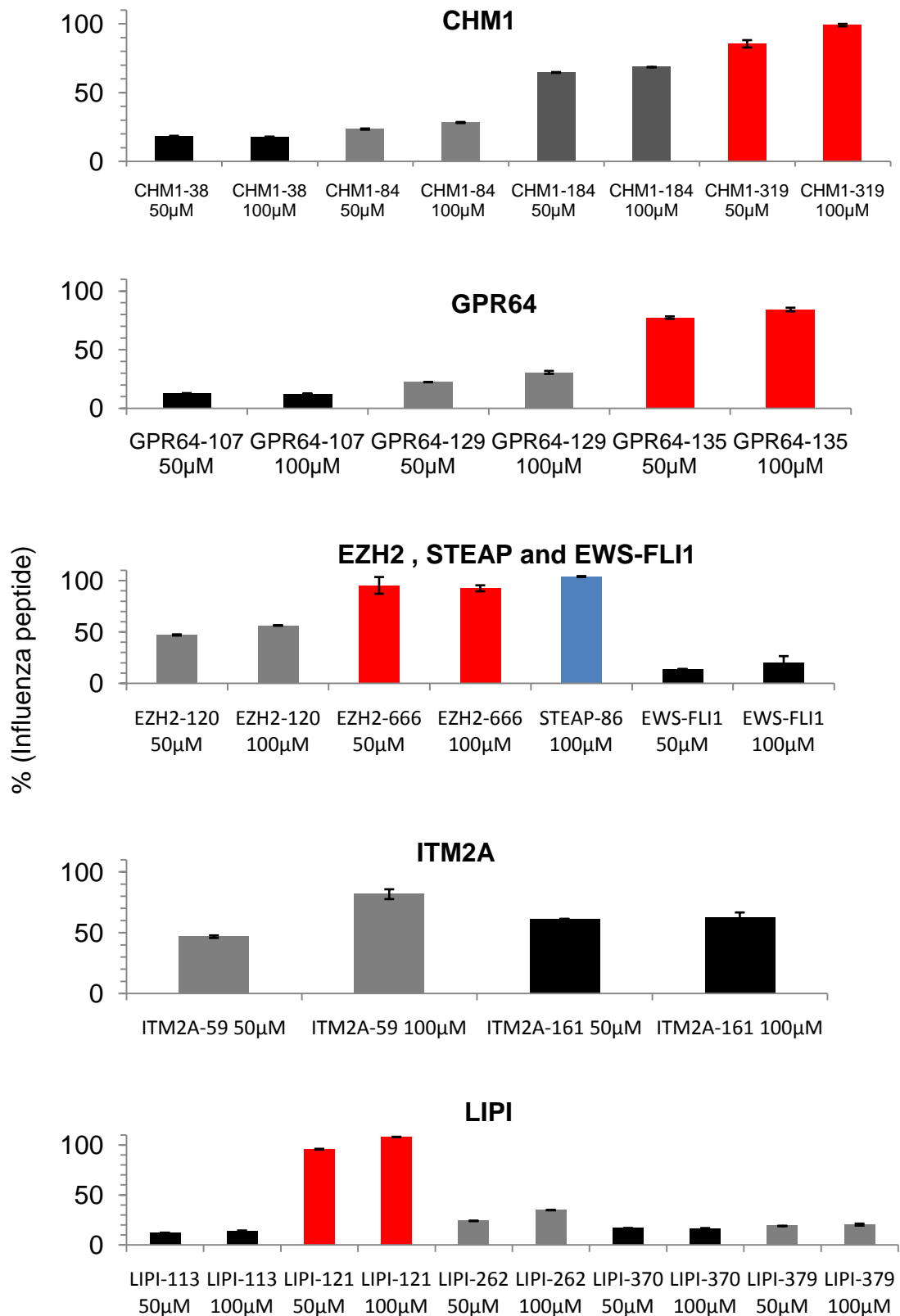


Figure 10: RA of EFT-specific peptides expressed in percentages of the influenza peptide

Raw data for these peptides can be found in Tab. 12.

Table 12: Peptide sequence, position and relative affinity

Gene	HLA-Allele	Sequence	Position of first N-terminal aa	RA [100µM]	% Influenza peptide [100µM]
CHM1	A*0201	RLLGVGAVV	38	0.97	17.86
	A*0201	KLQDGSMEI	84	1.54	28.26
	A*0201	FLSSKVLEL	184	3.73	68.54
	A*0201	VIMPCSWWV	319	5.40	99.11
EZH2	A*0201	FMVEDETVL	120	3.08	56.49
	A*0201	YMCSFLFNL	666	5.05	92.69
EWS-FLI1	A*0201	GQQNPSYDSV	-	1.08	13.94
GPR64	A*0201	GTLTGVLSSL	107	0.68	12.41
	A*0201	TLSETYFIM	129	1.67	30.67
	A*0201	FIMCATAEA	135	4.59	84.30
ITM2A	A*0201	GLSFILAGL	59	4.46	81.78
	A*0201	YLMPLNTSI	161	3.41	62.52
Influenza (FLU)	A*0201	GILGFVFTL	-	5.75	100.00
LIPI	A*0201	WLQNFVRIL	113	0.76	14.02
	A*0201	LLNEEDMNV	121	5.91	108.43
	A*0201	SIFSGIQFI	262	1.90	34.91
	A*0201	TMDGFSFSF	370	0.90	16.55
	A*0201	KLLNQLGMI	379	1.12	20.47
STEAP	A*0201	FLYTLLREV	86	5.67	104.13

4.4.1 CHM1

Four different peptides derived from the protein sequence of CHM1 were selected, ordered and tested for relative binding affinity to HLA-A*0201.

CHM1-38 and CHM1-84 were identified as non-binding peptides. CHM1-184 may be a moderate binder; CHM1-319 is a strong binder comparable to the influenza peptide (see Fig. 10).

4.4.2 GPR64

Three different peptides derived from the protein sequence of GPR64 were selected, ordered and tested for relative binding affinity to HLA-A*0201.

GPR64-107 and GPR64-129 were identified as non-binding peptides. GPR64-135 is a strong binder comparable to the influenza peptide (see Fig. 10).

4.4.3 EZH2

Two different peptides derived from the protein sequence of EZH2 were selected, ordered and tested for relative binding affinity to HLA-A*0201.

EZH2-120 was identified as weak binding peptide. EZH2-666 is a strong binder comparable to the influenza peptide (see Fig. 10).

4.4.4 STEAP and EWS-FLI1

One peptide derived from the protein sequence of STEAP was selected, ordered and tested for relative binding affinity to HLA-A*0201. Additionally, one peptide derived from the protein sequence of the fusion region of EWS-FLI1 was selected, ordered and tested for relative binding affinity to HLA-A*0201.

STEAP-86 is a strong binder comparable to the influenza peptide. The EWS-FLI1 peptide was a non-binding peptide. No HLA-A*0201-binding peptide derived from the fusion region of EWS-FLI1 was found. This confirms the data published by Meyer-Wentrup *et al.* in 2005 (66) (see Fig. 10).

4.4.5 ITM2A

Two different peptides derived from the protein sequence of ITM2A were selected, ordered and tested for relative binding affinity to HLA-A*0201.

ITM2A-59 and ITM2A-161 were identified as moderate to strong binders comparable to the influenza peptide (see Fig. 10).

4.4.6 LIPI

Five different peptides derived from the protein sequence of LIPI were selected, ordered and tested for relative binding affinity to HLA-A*0201.

LIPI-113, LIPI-262, LIPI-370 and LIPI-379 were identified as non-binding peptides. LIPI-121 is a strong binder comparable to the influenza peptide (see Fig. 10).

4.4.7 Detailed peptide-binding assay

For strong binding peptides CHM1-319 and EZH2-666 a more detailed assay was performed with peptide concentration ranging from 0.1 μM to 100 μM (see 3.21). Included in this assay was the influenza peptide as positive control and the non-binding peptide CHM1-38 as negative control.

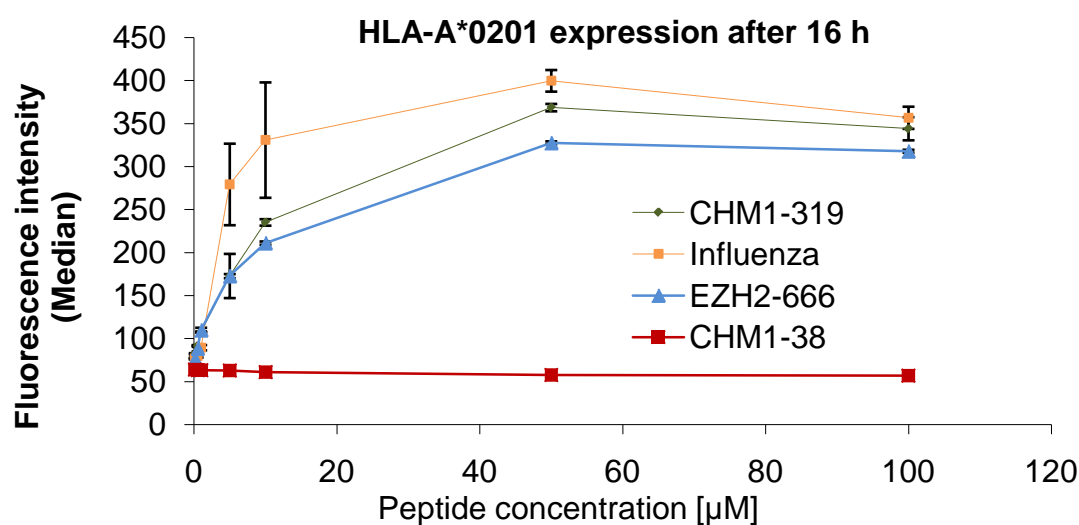
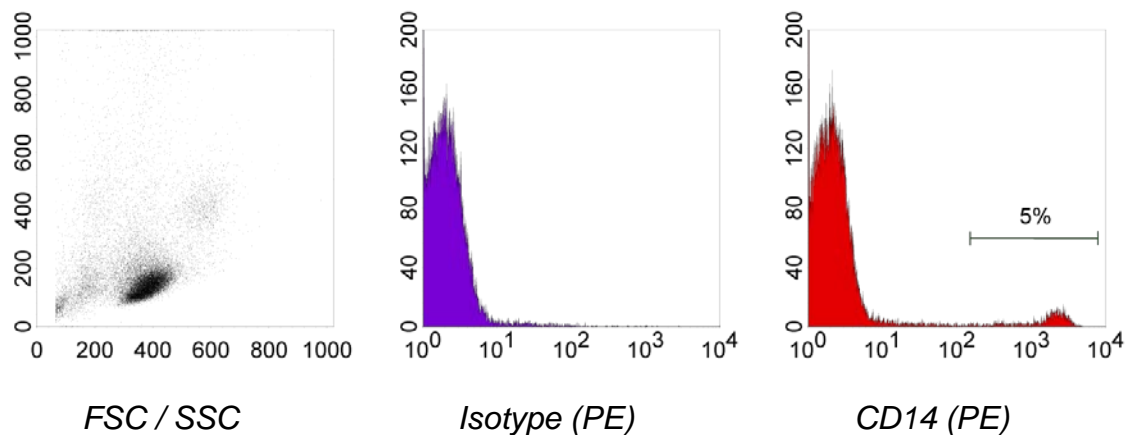


Figure 11: Fluorescence intensity representing relative affinity of CHM1-319 and EZH2-666; as positive control the influenza peptide is included; CHM1-38 is an example of a non-binding peptide

4.5 CD14 selection

Dendritic cells were generated from CD14⁺ PBL from healthy donors. The immuno-magnetic selection was controlled by flow cytometry. The cells were stained with CD14-PE antibody before and after separation.

Pre-selection



Post-selection

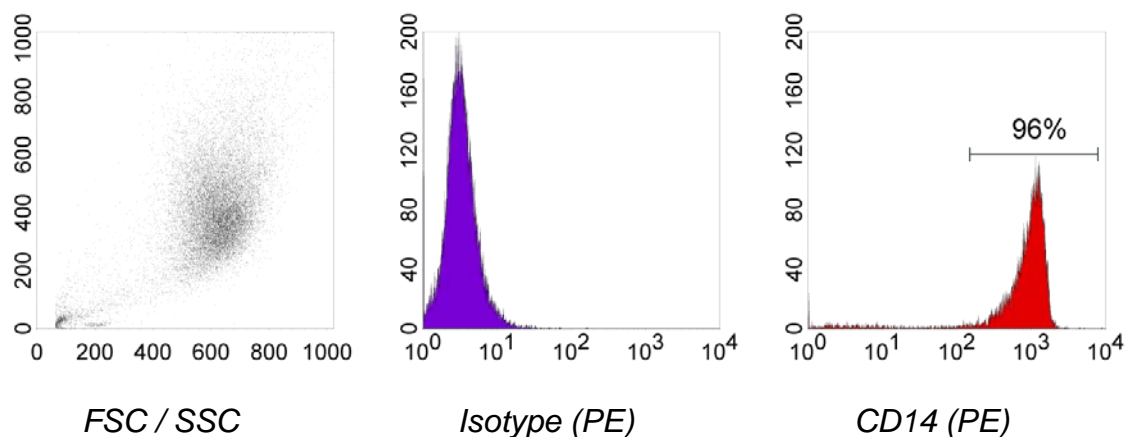


Figure 12: Flow cytometric control of immuno-magnetic CD14⁺ positive selection; ordinate of dot plots (left) was SSC, abscissa was FSC; ordinate for the histograms was event count

Fig. 12 is a representative example of all performed CD14 selections.

The positive fraction was very pure (> 95 %). Only pure CD14⁺ cells were used to generate DCs.

4.6 Dendritic cells

Dendritic cells were generated from the selected CD14⁺ cells as described (see 3.3 and 3.5). Cells were evaluated microscopically (Fig. 13) and by flow cytometry (Fig. 14).

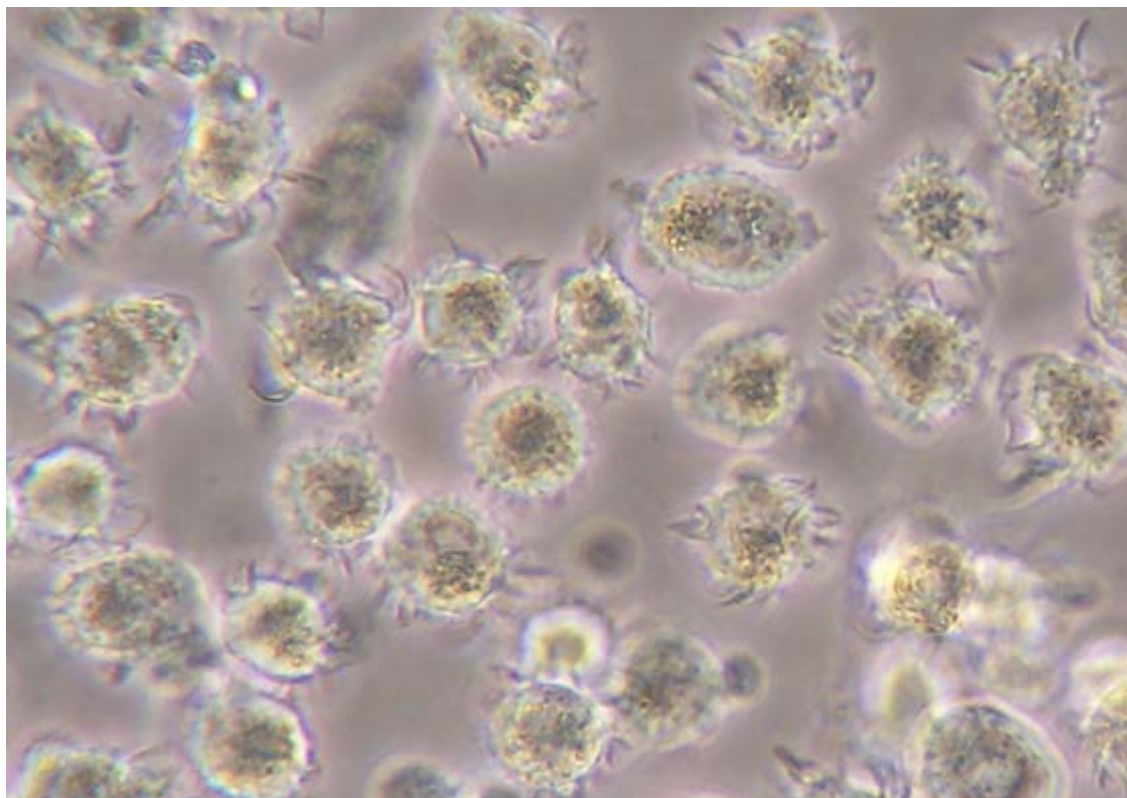


Figure 13: Mature DC, 10x (detail)

Fig. 13 shows mature DC displaying the characteristic fuzzy ball phenotype.

To control for maturity markers the DCs were stained for HLA-DR, CD86 and CD83.

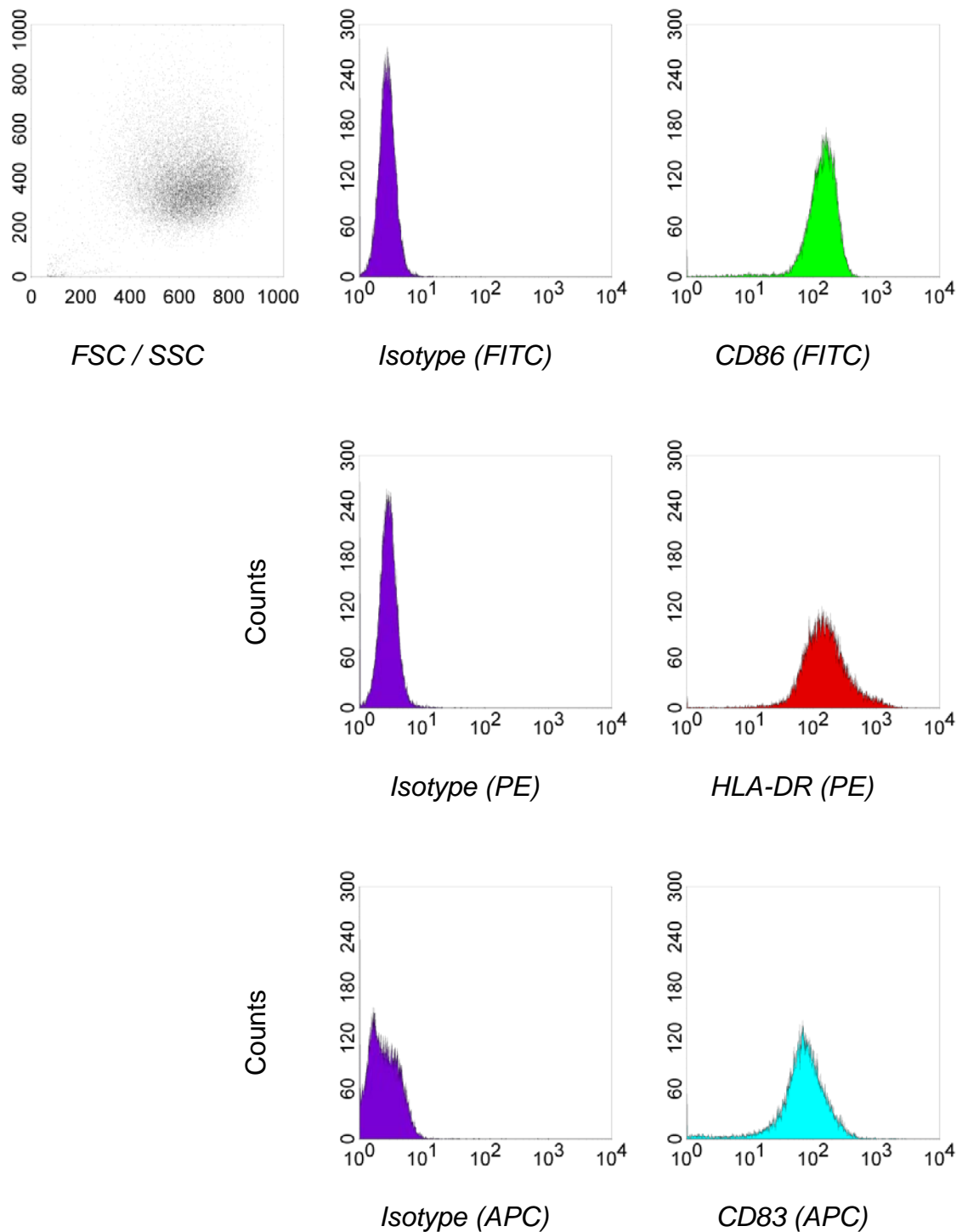


Figure 14: Markers of matured DCs; ordinate of dot plot (upper left) was SSC, abscissa was FSC; ordinate for the histograms was event count

Fig. 14 is a representative example of mature DC stained for the maturity markers CD86, HLA-DR and CD83. Only DCs that showed this maturity

phenotype cytometrically and microscopically (Fig. 13) were used in subsequent experiments.

4.7 CD8 selection

CD8⁺ T cells used for IVP were isolated from PBL from healthy donors. The immuno-magnetic untouched negative selection was controlled by flow cytometry. The cells were stained with CD8-PE antibody and CD3-FITC antibody before and after separation. The CD3-FITC antibody was included to show the effect of the selection on the whole T cell population in the sample.

Pre-selection

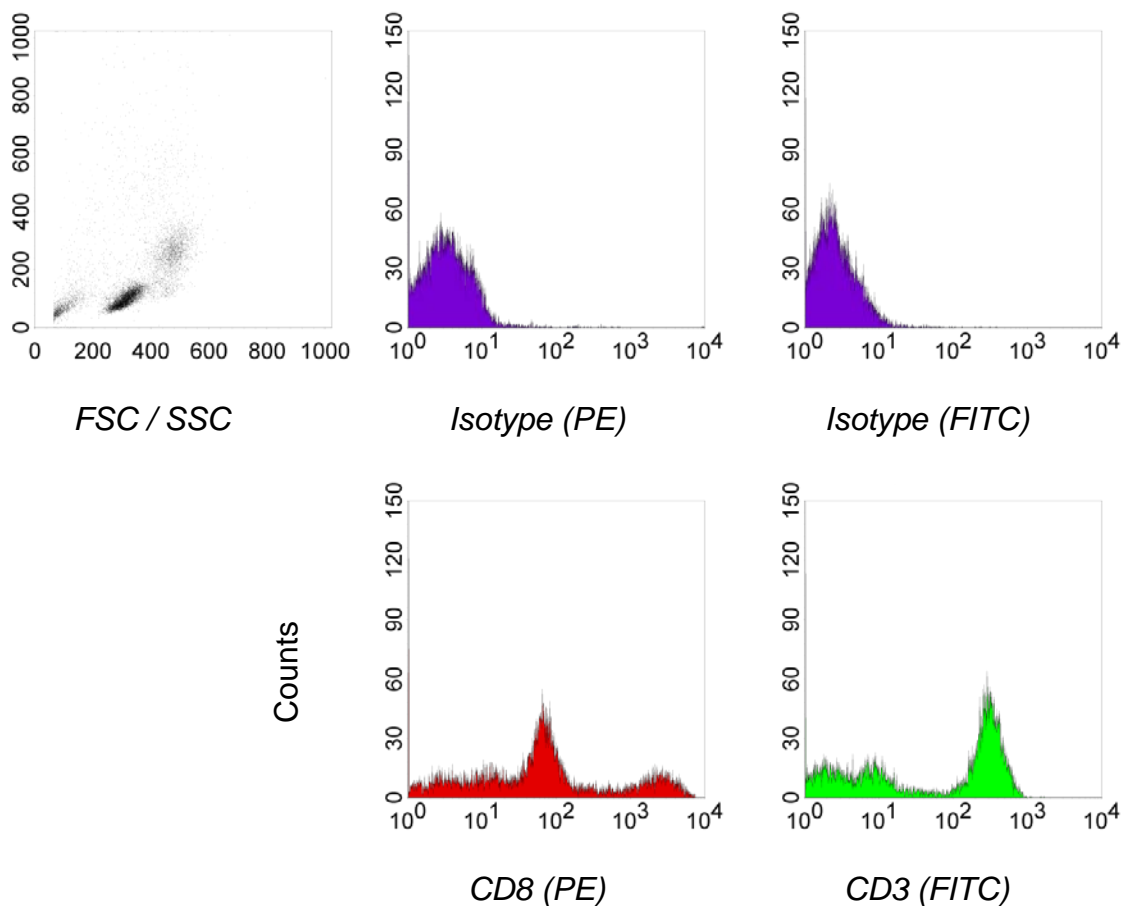
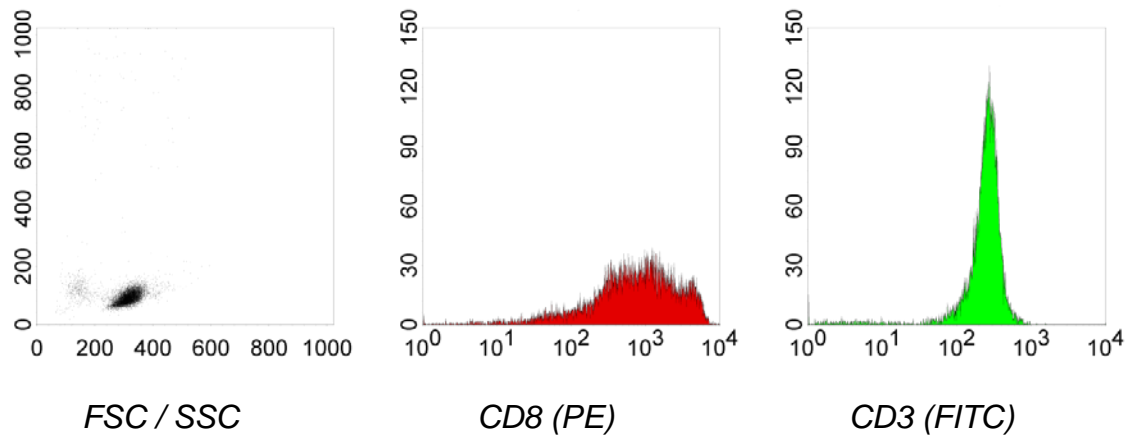


Figure 15: CD8 and CD3 T cell populations before selection; ordinate of dot plot (upper left) was SSC, abscissa was FSC; ordinate for the histograms was event count

The CD8-PE staining shows two T cell populations with differing expression levels of CD8. The selection targeted the CD8^{high} T cells.

Post-selection

Positive Fraction:



Negative fraction:

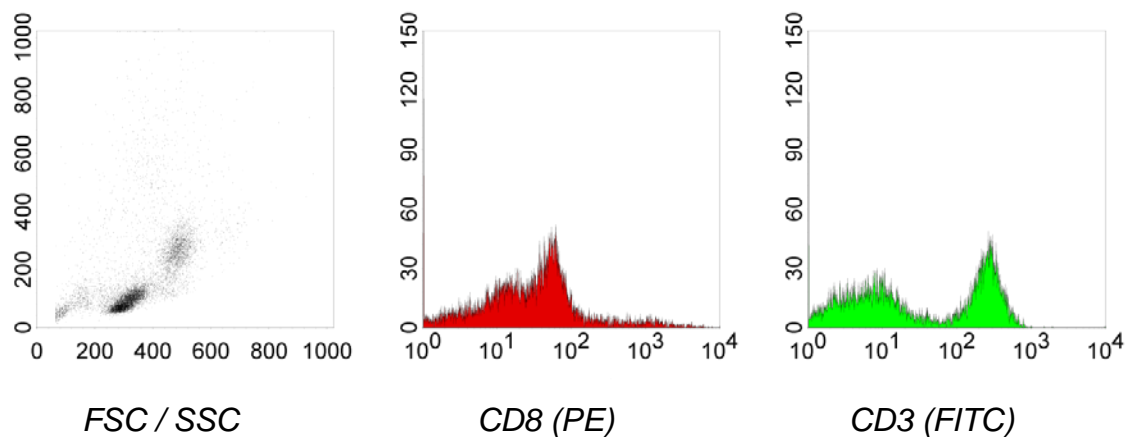


Figure 16: CD8 and CD3 T cell populations before and after selection in positive and negative fraction: ordinate of dot plot (left) was SSC, abscissa was FSC; ordinate for the histograms was event count

Fig. 15 - 16 are representative examples of CD8⁺ T cells before and after untouched negative selection. The positive fraction post-selection contains the enriched T cells expressing a high level of CD8. The negative fraction contains other lymphocytes including CD3⁺ T cells with a low expression level of CD8⁺ and the CD4⁺ T cell subset.

4.8 Autologous *in vitro* priming

Mature DCs were pulsed with EFT-specific peptides and mixed with CD8⁺ T cells present in a whole PBMC population. *In vitro* priming involved two consecutive stimulations as described in 3.16. The EFT-specific peptides identified as good HLA-A*0201 binders (see 4.4, Fig.10) were used.



Figure 17: DCs surrounded by T cells (one example circled in red) 30 minutes after start of IVP; 10x (detail)

Fig. 17 shows dendritic cells surrounded by T cells approximately 30 minutes after mixing them.

4.8.1 CHM1

Two weeks after start of the IVP peptide-specificity of T cells was assayed by IFN γ ELISpot. T cells from every priming well were brought in contact with T2 cells pulsed with the CHM1-319 peptide (VIMPCSWWV) and with T2 cells pulsed with influenza peptide (FLU) as negative control. The most promising clone was No 22 (see Fig. 18).

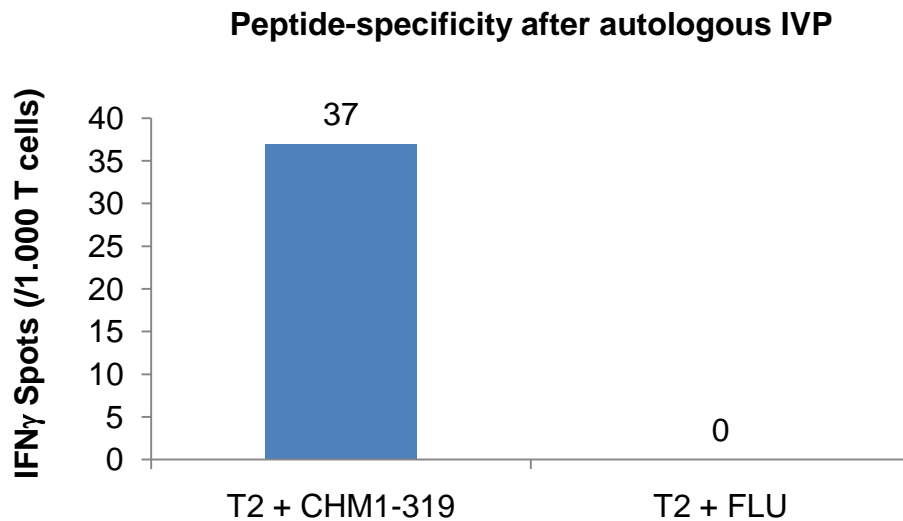


Figure 18: Peptide-specificity of T cells (clone 22) after autologous IVP; CHM1-319

T cells from this well were cloned by limiting dilution. Expanded “clones” were again tested for peptide specificity by IFN γ ELISpot.

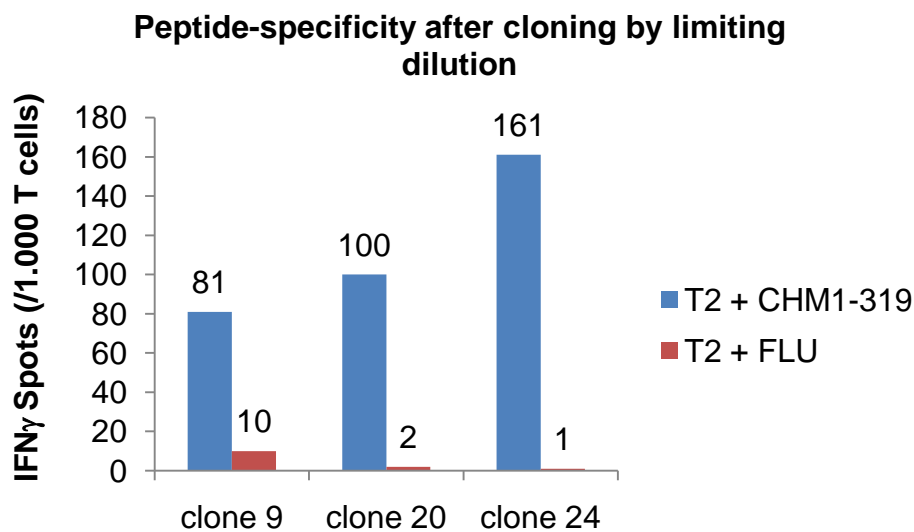


Figure 19: Peptide-specificity after cloning by limiting dilution; CHM1-319

All clones shown in Fig. 19 were expanded and stored in aliquots of 1×10^6 T cells per 100 μ l freezing medium aliquots. Clone 24 was selected for further testing and named CHM1-319-24.

Clone 24 was tested for clonality by flow cytometry based V β analysis. As described in 3.22 this allows rapid testing of presence of 24 TCR V β families.

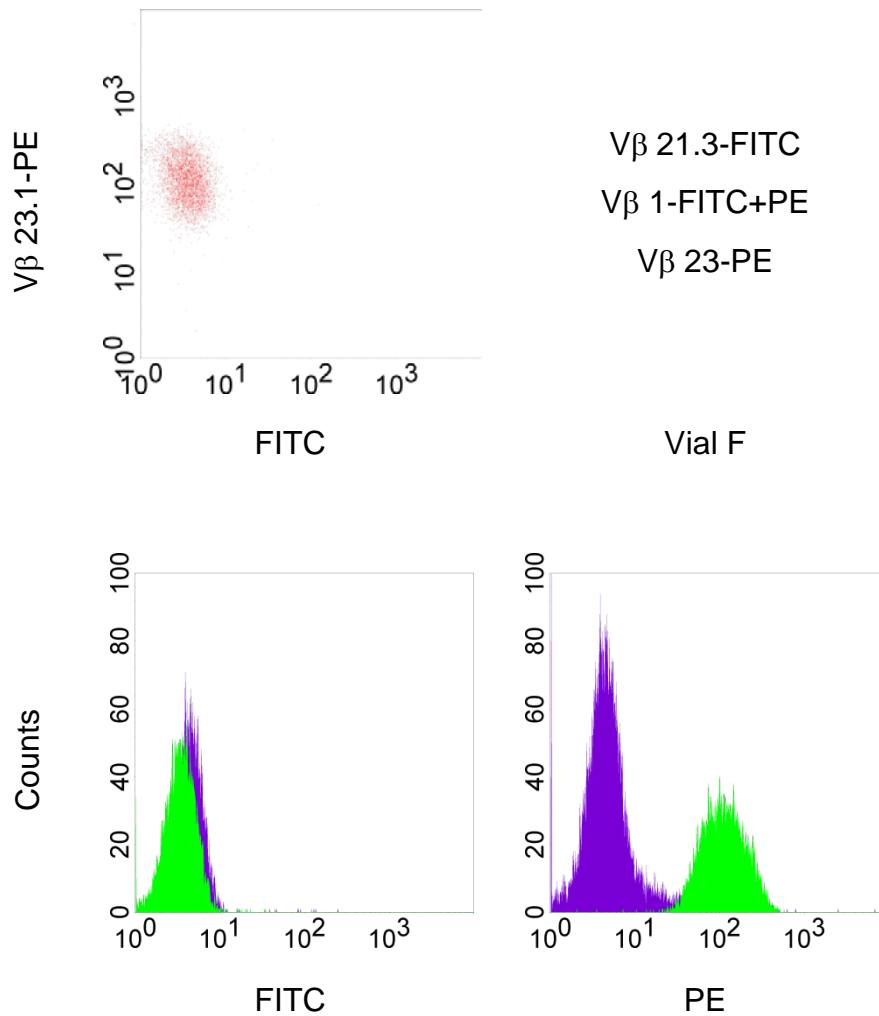


Figure 20: Dot plot (upper left) **and histograms** (bottom) **of CHM1-319-24**; vial F contains antibodies for three different V β families as shown on the upper right.

Of the eight vials containing 24 different TCR V β families only vial F gave a positive result. Vial F contains V β 21.3-FITC, V β 1-FITC+PE and V β 23-PE. As shown in Fig. 20 only the PE-marked V β is expressed. CHM1-319-24 is positive for V β 23 and negative for all other tested V β families.

Clone 24 was tested again for IFN γ and Perforin release to monitor behavior.

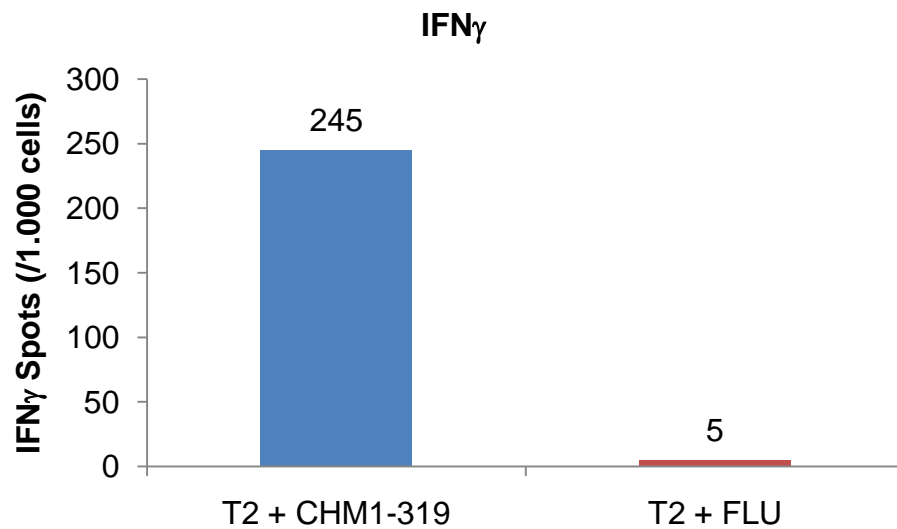


Figure 21: Peptide-specificity of clone CHM1-319-24 in IFN γ ELISpot

The peptide-specific clone was tested for Perforin release by ELISpot assay.

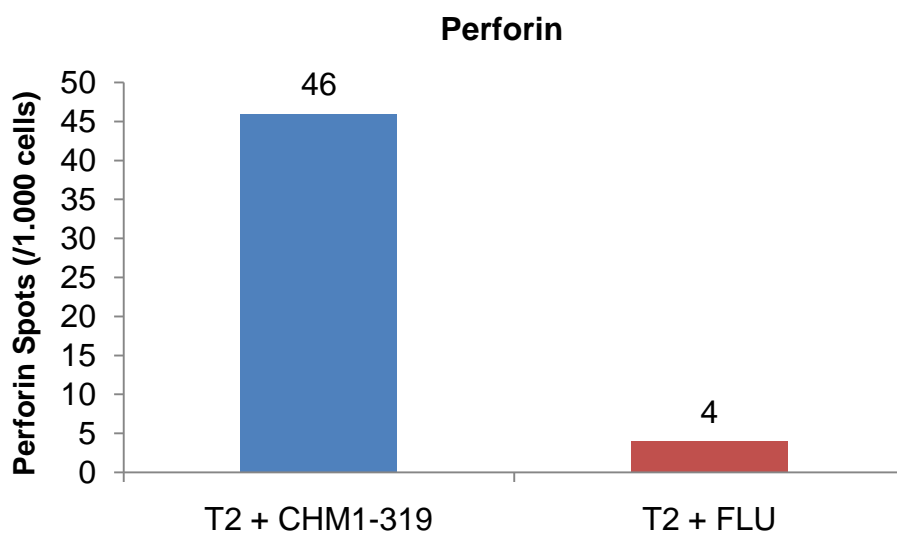


Figure 22: Peptide-specificity of clone CHM1-319-24 in Perforin ELISpot

CHM1-319-24 showed specificity in IFN γ ELISpot and in Perforin ELISpot when compared to reaction to the influenza peptide.

The peptide-specific clone was tested for IFN γ release upon contact with EFT cell lines. A673 and TC-71 are HLA-A*0201⁺. SBSR-AKS does not express HLA-A*0201.

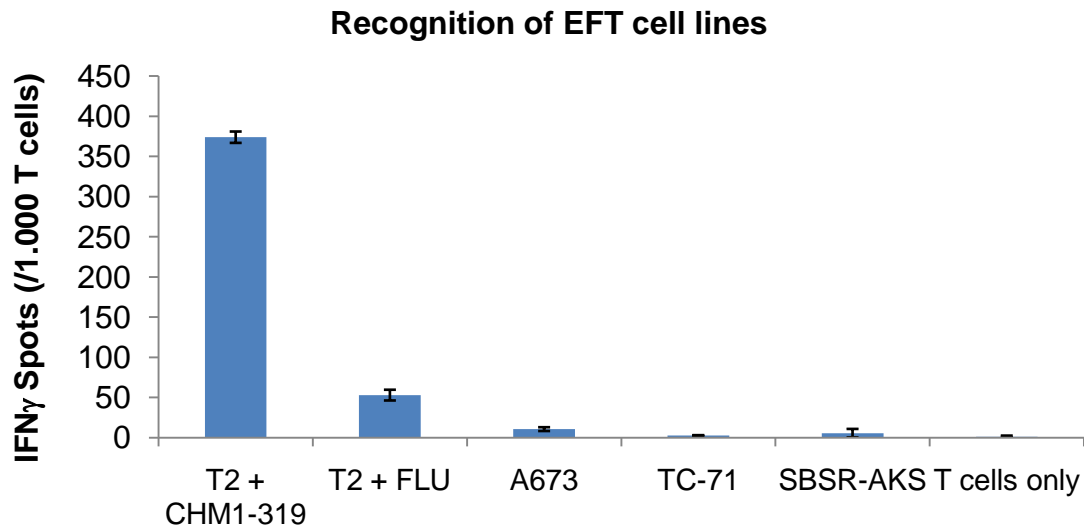


Figure 23: IFN γ release after contact with EFT cell lines, CHM1-319-24

CHM1-319-24 is peptide-specific but does not release significant amounts of IFN γ when brought in contact with EFT cell lines. This indicates that the CTL culture despite its proven peptide specificity cannot recognize EFT cell lines.

4.8.2 GPR64

GPR64-135 (FIMCATAEA) was found to be a HLA-A*0201-binding peptide (see 4.4, Fig. 10). An autologous IVP was done to obtain a peptide-specific T cell clone. The T cells of the most promising well (not shown) were cloned by limiting dilution similar to the CHM1 clone and tested again for peptide-specificity by IFN γ ELISpot.

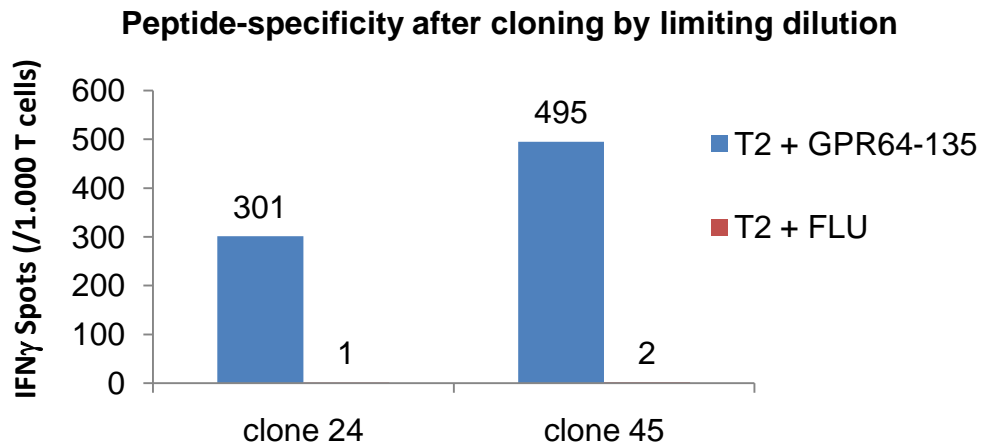


Figure 24: Peptide-specificity after cloning by limiting dilution; GPR64-135

Both clones were expanded, stored and clone 45 was tested for clonality by flow cytometry based V β analysis. As described in 3.22 this allows rapid testing of presence of 24 TCR V β families.

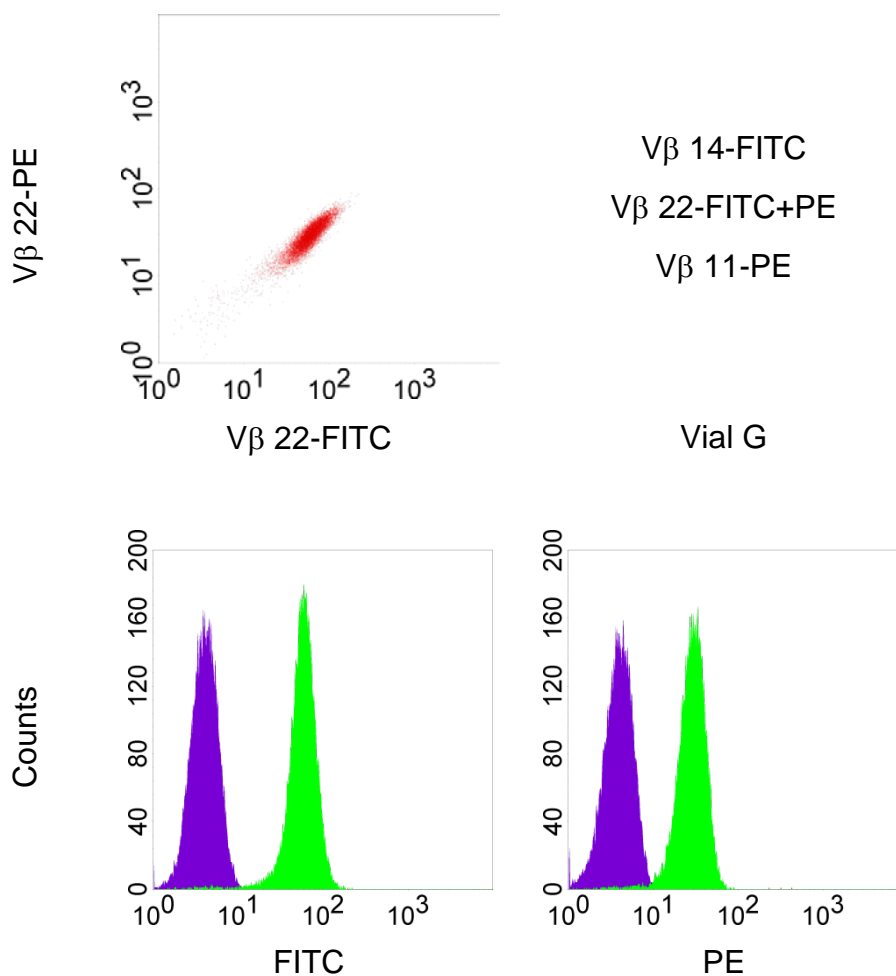


Figure 25: Dot plot (upper left) and histograms (bottom) of GPR64-135-45, vial G contains antibodies for three different V β families as shown in the upper right.

Of the eight vials containing 24 different TCR V β families only vial G gave a positive result. Vial G contains V β 14-FITC, V β 22-FITC+PE and V β 11-PE. As shown in Fig. 25, only the FITC+PE-marked V β is expressed. GPR64-135-45 is positive for V β 22 and negative for all other tested V β families.

The peptide-specific clone GPR64-135-45 was tested for IFN γ release upon contact with EFT cell lines.

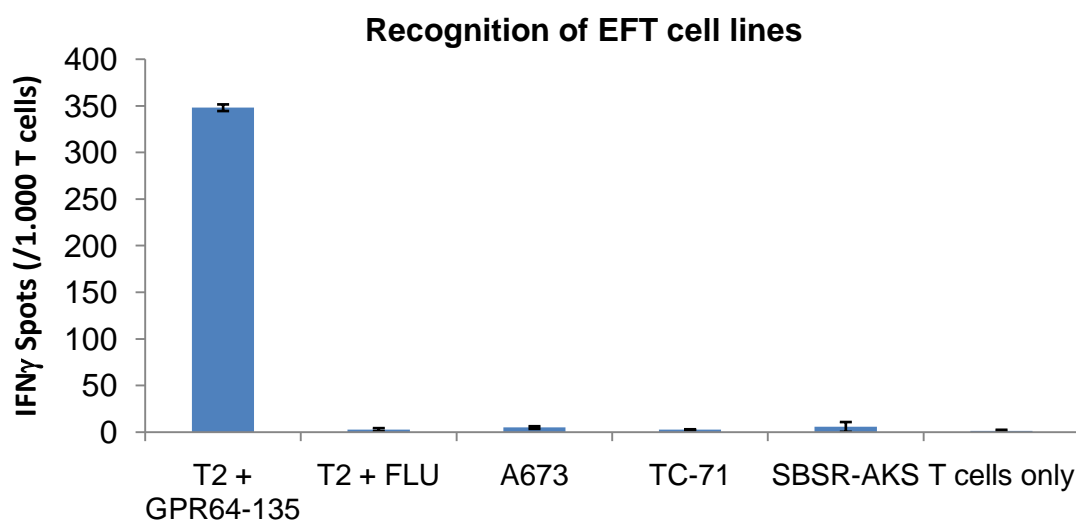


Figure 26: IFN γ release after contact with EFT cell lines, GPR64-135-45

As seen with the CHM1-319 CTL culture, GPR64-135-45 is also peptide-specific but does not release significant amounts of IFN γ when brought in contact with EFT cell lines.

4.8.3 EZH2

To control for false binding candidates and to evaluate the assays performed so far, published HLA-A*0201-binding peptides able to generate a T cell response against different tumor entities (EZH2-666 and STEAP-86) were used in subsequent IVP experiments.

An autologous IVP was done to obtain a peptide-specific T cell clone for the HLA-A*0201-binding peptide EZH2-666 (YMCSFLFNL (98)). The T cells of the most promising well (not shown) were cloned by limiting dilution similar to the CHM1 clone and tested again for peptide specificity by IFN γ ELISpot.

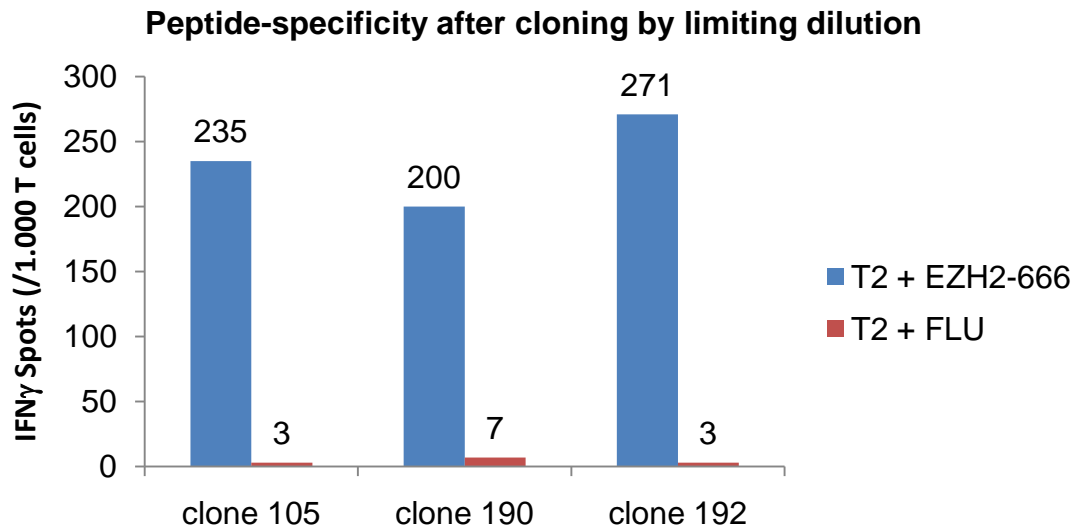


Figure 27: Peptide-specificity after cloning by limiting dilution; EZH2-666

All shown clones were expanded and stored in 1×10^6 / 100 μ l freezing medium aliquots. Clone 192 was selected for further testing.

The peptide-specific clone was tested for IFN γ release upon contact with EFT cell lines.

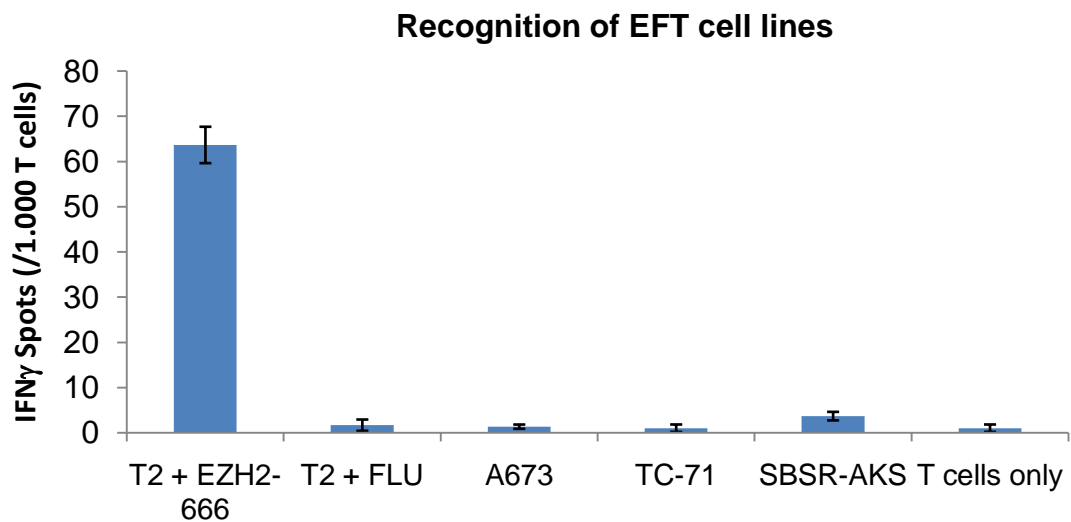


Figure 28: IFN γ release after contact with EFT cell lines, EZH2-666-192

EZH2-666-192 is peptide-specific but does not release significant amounts of IFN γ when brought in contact with EFT cell lines.

4.8.4 STEAP

An autologous IVP was performed to obtain a peptide-specific T cell clone for the HLA-A*0201-binding peptide STEAP-86 (FLYTLLEEV (99)). The T cells of the most promising well (not shown) were cloned by limiting dilution similar to the CHM1 clone and tested again for peptide-specificity by IFN γ ELISpot.

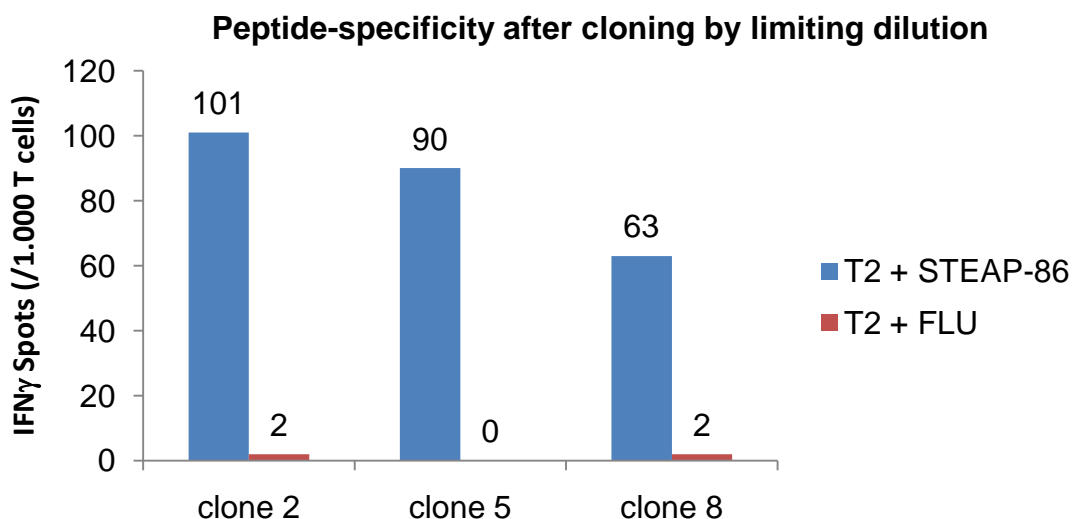


Figure 29: Peptide-specificity after cloning by limiting dilution; STEAP-86

All clones shown in Fig. 29 were expanded and stored in 1×10^6 / 100 μ l freezing medium aliquots. Upon further testing clone No 8 appeared to be the most specific and reactive.

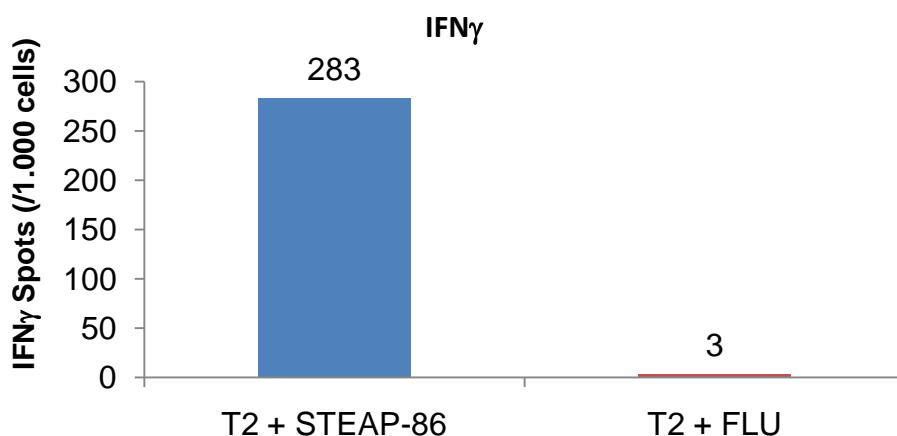


Figure 30: Peptide-specificity; STEAP-86-8

STEAP-86-8 was tested for clonality by flow cytometry based V β analysis.

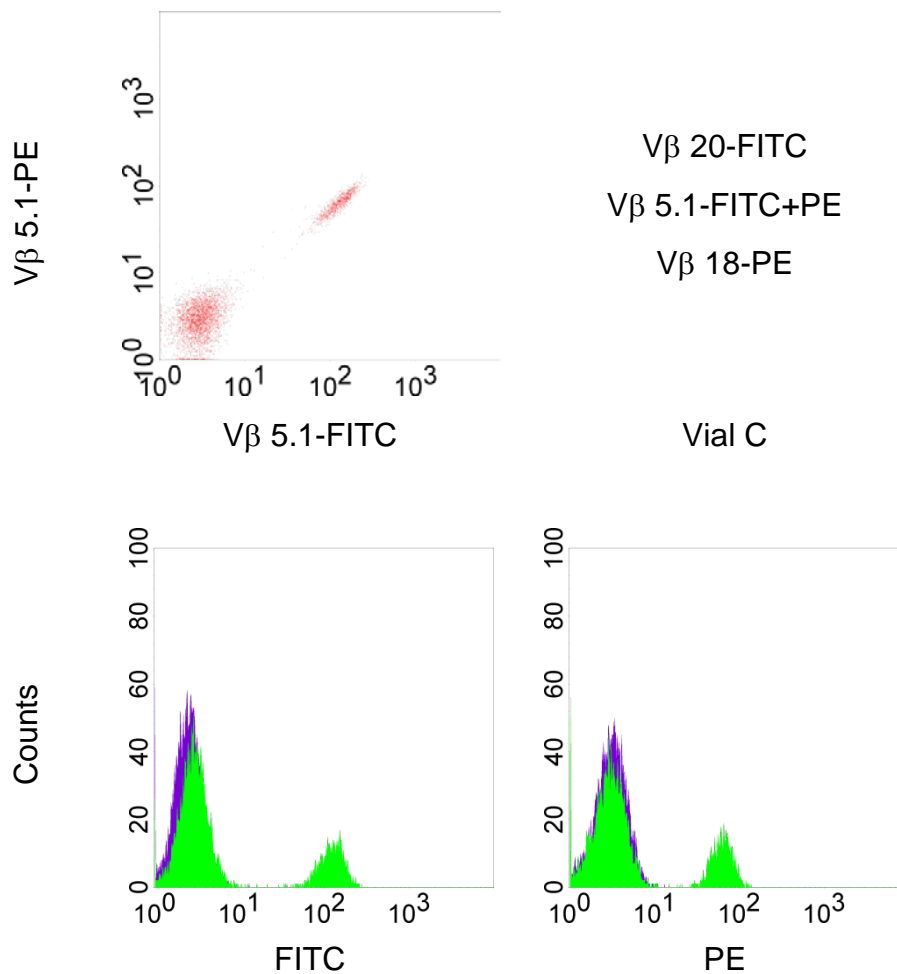


Figure 31: Dot plot (upper left) and histograms (bottom) of STEAP-86-8; vial C contains antibodies for three different V β families as shown in the upper right.

Of the eight vials containing 24 different TCR V β families only vial C gave a positive result. Vial C contains V β 20-FITC, V β 5.1-FITC+PE and V β 18-PE. As shown in Fig. 31, only the FITC+PE-marked V β is expressed. STEAP-86-8 is positive for V β 5.1 and negative for all other tested V β families. However, it is clear from this analysis that the STEAP-86-8 CTLs are a mixed culture containing CTLs of another V β family which was not represented in the kit.

STEAP-86-8 was tested for IFN γ release upon contact with EFT cell lines by ELISpot.

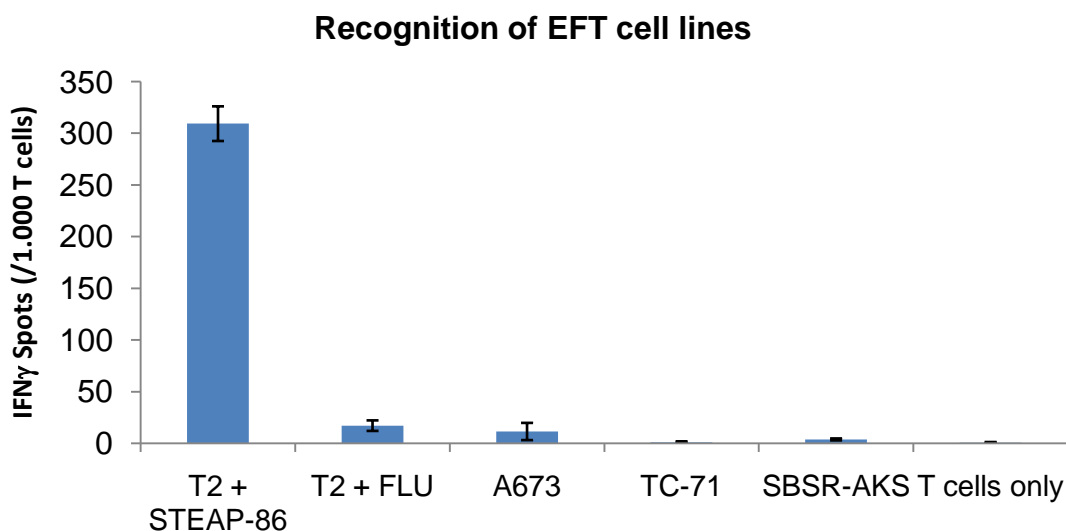


Figure 32: IFN γ release after contact with EFT cell lines, STEAP-86-8

STEAP-86-8 is peptide-specific but does not release significant amounts of IFN γ when brought in contact with EFT cell lines.

4.8.5 ITM2A

An autologous IVP was done to obtain peptide-specific T cell clones for the probably HLA-A*0201-binding peptides ITM2A-59 (GLSFILAGL) and ITM2A-161 (YLMPLNTSI). Unfortunately, no well with promising T cells was detected.

4.8.6 LIPI

An autologous IVP was done to obtain peptide-specific T cell clones for the probably HLA-A*0201-binding peptides LIPI-121 (LLNEEDMNV) and LIPI-262 (SIFSGIQFI). Unfortunately no well with promising T cells was detected. Additionally, a futile attempt to obtain a peptide-specific T cell clone for LIPI-370 (TMMDGSFSF) was carried out in the beginning before a peptide-binding assay was established.

4.8.7 Summary of the autologous *in vitro* priming

All T cell clones obtained in the autologous setting usually displayed a high peptide specificity and even secreted Perforin upon peptide contact (Fig. 22), but were unable to recognize any EFT line in the correct HLA-A*0201 context. Experimental problems were ruled out. T cell clones generated against novel unconfirmed peptide epitopes as well as against published peptide epitopes revealed an identical behavior suggesting a problem in the recognition of the EFT lines that I hoped to address with the subsequent generation of allorestricted T cells.

4.9 Allogeneic in vitro priming

During the past years methods emerged to identify, isolate, and expand tumor peptide-specific allorestricted T cells *ex vivo* (100-104), anticipating their potential use for adoptive immunotherapy (54) e.g. to replace common DLI with tumor-specific, allorestricted T cells. The approach used here was to mismatch purified CD8⁺ T cells and mature peptide pulsed DCs for HLA-A*0201 expression and to stimulate HLA-A*0201⁻ CD8⁺ T cells like those in the autologous setting, purify them with a specific peptide-pentamer and characterize their immunologic features.

4.9.1 CHM1

HLA-A*0201⁺ DCs were pulsed with 30 μ M CHM1-319 peptide and used to prime HLA-A*0201⁻ CD8⁺ T cells. After restimulation all T cells were pooled and stained for cell sorting.

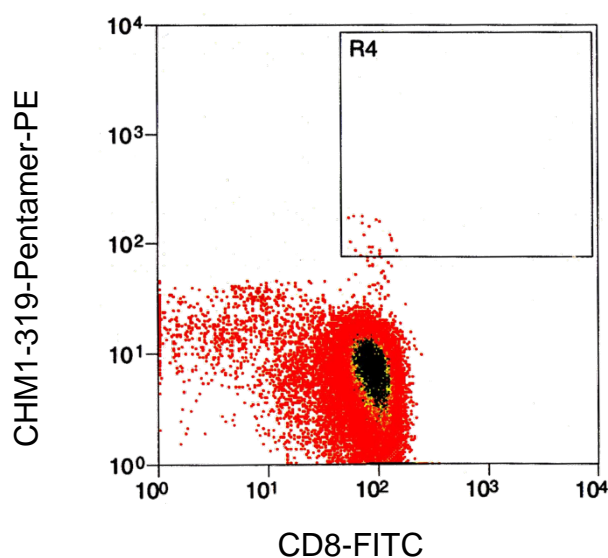


Figure 33: Sorting the CD8-FITC / CHM1-319-Pentamer-PE double positive T cells in gate R4: 1.560 events

Approximately 1.5×10^7 viable T cells were sorted. 1.560 events (= 0.01 %) were counted in gate R4 and collected in human serum. Those T cells were regarded as HLA-A*0201 peptide-specific and cloned by limiting dilution in three 96-well plates. Every well contained five T cells statistically. 96 clones were tested by IFN γ ELISpot screening for peptide specificity with T2 cells

pulsed with the CHM1-319 peptide and the influenza peptide as negative control (not shown). 18 clones passed the screen and were tested again for specificity, this time including the EFT cell line A673 and an artificial construct of the simian cell line Cos-7. This cell line is easily transfected with the gene of interest (CHM1 in this case) and the human HLA-A*0201 and expresses the transfected genes at high levels. If the peptide-epitope is processed and presented as predicted *in silico* the peptide-specific CTL culture should be able to recognize the artificial Cos-7 construct.

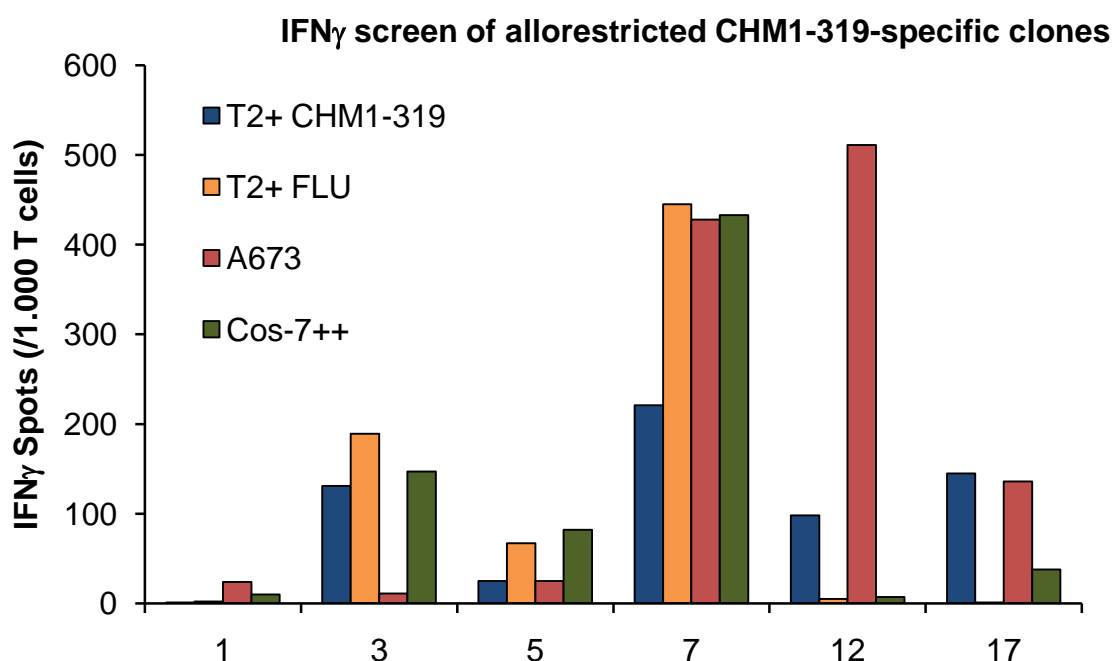


Figure 34: Sorted T cells were cloned by limiting dilution and screened for peptide- and EFT-cell line specificity in IFN γ -ELISpot, (A673: + 100 U / ml IFN γ 48 h prior to ELISpot; Cos-7++: transient lipofection with human HLA-A*0201 and CHM1 gene)

Three clones passed this screen: 7, 12 and 17. Those clones were able to release IFN γ after contact with the HLA-A*0201⁺ EFT cell line A673. Those clones were tested again in triplicates.

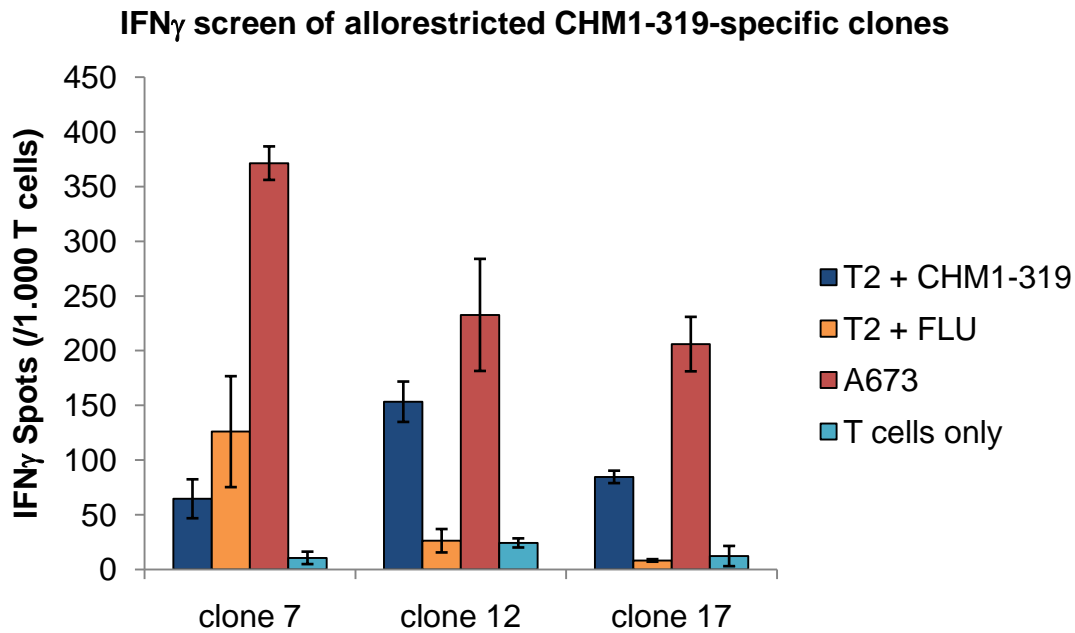


Figure 35: Re-evaluation of allorestricted T cell clones specific for CHM1-319

CHM1-319-17 was found to be the best of these three. Clone 7 lacked peptide specificity. Clone 12, while looking good in Fig. 34 - 35, was not used in further experiments because, unfortunately, it did not expand (not shown).

CHM1-319-17 was stained with specific and unspecific Pentamer-PE after expansion to control for peptide specificity via flow cytometry.

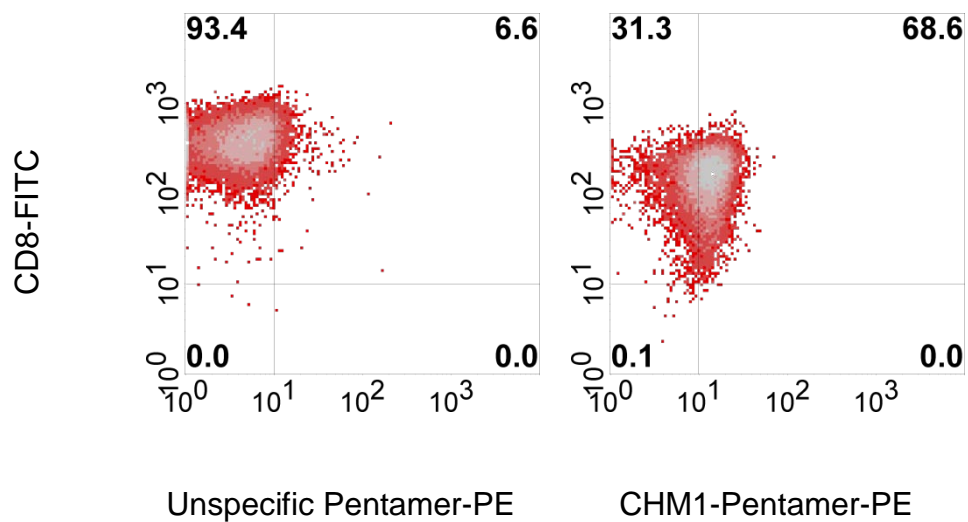


Figure 36: Pentamer staining of CHM1-319-17

Compared to staining with an unspecific Pentamer-PE, CHM1-319-17 showed a significant shift resulting in more than 68 percent CD8 / CHM1-Pentamer double positives (see Fig. 36).

CHM1-319-17 maintained peptide specificity in IFN γ ELISpot and maintained the ability to recognize the EFT cell line A673.

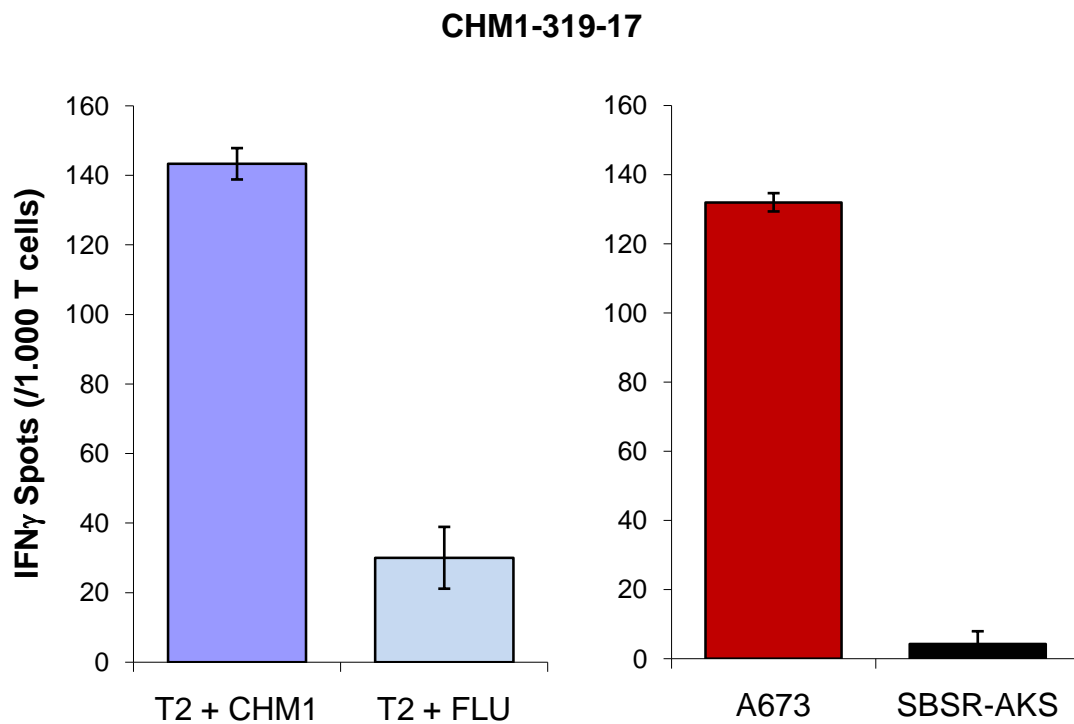


Figure 37: Peptide specificity of CHM1-319-17 and HLA-A*0201-specific recognition of EFT cell lines

CHM1-319-17 was tested for IFN γ release after contact with two EFT cell lines. It recognized the HLA-A*0201⁺ cell line A673 and did not recognize the HLA-A*0201⁻ cell line SBSR-AKS indicating the correct HLA-A*0201 restriction.

The TCR V β repertoire of CHM1-319-17 was tested to get information about possible clonality of the CTL culture.

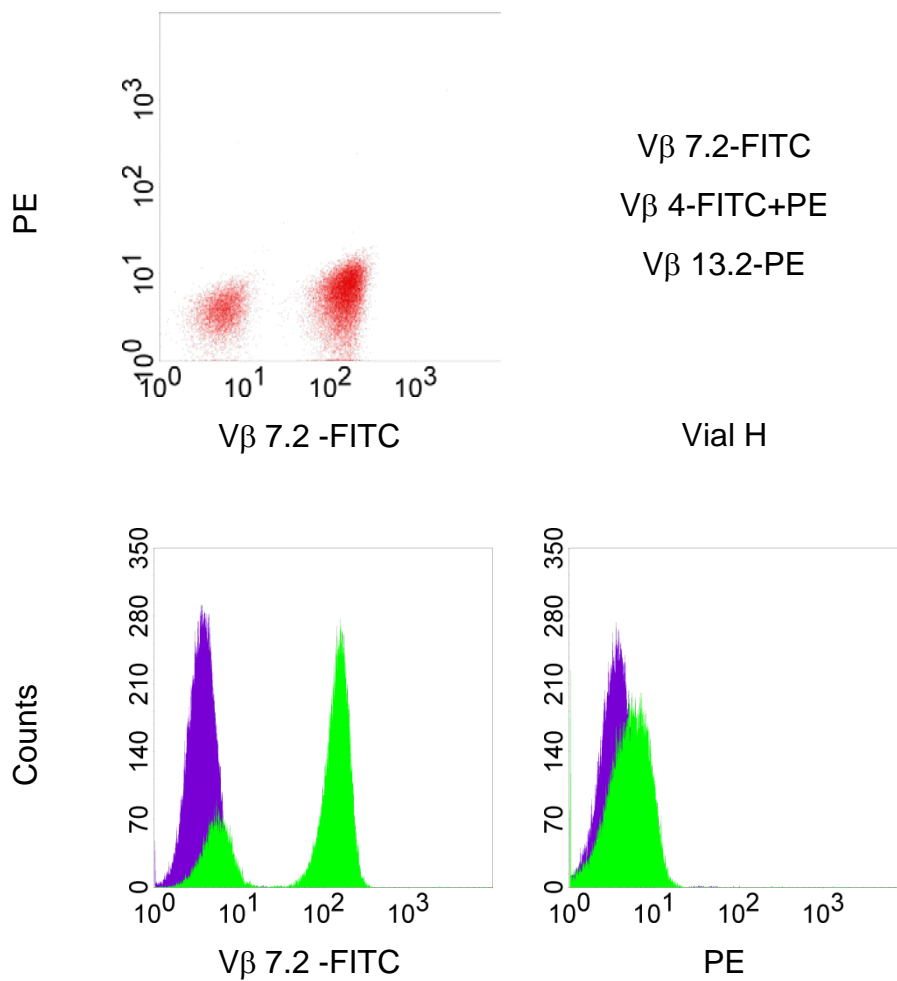


Figure 38: Dot plot (upper left) and histograms (bottom) of CHM1-319 -17; vial H contains antibodies for three different V β families as shown on the upper right.

CHM1-319-17 is positive for V β 7.2-FITC as shown in the dot plot and histograms (Fig. 38). A big part of the T cell population is positive for this V β .

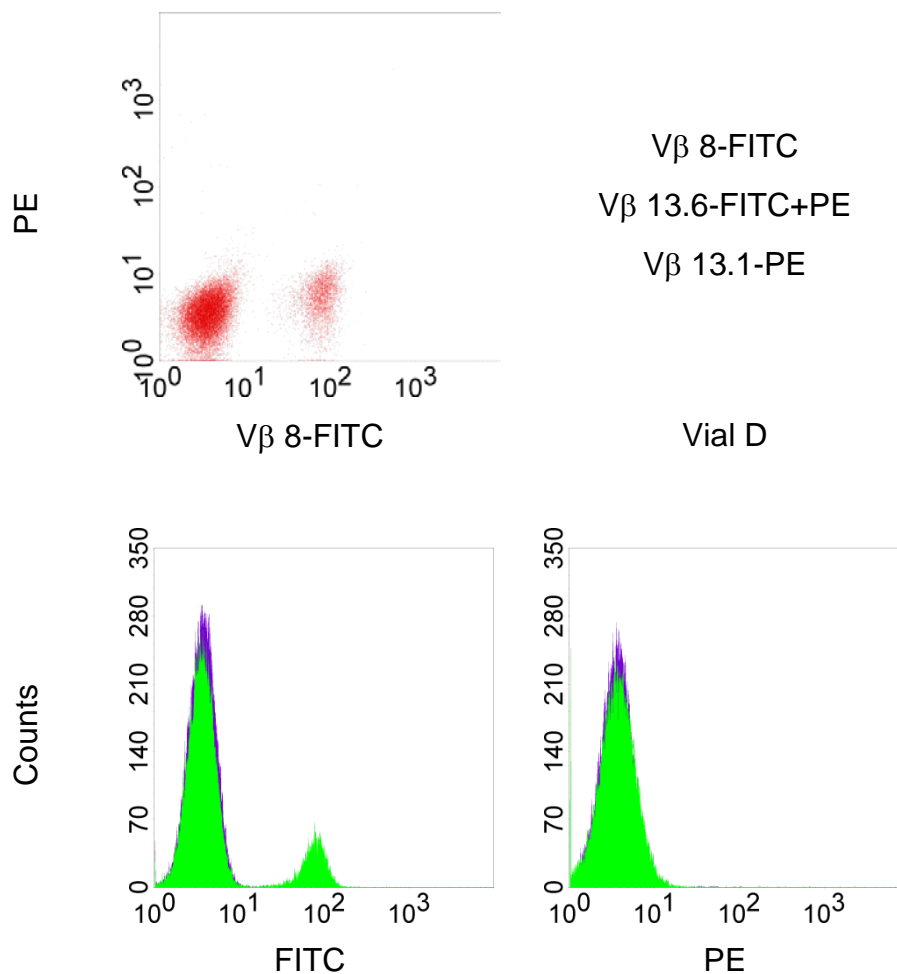


Figure 39: Dot plot (upper left) **and histograms** (bottom) of **CHM1-319 -17**; vial D contains antibodies for three different V β families as shown on the upper right.

CHM1-319-17 is also positive for V β 8-FITC as shown in the dot plot and histograms (Fig. 39). But only a small part of the population is positive for this V β .

Of the eight vials containing 24 different TCR V β families vial D gave a positive result. Vial D contains V β 8-FITC, V β 13.6-FITC+PE and V β 13.1-PE. As shown in Fig. 39, of these three, only the FITC-marked V β 8 is expressed. There is another positive result with vial H. Vial H contains V β 7.2-FITC, V β 4-FITC+PE and V β 13.2-PE. As shown in Fig. 38, of these three, only the FITC-marked V β 7.2 is expressed. CHM1-319-17 is positive for V β 8 and V β 7.2 and negative for all other tested V β families. So the CTL culture contains at least two clones.

To ascertain the peptide affinity of the CTL culture a peptide titration assay was conducted. T2 cells were loaded with either the CHM1-319 peptide or – for negative control – the influenza peptide at different concentrations. IFN γ release was measured by ELISpot.

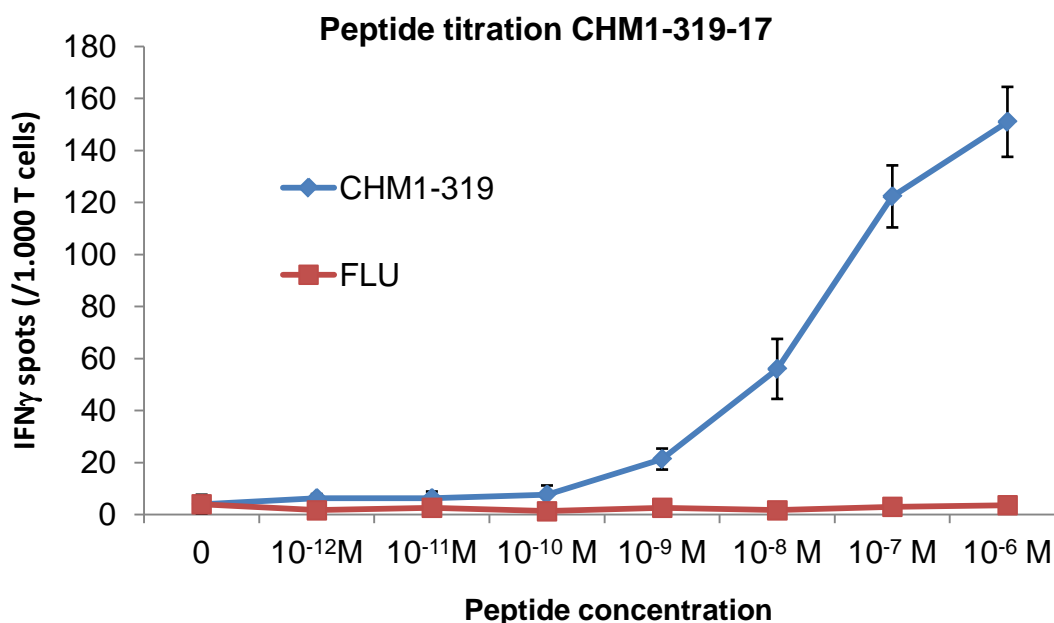


Figure 40: Peptide titration assay for CHM1-319-17; error bars are standard deviation of triplicates

At concentration as low as 10^{-9} M IFN γ release was detectable and it was specifically released compared to the reaction to influenza peptide-pulsed T2 cells. A plateau was not reached even at the concentration of 10^{-6} M. This shows a low affinity of the CTL culture CHM1-319 to the peptide, as a CTL culture with higher affinity for the peptide would need much less peptide to trigger detectable IFN γ release (compare EZH2-666, Fig. 51).

The CTL culture CHM1-319-17 was shown to be peptide-specific, able to recognize within HLA context EFT cell lines expressing CHM1. Left to show was the ability to kill this cell line specifically. This was done by a granzyme B ELISpot.

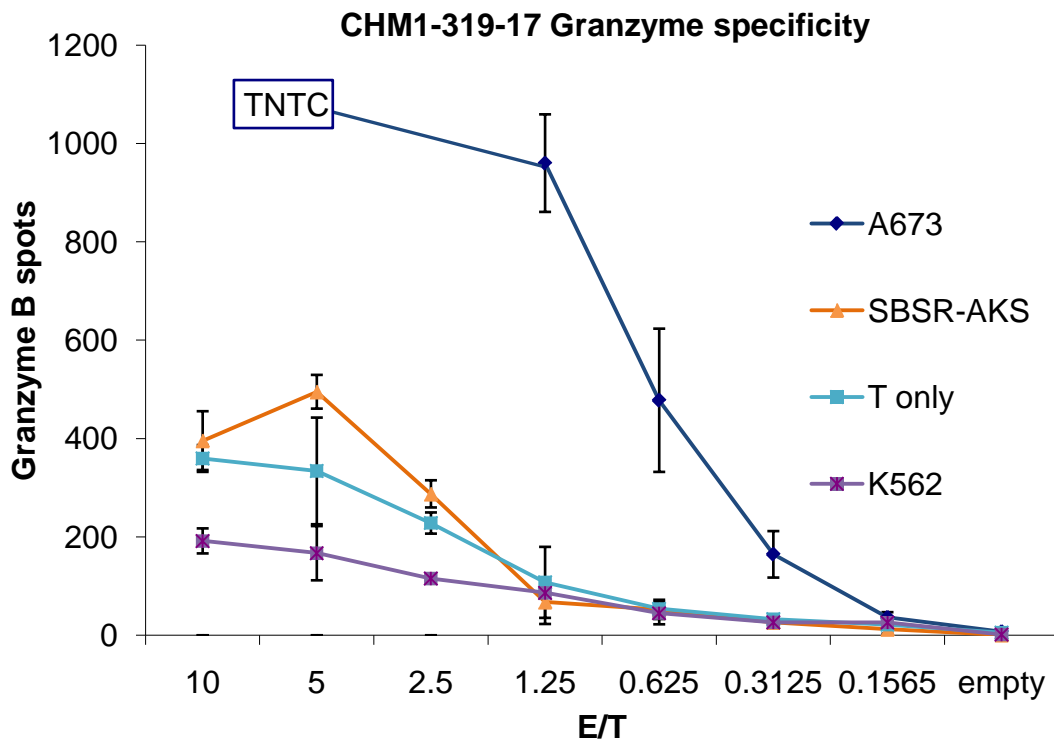


Figure 41: Specific cytotoxicity of CHM1-319-17; E / T: effector / target ratio; TNTC: too numerous to count

CHM1-319-17 specifically released granzyme B when mixed with the A673 cell line.

At higher effector to target ratio the granzyme B spots were almost confluent and no more countable for the software. T cells only controlled for spontaneous release. SBSR-AKS controlled the HLA context. K562 controlled for natural killer cell activity.

An additional control experiment (see Fig. 42) was conducted to show the cytotoxic specificity of the CHM1-319-17 CTL culture. For this experiment, the two E / T ratios, where the difference in granzyme release between the EFT cell line A673 and the controls were most significant ($p < 0.01$) and producing countable spots, were used. The CTL culture releases more granzyme B when brought in contact with the HLA-A*0201⁺ EFT cell line A673 which expresses CHM1 at a high level than when brought in contact with the HLA-A*0201⁺ cALL cell line 697 which does not express CHM1. The p values for the E / T ratios of 1.25 and 0.625 were 0.016 and 0.17 respectively.

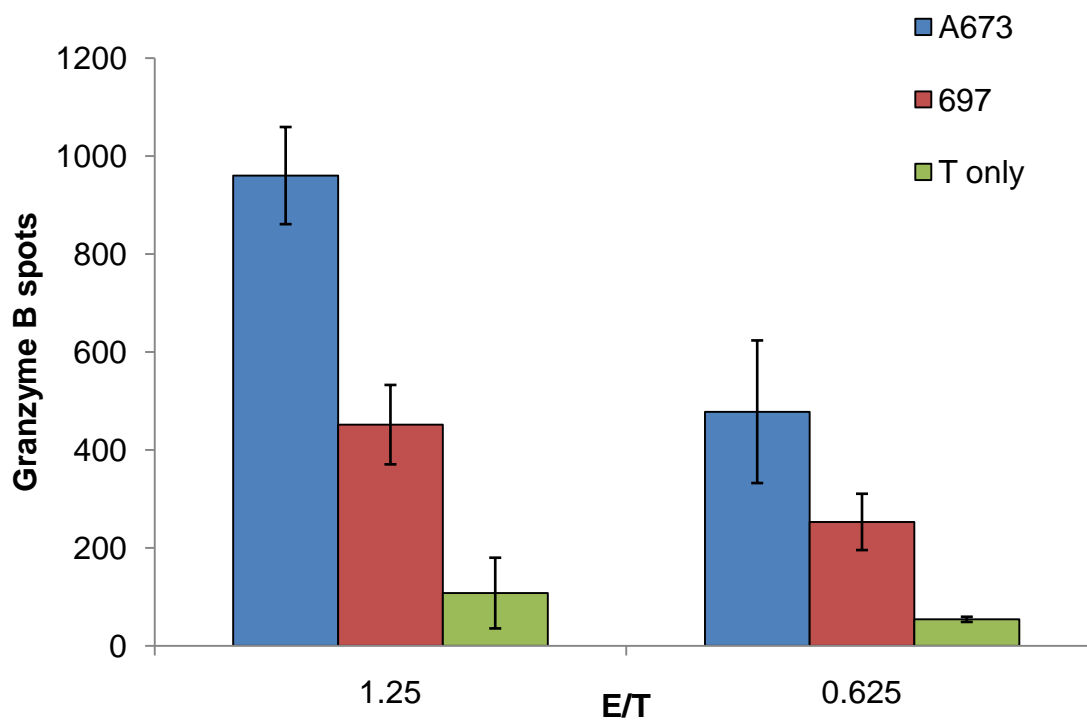


Figure 42: Granzyme B release after contact with two HLA-A*0201⁺ cell lines, CHM1-319-17

While peptide specificity of this CTL culture was shown several times, the pentamer staining only yielded approximately 64 percent specific T cells (see Fig. 36). Therefore an additional cytotoxicity experiment was conducted. T2 cells pulsed with the CHM1-319 peptide and T2 cells pulsed with influenza peptide were added as controls for peptide specificity. CHM1-319-17 specifically released granzyme B when mixed with the EFT cell line A673 and the T2 cell line pulsed with the CHM1-319 peptide, but did not release granzyme B when mixed with T2 cells pulsed with the influenza peptide. T cells alone were added to control for spontaneous release (see Fig. 43).

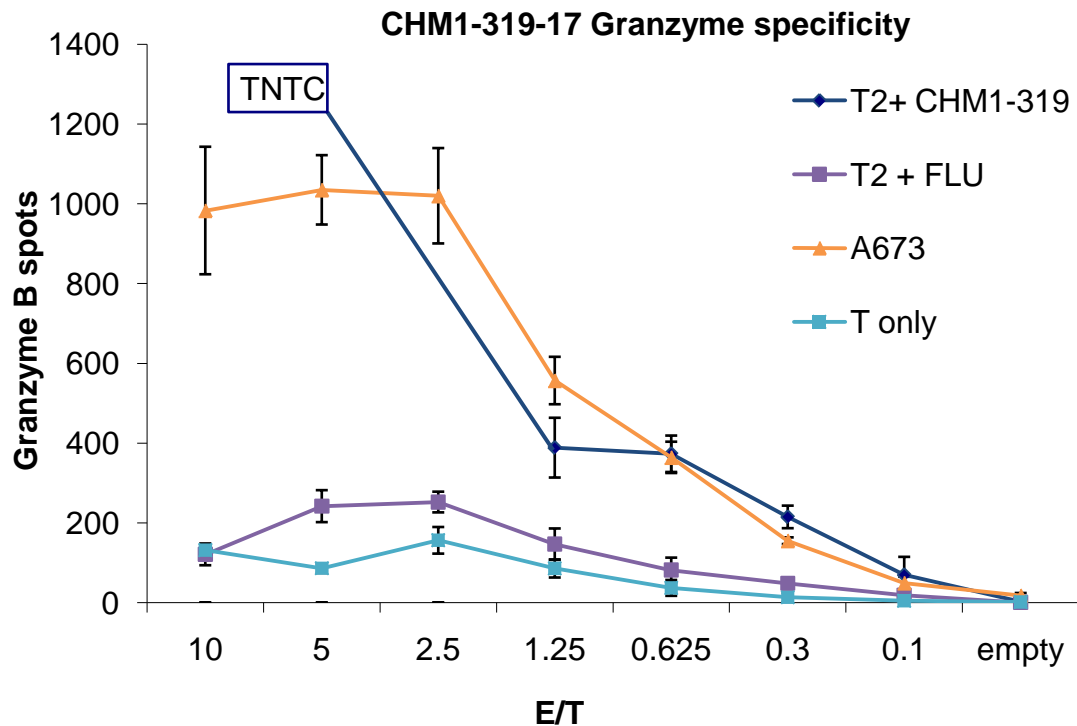


Figure 43: Specific cytotoxicity of CHM1-319 17; E / T: effector / target ratio; TNTC: too numerous to count

The CHM1-319 CTL culture was identified as effector memory T cells (T_{EM}) by observing the capability of releasing $IFN\gamma$ and the absence of central memory T cell (T_{CM}) markers. The CTL culture was negative for CD27, CD28, CD45RA, CD62L, CCR5, CCR7 and CD127 as evaluated by flow cytometry (not shown).

4.9.2 EZH2

HLA-A*0201⁺ DCs were pulsed with 30 μ M EZH2-666 peptide and used to prime HLA-A*0201⁻ CD8⁺ T cells. After restimulation all T cells were pooled and stained for cell sorting.

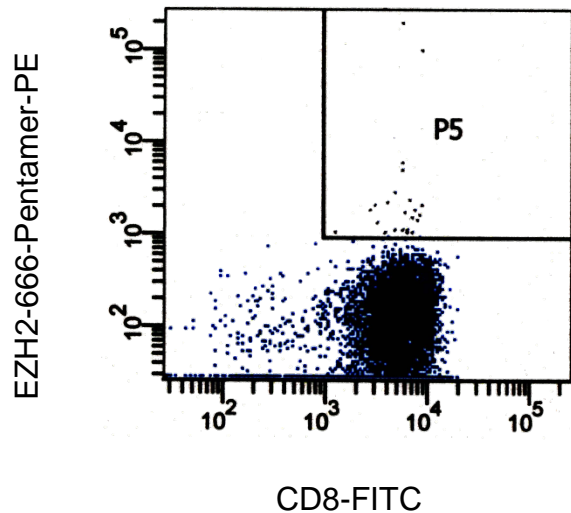


Figure 44: Sorting the CD8-FITC / EZH2-666-Pentamer-PE double positive T cells in gate P5: 5148 events

Approximately 1.5×10^7 viable T cells were sorted. 5.418 events (= 0.03 %) were counted in gate P5 and collected in human serum. Those T cells were then cloned by limiting dilution in 96-well plates. Two plates contained one T cell per well statistically, another two contained five T cells per well, and a final two plates contained ten T cells per well statistically. 96 clones were tested by IFN γ ELISpot screening for peptide specificity with T2 cells pulsed with the EZH2-666 peptide and the influenza peptide as negative control (not shown). 24 clones passed the screen and were tested again for specificity, this time including the EFT cell line A673 and an artificial construct of the simian cell line Cos-7 transfected with the human HLA-A*0201 gene and the EZH2 gene.

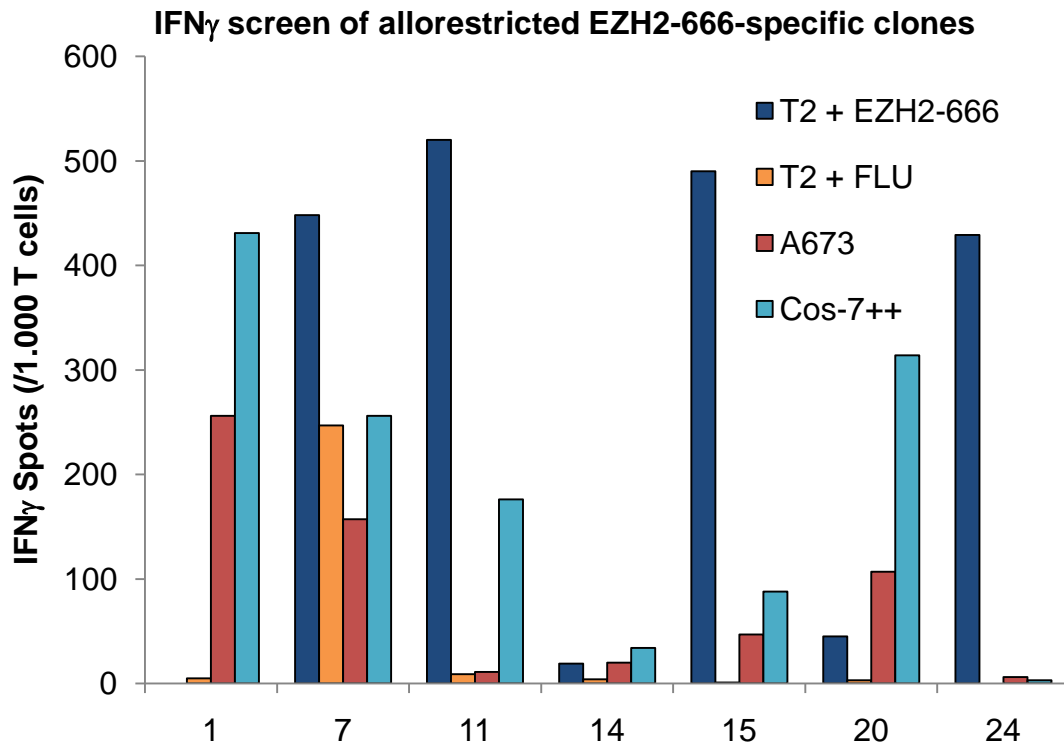


Figure 45: Sorted T cells were cloned by limiting dilution and screened for peptide- and EFT-cell line specificity in IFN γ -ELISpot, (A673: + 100 U / ml IFN γ 48 h prior to ELISpot; Cos-7++: transient lipofection with human HLA-A*0201 and gene of interest)

Four clones passed this screen: 7, 11, 15 and 20. Those clones were expanded and tested again in triplicates. Especially clone 7 however seemed to lack peptide-specificity, but was nevertheless expanded because of its strong recognition of the EFT cell line A673.

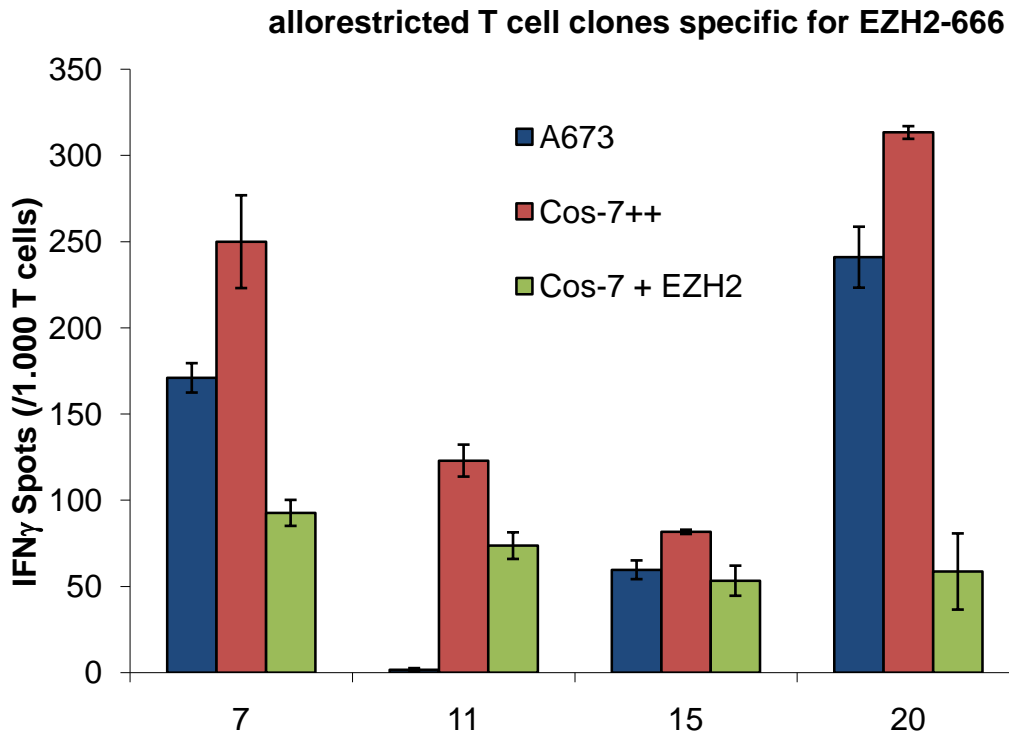


Figure 46: T cells that passed the first screen were expanded and screened for peptide- and EFT-cell line specificity in IFN γ -ELISpot, (A673: + 100 U / ml IFN γ 48 h prior to ELISpot; Cos-7++: transient lipofection with human HLA-A*0201 and gene of interest; Cos-7 + EZH2: transient lipofection with EZH2 but without human HLA-A*0201);

The clones were retested for recognition of the EFT cell line A673 and the artificial constructs with the simian cell line Cos-7. Clone 11 did not recognize A673, as seen in Fig. 45 – 46, but released IFN γ after contact with the artificial Cos-7 construct.

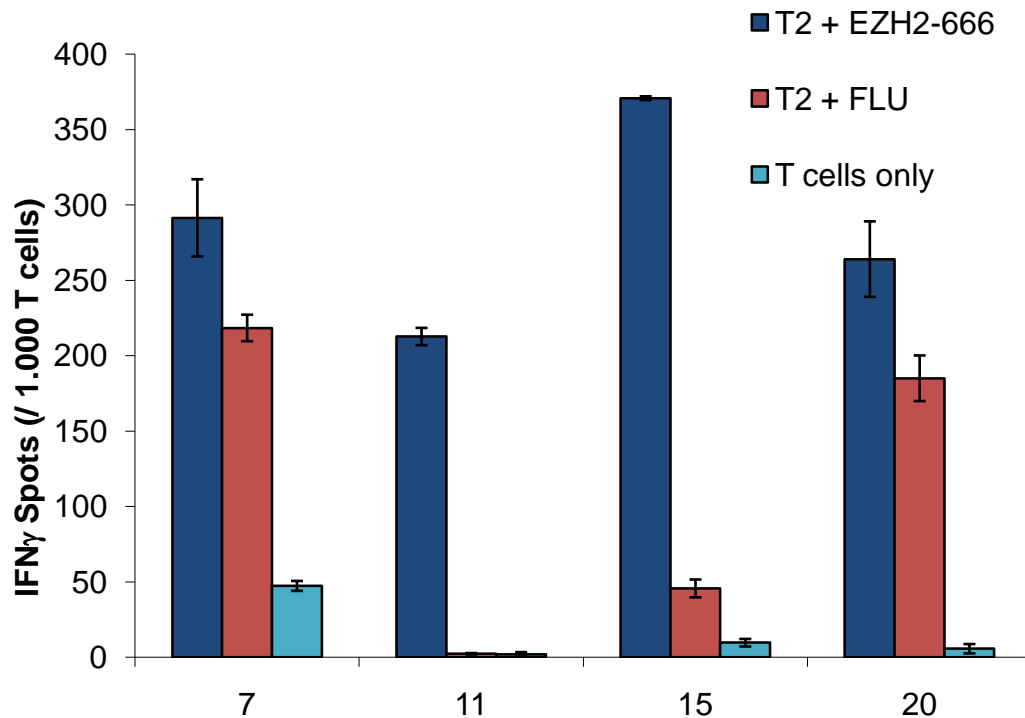


Figure 47: Allogeneic T cell clones specific for EZH2-666; test for peptide specificity

The clones were at the same time tested for peptide-specificity.

EZH2-666-15 was found to be the best of these four clones. Clone 7 and 20 lacked peptide-specificity; clone 11 did not recognize the EFT cell line.

EZH2-666-15 was stained with specific and unspecific Pentamer-PE after expansion to control for peptide-specificity via flow cytometry.

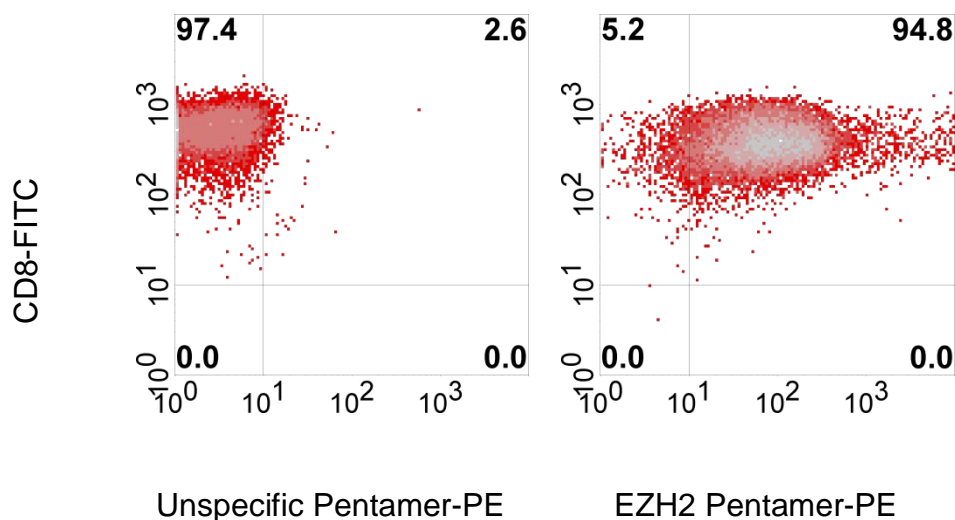


Figure 48: Pentamer staining of EZH2-666-15

Compared to staining with an unspecific Pentamer-PE, EZH2-666-15 showed a significant shift resulting in more than 94 percent CD8 EZH2-Pentamer double positives.

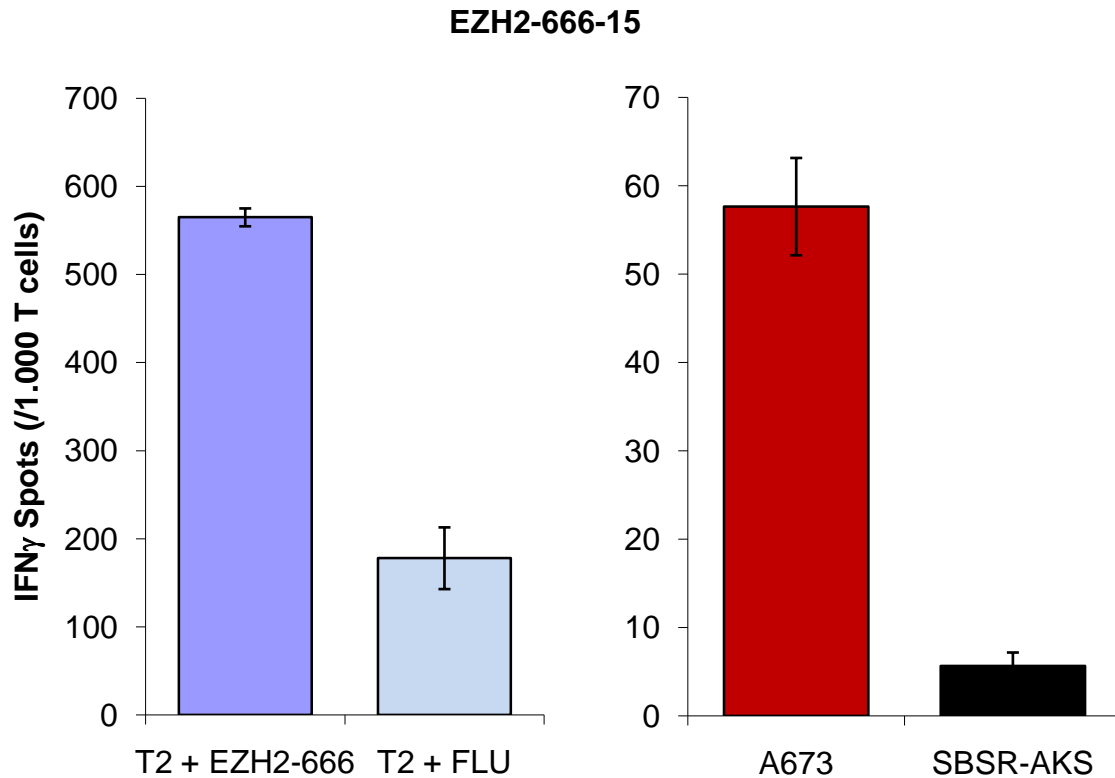


Figure 49: Peptide specificity of EZH2-666 15 and HLA-A*0201-specific recognition of EFT cell lines

EZH2-666-15 maintained peptide specificity and the ability to recognize the EFT cell line A673.

EZH2-666-15 was tested for IFN γ release after contact with two EFT cell lines. It recognized the HLA-A*0201⁺ cell line A673 and did not recognize the HLA-A*0201⁻ cell line SBSR-AKS.

The TCR V β repertoire of EZH2-666-15 was tested to get information about potential clonality of the CTL culture.

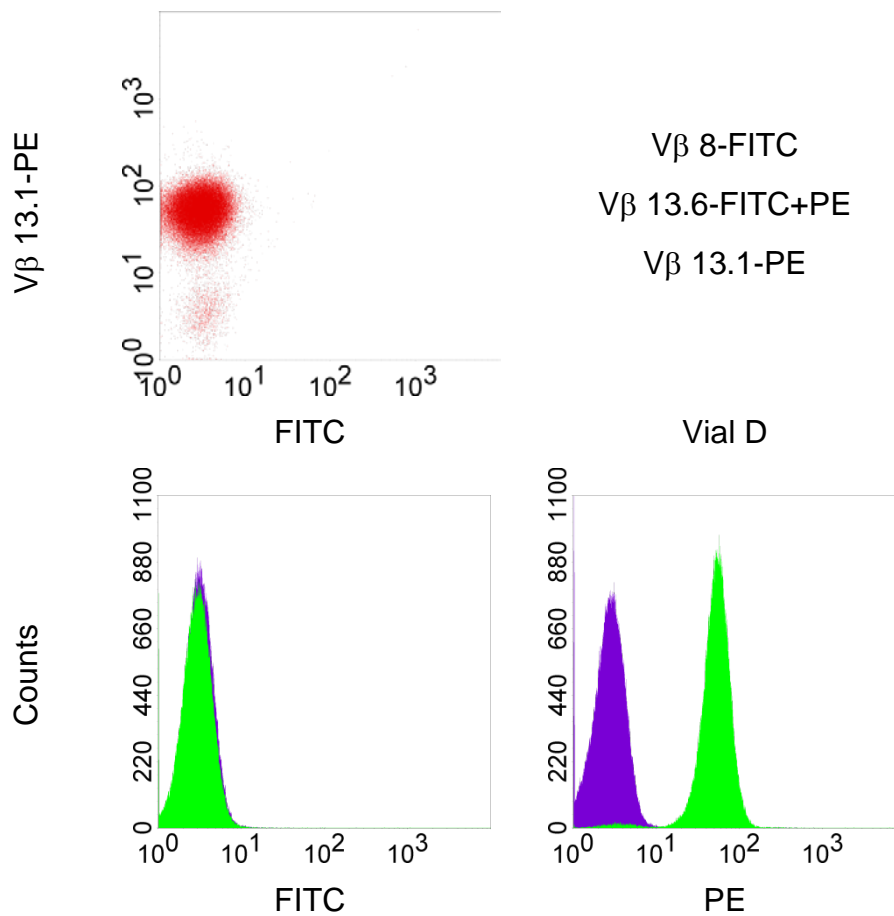


Figure 50: Dot plot (upper left) **and histograms** (bottom) **of EZH2-666-15**; vial D contains antibodies for three different V β families as shown on the upper right.

Of the eight vials containing 24 different TCR V β families only vial D gave a positive result. Vial D contains V β 8-FITC, V β 13.6-FITC+PE and V β 13.1-PE. As shown in Fig. 50 of these three, only the PE-marked V β 13.1 is expressed. EZH2-666-15 is positive for V β 13.1 and negative for all other tested V β families.

To ascertain the peptide affinity of the CTL clone a peptide titration assay was conducted. T2 cells were loaded with either the EZH2-666 peptide or – for negative control – the influenza peptide at different concentrations. IFN γ release was measured by ELISpot.

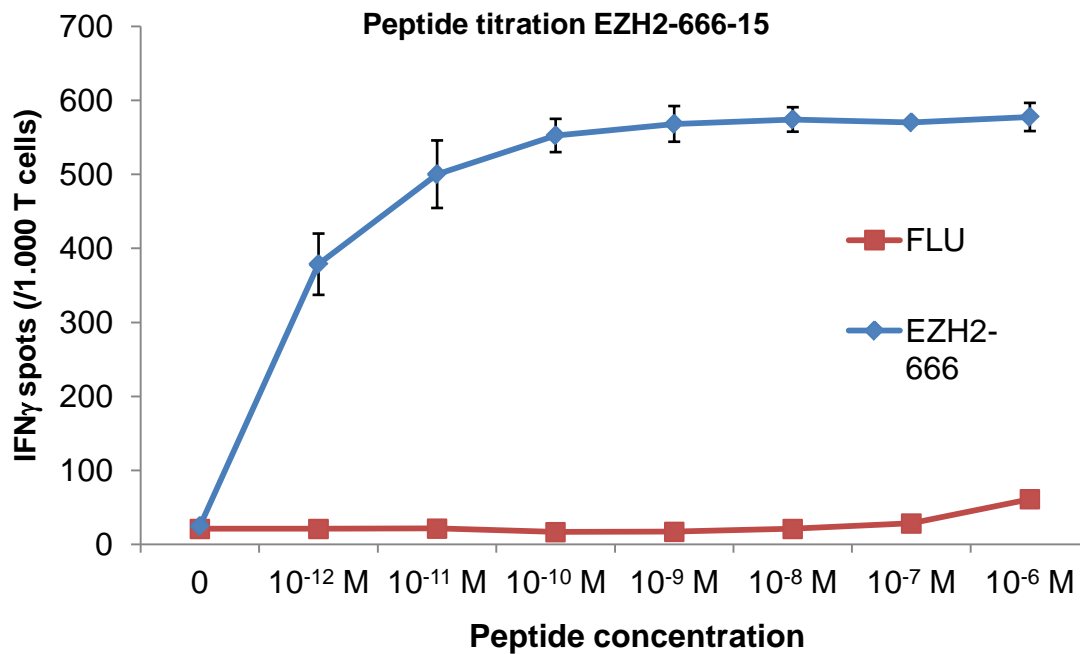


Figure 51: Peptide titration of clone 15 specific for EZH2-666

At concentration as low as 10⁻¹² M significant amounts of IFN γ were specifically released compared to the reaction to influenza peptide-pulsed T2 cells. At concentration of 10⁻¹⁰ M a plateau was reached.

The CTL culture EZH2-666-15 was shown to be peptide specific, able to recognize within HLA context EFT cell lines expressing EZH2. Left to show was the ability to kill this cell line specifically. This was done by granzyme B ELISpot (see Fig. 52).

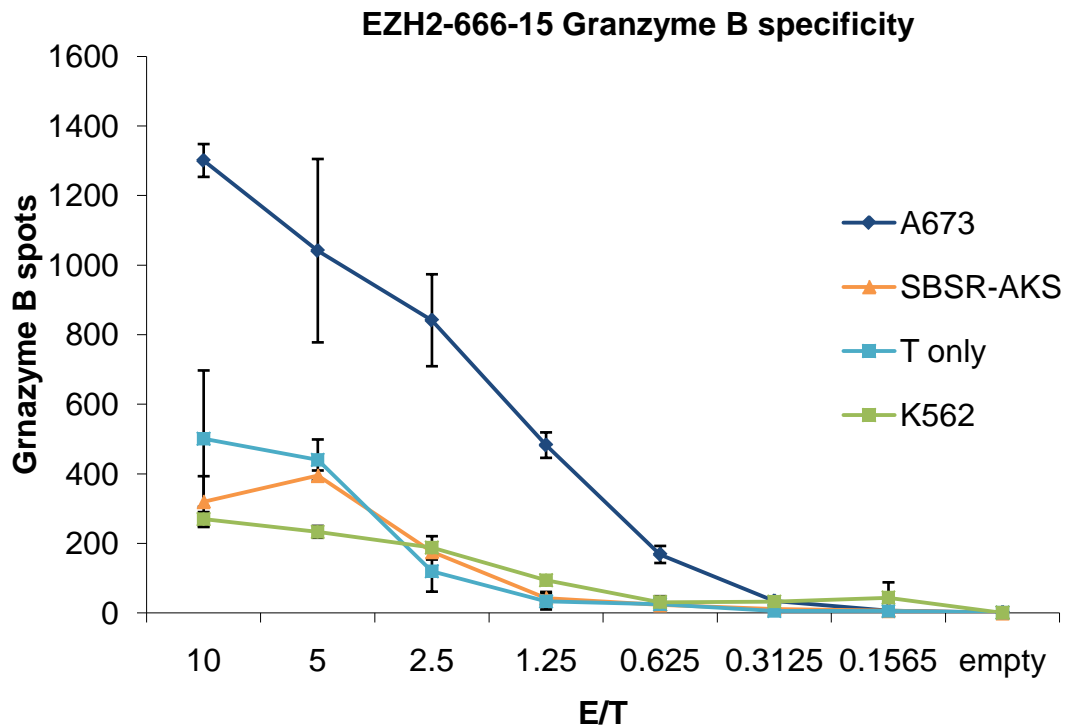


Figure 52: Specific cytotoxicity of EZH2-666-15; E/T: effector / target ratio

EZH2-666-15 specifically released granzyme B when mixed with the A673 cell line.

T cells alone controlled for spontaneous release. SBSR-AKS controlled the HLA context. K562 controlled for natural killer cell activity.

An additional control experiment was conducted to show the cytotoxic specificity of the EZH2-666-15 CTL clone (see Fig. 53). For this experiment, the two E / T ratios, where the difference in granzyme release between the EFT cell line A673 and the controls were most significant ($p < 0.01$), were used. The CTL culture releases more granzyme B when brought in contact with the HLA-A*0201⁺ EFT cell line A673 which expresses EZH2 at a high level than when brought in contact with the HLA-A*0201⁺ cALL cell line 697 which expresses EZH2 at a low level. The p values for the E / T ratios of 2.5 and 1.25 were 0.04 and 0.003 respectively.

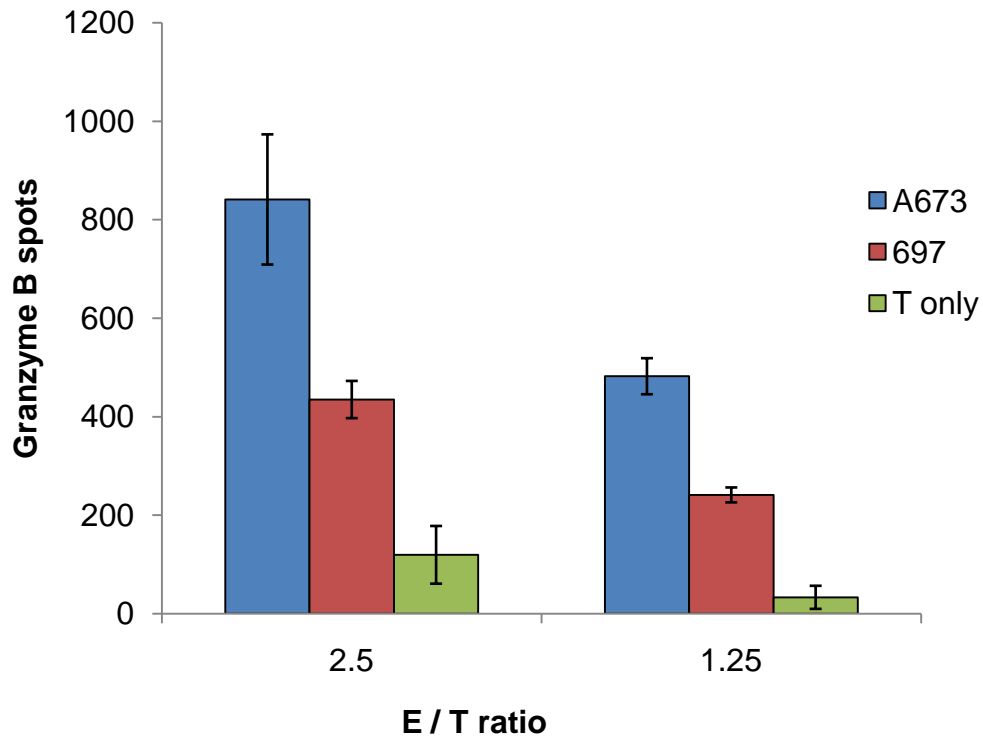


Figure 53: Granzyme B release after contact with two HLA-A*0201 positive cell lines; EZH2-666-15

The EZH2-666-15 CTL clone was identified as effector memory T cells (T_{EM}) by observing the capability of releasing $IFN\gamma$ and the absence of central memory T cell (T_{CM}) markers. The CTL culture was negative for CD27, CD28, CD45RA, CD62L, CCR5, CCR7 and CD127 as evaluated by flow cytometry (not shown).

5 Discussion

The EWS-FLI1 fusion protein which is pathognomonic in 85 percent of EFTs represents an ideal immunological target in search of immunogenic peptides for T cell based therapy. However, we were not able to validate any peptide from this fusion region as a good binder to HLA-A*0201 (66). Therefore we tried to identify CTL epitopes of other antigens that are specifically expressed in EFTs. In a previous microarray analysis we identified several genes as strongly up-regulated in EFTs (65). In this work six genes were classified as EFT-specific or EFT associated. STEAP and EZH2 are known genes associated with prostate cancer (94, 95). CHM1, LIPI, GPR64 and ITM2A were not previously known as tumor associated. ITM2A, as EZH2, is not EFT-specific as it is expressed in a wide variety of normal body tissue, but it is still over-expressed in EFT. The microarray data was verified by real-time PCR in the laboratory and the over-expression in EFT cell lines compared to other tumor cell lines and normal body tissue (not shown) was established.

A decision was made to focus on the HLA-A*0201 allele as it is the most frequent allele in “Caucasian” populations (105), and while not the most frequent allele, still very frequent in Asian and Black populations (106). In 2005, HLA-A*2 frequency in a sample group of 11.407 Germans included into the Bone Marrow Registry was determined to be 49.9 % (107). Reliable *in silico* prediction algorithms are very helpful to identify a CTL epitope. Those algorithms are trained with data sets of known epitopes. Many known published epitopes are HLA-A*0201-binding, so the accuracy for this allele is supposedly higher (85). Still, *in silico* high scoring epitope candidates have to be confirmed as HLA-binding *in vitro* before using them in assays. This was done and of 18 peptides tested six were identified as strong binders, including the previously described EZH2-666 and STEAP-86. This highlights the importance of this verification step.

The HLA-A*0201 status of the cell lines which expressed the gene of interest had to be determined, and cell lines were selected to establish an assay with controls for HLA restriction and gene specificity. SBSR-AKS was used as a control for HLA-A*0201 restriction. The cALL cell line 697 was used as a control

for gene specificity, as it is HLA-A*0201⁺ and does not express the gene of interest at high level (EZH2) or at all (CHM1).

Cell selection steps to obtain CD14⁺ PBMCs were controlled by flow cytometry. Only pure (> 95 percent) CD14 populations were used to generate DCs. DC generation and maturation was observed microscopically and controlled by flow cytometry. Only DC cultures expressing DC markers CD86, CD83 and HLA-DR at high level were used in IVP experiments. For the allogeneic approach purified CD8⁺ T cells were used for IVP. The efficacy of the T cell selection was also controlled by flow cytometry.

5.1 Autologous in vitro priming

To establish the method in our laboratory the first approach to obtain tumor-specific CTL was within the autologous context. T cells and DCs were isolated or generated from the same healthy donor. This simulates the situation where CD14⁺ PBMCs of a tumor-bearing host are isolated to generate DCs and the mature DCs are used to prime T cells of the same patient. Autologous CTLs will not induce the toxic side effects known as GvHD but the patient will also not benefit from the desired side effect called GvT. Another problem is the already compromised immune system of the patient. The T cell pool of the patient may be diminished by central tolerance effects resulting in clonal deletion of potential tumor-specific CTLs in the thymus (108). Another problem is the already compromised immune system of the patient, since most patients are already in treatment, mostly chemotherapy, which impairs their immune system. Ideally for the researcher, cells of a patient are harvested at the time point of tumor diagnosis before the beginning of treatment.

The first attempts to obtain EFT-specific CTLs were done with the epitopes CHM1-319 and LIPI-370. The experiment with LIPI-370 did not lead to isolation of specific T cells. Later, after establishing and conducting the peptide-binding assay with all peptides, this was obvious in hindsight, because LIPI-370 turned out not to be a binding peptide. After this failed attempt no further experiments were done without first testing the ordered peptide for specific binding *in vitro*. Still, the attempt to obtain peptide-specific CTLs for CHM1-319 was successful. After initially screening the T cells from the most promising well those cells

were cloned by limiting dilution and the best “clone” was selected for further testing. CHM1-319-24 was tested for clonality by flow cytometric based V β family analysis and was found to be “clonal” because only one of 24 tested V β families was detectable. To actually define clonality however, this approach is not sufficient. Not all V β families are represented in the test kit, families have subfamilies, and no statement about V α can be made. This, however, is not a proof of actual clonality. A complete TCR V β and V α analysis by PCR is needed to prove this. The CHM1-319-24 “clone” was found to be able to specifically release IFN γ and Perforin when mixed with T2 cells pulsed with the correct peptide compared to T2 cells pulsed with the irrelevant influenza peptide.

One significant problem associated with this of approach is the inability of predicting if a binding peptide is actually processed and presented *in vitro* as predicted *in silico*. The only way to explore this is to find out whether the candidate peptide is a native peptide, generated by proteasomal cleavage and by transport via TAP into the ER is to show recognition of the peptide by specific CTLs when confronted with cells expressing the target protein and the corresponding HLA allele. I was not able to demonstrate this with CHM1-319 in the autologous context (data not shown). The possible reasons for this are manifold: (i) It is possible that this specific clone was incapable of recognizing the epitope when presented by cell lines while another clone might be able to. (ii) The antigen density as presented by cell lines can never match that of a pulsed T2 cell. (iii) Low avid CTLs may not be able to react to low concentrations of antigen (109). (iv) The cell line might be a bad presenter, which cannot be remedied by up-regulating the HLA expression by co-culturing with IFN γ . (v) The worst case scenario is that the candidate epitope is not processed as predicted. This scenario was proven to be wrong by the results of the allogeneic experiments concerning the CHM1-319 and EZH2-666 epitopes. Several unsuccessful attempts were made to obtain specific CTLs for peptides derived from ITM2A, LIPI and additional peptides from GPR64 and CHM1. Partially successful attempts led to autologous CTLs specific for STEAP-86, GPR64-135 and EZH2-666. All these CTLs were specific when comparing IFN γ

and Perforin release after confrontation with T2 cells pulsed with either the correct peptide or the control peptide.

Alas, the same problem as with CHM1-319 was observed with GPR64-135. The CTLs were not able to recognize the peptide when possibly presented by EFT cell lines. GPR64-135, as CHM1-319, is a novel potential epitope, and it is possible that it is an artificial epitope. STEAP-86, however, is a known, previously published epitope (99). Another publication showed that the EFT cell line A673 is capable of presenting STEAP effectively, resulting in specific recognition and killing of the cell line by a CTL clone specific for another STEAP derived peptide epitope (110). EZH2-666 is also a previously published epitope detected in hepatocellular carcinoma and colorectal cancer (98).

Those findings established the EFT cell line A673 as a suitable cell line that is capable of presenting antigens. Failure to recognize EFT cell lines *in vitro* cannot be collectively explained by the epitopes not being processed as predicted because previously published and confirmed epitopes were similarly not recognized when presented by cell lines in my hands. But the method in principle was shown to be capable of obtaining peptide-specific CTLs. However, our goal from the beginning was to emulate an allogeneic approach, and with the commercial availability of custom MHC pentamers we switched to this method and hoped it would solve the problem with the CTL cultures not being able to recognize our tumor cell lines.

5.2 Allogeneic *in vitro* priming

Traditionally, cancer-specific immunity has been aimed at activating CD8⁺ CTLs directed against major MHC class I-binding peptide epitopes in the patient's body. Other approaches utilize T cell adoptive therapy where autologous, tumor-specific T cells propagated *in vitro* are transferred back into recipients. However, these strategies have met with limited success in part due to the regulatory mechanisms of T cell tolerance, which pose a considerable challenge to cancer immunotherapy (111). T cells with a high avidity to self antigens are eliminated in the thymus by clonal deletion. Remaining low-avidity T cells are not as effective in recognizing and killing cells presenting the antigen. To by-pass the tolerance related problems and problems with low-

avidity autologous T cells we tried an allogeneic approach where DCs presenting the antigen were HLA-A*0201 positive and the T cells to be primed were HLA-A*0201 negative.

In the autologous context it was possible to find the specific T cells by a simple ELISpot screening comparing IFN γ release of T cells from one well after contact with the correct antigen with the IFN γ release of T cells from the same well after contact with a negative control antigen. T cells from a well passing this screen were then cloned by limiting dilution. In the allogeneic setup the methodical problem is to detect and isolate the rare peptide-specific allorestricted CTLs amidst the vast majority of unspecific alloreactive T cells. This problem was solved by using the MHC-Pentamer-staining and sorting technology. After IVP T cells were pooled and stained with CD8-FITC antibody and the PE-linked peptide-specific pentamer. Double positive events were then detected and collected via flow cytometric cell sorting. This allowed obtaining specific T cells as rare as 0.01 % of the whole T cell bulk culture. The sorted cells were then cloned by limiting dilution. In the following IFN γ ELISpot screen an additional control was used to help solve the question if the *in silico* predicted peptide was actually processed *in vitro*. The simian cell line Cos-7 was co-transfected with vectors containing the human HLA-A*0201 gene and the gene of interest. Cos-7 is easily transfected and expresses the gene of interest at high levels. If the epitope is processed as predicted it should be presented to the T cells. However, as it is a transient transfection of two genes, the percentage of double positive Cos-7 is expected to be low (around 30 percent as measured cytometrically after transfection with HLA-A*0201 and the reporter gene GFP, not shown). Nevertheless, specific T cells should be able to release IFN γ after contact with double transfected Cos-7 if the epitope exists. As an additional negative control, Cos-7 cells were transfected only with the gene of interest. Those cells were not able to present the epitope, as the simian cell line lacks the human HLA allele.

5.2.1 EZH2-666

The custom pentamers synthesized by ProImmune are quite expensive. That's why we started the first experiment with an epitope previously described, EZH2-666. To my knowledge this epitope was not shown to be detected in EFT cell lines or patients.

0.03 percent of the stained T cells after allogeneic IVP were double positive for CD8 and EZH2-666-Pentamer-PE and were cloned by limiting dilution. The following IFN γ ELISpot screen showed clones with very differing behavior. But several clones passed the screen based on specificity and recognizing the artificial construct of the double transfected simian cell line.

This first result was the proof-of-principle needed. Epitope-specific T cells were isolated and expanded in the allogeneic context. Even more important, some allorestricted T cell clones were able to release IFN γ after contact with the EFT cell line A673, which I was unable to show with autologous T cells in this work.

The T cell culture No 15, which was performing best in the screens, was further characterized. It demonstrated sustained peptide-specificity proven by specific IFN γ release after contact with T2 cells pulsed with the EZH2-666 peptide. Peptide-specificity was also shown cytometrically, where more than 94 percent of the CTL culture was shown to bind to the specific pentamer. Furthermore, EZH2-666-15 was capable of recognizing the cell line A673. HLA-A*0201 specificity was further evidenced by showing that these T cells did not release IFN γ after contact with the HLA-A*0201⁻ cell line SBSR-AKS. As shown by real-time PCR, SBSR-AKS is expressing EZH2 at high levels. The CTL culture seemed to be a clone as it tested positive for only one of 24 TCR V β families as analyzed by flow cytometry. This, however, is not a proof of actual clonality as already mentioned for the autologous T cells (see 5.1, page 101).

To show the affinity of the CTL culture to the HLA-A*0201 bound peptide a peptide titration assay was performed and showed a half-maximal release of IFN γ at a peptide concentration lower than 1 pM. This supports the idea of having isolated a high avidity T cell clone.

The most important role of CTLs however is the cytotoxic effect on target cells. We measured this effect by granzyme B ELISpot which was published to be a suitable replacement for the more traditional chromium release assay (112).

EZH2-666-specific CTL culture No 15 specifically released granzyme B when mixed with the A673 cell line at E / T ratios from 0.625:1 to 10:1. The experiment was controlled for target specificity, HLA specificity and for spontaneous release. The biggest difference between signals was at ratios 1.25:1 and 2.5:1. For these E / T ratios an additional granzyme B ELISpot including the HLA-A*0201⁺ cALL cell line 697 was performed. 697 expressed EZH2 at a low level. A better control would be a HLA-A*0201 cell line that did not express EZH2 at all, but we were not able to find such a cell line, as EZH2 seems to be expressed in most tumor cell lines. Nevertheless, the number of granzyme B spots after contact with 697 was considerably less.

With these tests the CTL clone 15 was shown to be capable of recognizing and killing target cells that presented the peptide EZH2-666 specifically and within the expected HLA context.

5.2.2 CHM1-319

After the successful attempt with the published epitope for EZH2 we ordered custom pentamers for the novel epitope of the novel EFT-specific antigen CHM1. IVP was done as described and after sorting. 0.01 percent of the initial number of T cells (1.5×10^7) was cloned by limiting dilution. This was less than after sorting the CTLs for EZH2-666, but still successful which again highlights the efficiency of this method. Expanded clones were screened for IFN γ release; three clones passed the specificity test. The most promising clone No 12 unfortunately did not expand after this screening step. No 7 turned out to be not peptide-specific enough, so CHM1-319-17 was selected and further characterized.

This clone showed sustained peptide-specificity proven by specific IFN γ release after contact with T2 cells pulsed with the CHM1-319 peptide. Peptide-specificity was also shown cytometrically, where more than 68 percent of the CTL culture was observed to bind to the specific pentamer. The percentage and the fluorescence intensity were considerably less compared to EZH2-666-15. However, CHM1-319 was capable of recognizing the cell line A673. HLA-A*0201 specificity was shown because the culture did not release IFN γ after contact with the HLA-A*0201⁻ cell line SBSR-AKS. As shown by real-time PCR,

SBSR-AKS is expressing CHM1 at high levels. The CTL culture was definitely not a clone as it tested positive for two of 24 TCR V β families as tested by flow cytometry, V β 8 and V β 7.2. This can be a problem in further expansion steps, as it is possible that only one of these CTL clones in the culture is actually CHM1-319-specific and this clone may have been lost or overgrown by unspecific CTLs. This problem could be addressed by re-sorting the expanded culture, in the future.

The granzyme B ELISpot of this CTL culture showed that CHM1-319-17 specifically released granzyme B when mixed with the A673 cell line at E / T ratios from 0.3125:1 to 10:1. At E / T ratios above 2.5:1 however, granzyme B spots became confluent and were too numerous to count by the software. The experiment was controlled for target specificity, HLA specificity and for spontaneous release. The biggest difference between signals was at ratios 0.625:1 and 1.25:1. For these E / T ratios an additional granzyme B ELISpot including the HLA-A*0201⁺ cALL cell line 697 was performed. 697 cells do not express CHM1 at a detectable level in real-time PCR. The difference in granzyme B release was observable but not as clear-cut as desired, considering that 697 cells do not express CHM1 at all. Additionally, a peptide titration assay showed a reduced avidity of the CTL culture to the HLA-A*0201 bound peptide. Detectable levels of IFN γ started at a peptide concentration of 1 nM and did not yet reach a clear plateau at the highest concentration of 1 μ M. The overall level of IFN γ release was also lower when compared with EZH2-666-15.

These mixed signals led to doubts if the CTL culture actually was still CHM1-319-specific or if it had lost this ability in one of the expansion steps by being overgrown by unspecific T cells present in the culture. I repeated the cytotoxicity assay including this time T2 cells pulsed with the target peptide and T2 cells pulsed with the influenza peptide as a negative control. In this test the CTL of this expansion step showed a clear specificity. The granzyme B spots after contact with T2 cells loaded with CHM1 peptide were too numerous to count above an E / T ratio of 1.25:1. A673 cells were killed specifically, too, while T2 cells loaded with control peptide were not confronted with granzyme B release above a level of spontaneous release.

With these tests the CTL clone No 17 was shown to be capable of recognizing and killing target cells that presented the peptide CHM1-319 specifically and within HLA context.

CHM1-319-17 showed very varying behavior depending on the expansion. Most probable cause is the nature of the bulk culture. A clone is preferable but in this case the limiting dilution cloning was not successful. This is a common problem of the limiting dilution method (113). It is essential to guarantee expansion of the low number of cells collected by cell sorting. The statistical probability of cell expansion increases with the number of cells per well. Naturally, the increase in numbers of cells per well will lower the statistical probability of clonality of the expanded cells. This is a tradeoff which has to be made. To maximize my chances to obtain expansion of clones I used several plates with different numbers of T cells per well, screened the expanded clones and selected, whenever possible, the T cells stemming from a well with the lowest statistical number of T cells per well. In the case of EZH2-666-15 it seemed to be successful, in the case of CHM1-319 it clearly was not.

5.2.3 Comparison of autologous and allogeneic approach

The obvious difference between those two methods in my work was the success of the allogeneic approach in obtaining CTLs that were able to recognize and kill target cells that expressed the antigen endogenously. This established the epitopes CHM1-319 and EZH2-666 as valid targets specific for EFTs. The autologous approach is considerably less expensive, as no pentamer staining based cell sorting is involved. As previously published by several groups, it is possible to obtain autologous CTLs able to recognize the endogenously processed antigen. For STEAP-86 this was even shown with the EFT cell line A673 (99). In my hands, the allogeneic approach was superior and preferable as it is closer to the situation where these CTLs are given to a tumor patient after BMT as a replacement for bulk DLI. In the autologous approach no T cells could be generated that could recognize and kill EFT cell lines. The allogeneic approach also by-passes the problems associated with the possible absence of high avidity T cells due to clonal deletion in the autologous setting. It is possible to generate high avidity CTLs which can recognize low

concentrations of antigen. Those high avidity CTLs might be deleted from the repertoire by central tolerance mechanisms in the autologous context and not be available for IVP or activation. High avidity CTL clones are more likely to kill tumor cells *in vitro* (114) and *in vivo* (109). The case study of Koscielniak *et al.* in 2005 (34) also supports the idea of a better efficacy of allogeneic T cell therapy.

A general imponderability of the approach is the variability in behavior of the T cells which makes it hard to collect reproducible data. T cells react differently depending on activation status, expansion step and expansion conditions. The expansion conditions vary from expansion to expansion when using LCLs and PBMCs as feeder cells. In one case, the PBMCs overcame the irradiation and overgrew the CTLs. I ended up with an unspecific CD4⁺ clone! To minimize these differences it is essential to store the CTLs of the first expansion in very small aliquots (less than 1×10^6 per aliquot) and to start subsequent experiments by expanding these aliquots.

Furthermore, a problem of the whole approach however may be the discrepancy between *in vitro* results and *in vivo* results. Until recently, no mouse tumor model has been a good predictor of a successful human response to immunotherapy. New mouse models are emerging (e.g. Rag2 / γ c double knock-out mice; (115)) where a human immune system can be reconstituted by transplanting human hematopoietic stem cells into the liver after birth. These mice develop a competent human immune system and may present a better model. Another problem is the low immunogenic profile of the EFT. Melanoma (116) and renal cell carcinoma (117) are so far the only examples of immunogenic tumors which recruit TILs to the affected tissue.

Another key issue is that the method described in this work yields effector memory T cells which are able to recognize and kill antigen presenting target cells but may not be able to persist for a long time *in vivo* or maintain their cytotoxic repertoire. In 2005, Gattinoni *et al.* published that transferred CD8⁺ T cells were less efficacious in killing the tumor *in vivo* after acquiring full effector function *in vitro* than T cells that were still expressing T_{CM} markers like CD62L or CCR7 (118). T cell transfer experiments in mice have shown that T_{EM} cells persist only for a short time, whereas the transfer of T_{CM} results in a long-term

memory response and the differentiation of T_{EM} cells on antigen stimulation (119).

A more successful approach might be to change the interleukin treatment regimen during IVP culture to keep the T cells from fully differentiating into T_{EM}. The goal would be to obtain central memory T cells which can be given to a patient or a mouse with a human immune system. Those T_{CM} can then be differentiated into T_{EM} in the lymph nodes of the body in the natural and optimal environment. T_{CM} are expected to be persistent in the body and to be a lasting reservoir for optimal T_{EM} which can be activated anytime the target is re-detected (120, 121). Recently, a new method was published where the IVP was done with IL-21 instead of IL-2 resulting in T cells not able to release IFN γ *in vitro* but more effective in impeding tumor growth *in vivo* (122) than the *in vitro* IFN γ releasing T cells obtained by priming under the influence of IL-2. Selection of specific T cells for expansion was done by screening for specific IL-2 release. Such cells may have advantages over the cells generated here and this new approach is currently tried in our laboratory but is no longer part of this work.

The allorestricted T cells isolated in this thesis work not only specifically recognized peptide-pulsed or antigen-transfected cells in the context of HLA-A*0201 but also released granzyme B when recognizing HLA-A*0201⁺ EFT cell lines expressing the antigen while HLA-A*0201⁻ EFT cell lines were not affected. This emphasizes the high specificity and effectivity of the allorestricted T cells generated with this approach and opens the way for new therapeutic strategies in allogeneic stem and effector cell transplantation.

6 Summary

A set of genes was identified by previous DNA-microarray analysis as EFT-specific or EFT associated. These findings were validated by comparing mRNA levels of those genes in tissue derived from a normal body atlas and EFT cell lines. Several genes were selected as potential targets for adoptive T cell therapy. Potential CTL epitopes derived from the protein sequence of these genes were predicted *in silico*. Peptides representing these epitopes were synthesized and tested *in vitro* for binding to the HLA molecule. For practical reasons we focused on the HLA-A*0201 allele. HLA-A*0201⁺ dendritic cells were pulsed with the EFT-specific peptide and were used to prime T cells. EFT-specific CTLs were identified by specific IFN γ release in ELISpot assay. Specific CTLs were cloned by limiting dilution and further characterized. The first approach was set in autologous context where DCs and T cells were generated and isolated, respectively, from a healthy donor. For several epitopes derived from several EFT-specific genes peptide-specific CTLs were isolated. However, the autologous CTLs were not able to recognize the epitope or even kill the cells when it was presented by EFT cell lines. This led to a different approach, where the T cells were HLA-A*0201⁻. To isolate the specific T cells from the bulk of alloreactive T cells after *in vitro* priming they were stained with HLA-A*0201/peptide pentamers and sorted by flow cytometry. In this allogeneic setting two CTL lines were isolated which were able to recognize and kill EFT cell lines presenting the antigen within the HLA-A*0201 context as evaluated by IFN γ and granzyme B ELISpot. One CTL line was specific for the previously published peptide EZH2-666. To date this peptide has not been described as an antigen specific for EFT. The other CTL line is specific for a novel antigen, CHM1-319. The allogeneic approach was superior to the autologous approach. We have optimized the techniques for isolating and expanding antigen-specific allogeneic T cells and established that allogeneic, tumor-specific cytotoxic CD8⁺ T cells can be easily isolated via Peptide/HLA-pentamer technology and may benefit new therapeutic strategies in allogeneic stem cell transplantation.

7 Zusammenfassung

In einer bereits vor dieser Doktorarbeit veröffentlichten Arbeit wurde eine Reihe von Genen mittels DNA-Microarray-Analyse als EFT-spezifisch oder EFT-assoziiert identifiziert. Diese Ergebnisse wurden im Labor mittels real-time PCR Experimenten überprüft. Dabei wurde die mRNA-Expression der Kandidatengene in EFT Zelllinien mit der in normalem gesunden Gewebe aus vielen unterschiedlichen Körperteilen und Organen verglichen. Mehrere Gene wurden ausgewählt als Zielstrukturen für eine adoptive T-Zelltherapie. Aus den Proteinsequenzen dieser Gene wurde mittels bioinformatischer Algorithmen potentielle Peptidepitope vorhergesagt. Diese Peptide wurden synthetisiert und im Labor auf ihre Bindungsfähigkeit an HLA-Molekülen überprüft. Aus praktischen Gründen beschränkten wir uns auf das HLA-A*0201 Allel. HLA-A*0201⁺ dendritische Zellen wurden mit EFT-spezifischen Peptiden gepulst und dann benutzt, um T-Zellen zu „*primen*“. EFT-spezifische zytotoxische T-Zellen wurden mittels spezifischer IFN γ -Ausschüttung in ELISpot-Assays identifiziert. Die T-Zellen wurden dann durch Vereinzelung kloniert und weiter charakterisiert. In einem ersten Ansatz wurde im autologen Kontext gearbeitet. Dendritische Zellen und T-Zellen stammten von demselben gesunden Spender. Für mehrere EFT-spezifische Peptide wurden spezifische T-Zellen isoliert. Die autologen T-Zellen waren jedoch nicht in der Lage, das Antigen zu erkennen geschweige denn die Antigen-präsentierenden Zellen zu töten, wenn sie von EFT-Zelllinien präsentiert wurden. Das führte zu einem anderen Ansatz, in dem die T-Zellen HLA-A*0201⁻ waren und mit HLA-A*0201⁺ dendritische Zellen gepulst mit EFT-Peptiden stimuliert wurden. Um aus der Menge von alloreaktiven T-Zellen nach *in vitro priming* im allogenen Kontext die spezifischen T-Zellen zu isolieren, färbten wir die T-Zellen mit Fluoreszenzmarkierten, Peptid-spezifischen HLA-A*0201-Pentameren. Die gefärbten Zellen konnten dann sortiert und gesammelt werden.

Im allogenen Ansatz konnten zwei T-Zelllinien generiert werden, die die EFT-Zelllinien Peptid-spezifisch und im HLA-Kontext erkennen und töten konnten. Dies wurde mittels IFN γ - und Granzym B-ELISpots gezeigt. Eine T-Zell-Kultur war spezifisch für das bereits in anderen Tumoren bekannte Peptid EZH2-666. Es wurde aber noch nicht für den EFT beschrieben. Eine andere T-Zell-Kultur

war spezifisch für ein Peptid aus einem neuen unbekanntem Antigen, CHM1-319. Der allogene Ansatz war dem autologen weit überlegen. Die Techniken für die Isolierung und Vermehrung Antigen-spezifischer allogener T-Zellen wurden optimiert und es wurde gezeigt, dass solche T-Zellen schnell und einfach generiert und isoliert werden können. Diese T-Zellen können in der Zukunft bei allogenen Stammzelltransplantationen zur Therapieunterstützung eingesetzt werden.

8 Acknowledgements

I would like to thank Prof. Dr. Stefan Burdach for giving me the opportunity to work with the newly established research group for Funktionelle Genomik und Transplantationsbiologie at the Klinik und Poliklinik für Kinder- und Jugendmedizin, Klinikum Rechts der Isar der Technischen Universität München. This project was supported by an intramural grant to SB (KKF 8739175) and by the Rotary Club Munich-Blutenburg who were so kind to contribute generously to the acquisition of an ELISpot Reader System.

I also want to thank Prof. Dr. Wolfgang Wurst, who agreed to be the first examiner of my doctoral thesis despite the administrative effort and time he had to put into this.

I also want to express my gratitude to Günther Richter who shouldered all the work in guiding me, setting strategies and connecting me with other research groups. He helped me enormously by countering my defeatism in the face of this long research project and the many setbacks common to this field. He provided me with optimism and new ideas and generally was essential to this work. Thank you, Günther!

The friendly and supportive atmosphere inherent to the whole research group contributed essentially to the final outcome of my studies. In this context I would like to thank particularly Andreas Mollweide, Sabine Rößler and Colette Zobywalski who were with me in the beginning when our group was small and confined to a basement filled with old equipment and very old files, and a dead hedgehog. This first group pioneered and began establishing all the methods used to obtain the results presented in this thesis. I was so impressed that only some years later I will marry one of you. After the move into the new laboratory full of sunlight and shiny new machines the research group grew, and I must express my gratitude to all of you. You were great colleagues, not only but also in beer gardens. Without your support the completion of this dissertation would not have been possible.

I want to express my sincere gratitude to Helga Bernhard and her research group who set me on the right trail with their protocols and work regarding T cell

priming and expansion. Especially Julia Neudorfer and Heinke Conrad were very helpful and supportive.

Heike Pohla and Birgit Stadlbauer helped me a lot with problems related to the ELISpot procedure and took time out of their busy schedule to share their knowledge.

I want to thank Dirk Busch, Matthias Schiemann and Katleen Götsch for their technical expertise in conducting the cell sorting experiments.

I would like to thank Josef Mautner and Uta Behrends who were always helpful with advice, ideas, motivation and discussions, and especially with all problems relating to LCL generation and culture.

Apart from my colleagues, I would like to thank my family and friends who maybe have never lost faith in this long-term project.

9 References

1. O. Delattre *et al.*, *The Ewing family of tumors--a subgroup of small-round-cell tumors defined by specific chimeric transcripts*, *N Engl J Med* **331**, 294 (Aug 4, 1994).
2. A. Aurias, C. Rimbaut, D. Buffe, J. M. Zucker, A. Mazabraud, *Translocation involving chromosome 22 in Ewing's sarcoma. A cytogenetic study of four fresh tumors*, *Cancer Genet Cytogenet* **12**, 21 (May, 1984).
3. C. Turc-Carel *et al.*, *Chromosomes in Ewing's sarcoma. I. An evaluation of 85 cases of remarkable consistency of t(11;22)(q24;q12)*, *Cancer Genet Cytogenet* **32**, 229 (Jun, 1988).
4. O. Delattre *et al.*, *Gene fusion with an ETS DNA-binding domain caused by chromosome translocation in human tumours*, *Nature* **359**, 162 (Sep 10, 1992).
5. D. Schmidt, D. Harms, S. Burdach, *Malignant peripheral neuroectodermal tumours of childhood and adolescence*, *Virchows Arch A Pathol Anat Histopathol* **406**, 351 (1985).
6. J. Whang-Peng *et al.*, *Chromosome translocation in peripheral neuroepithelioma*, *N Engl J Med* **311**, 584 (Aug 30, 1984).
7. H. Kovar, *Context matters: the hen or egg problem in Ewing's sarcoma*, *Semin Cancer Biol* **15**, 189 (Jun, 2005).
8. J. A. del Regato, *James Ewing*, *Int J Radiat Oncol Biol Phys* **2**, 185 (Jan-Feb, 1977).
9. J. Ewing, Ed., *Neoplastic Diseases: A Treatise on Tumors (2nd edition)* (WB Saunders, Philadelphia, New York (1919), 1922), pp.
10. J Ewing, *Diffuse endothelioma of bone*, *Proc NY Pathol Soc* **21**, pp. 17 (1921).
11. A. G. Huvos, *James Ewing: cancer man*, *Ann Diagn Pathol* **2**, 146 (Apr, 1998).
12. M. Lahl, V. L. Fisher, K. Laschinger, *Ewing's sarcoma family of tumors: an overview from diagnosis to survivorship*, *Clin J Oncol Nurs* **12**, 89 (Feb, 2008).

13. K. L. Weber, A. Makimoto, A. K. Raymond, M. G. Pearson, N. Jaffe, *Ewing sarcoma of the clavicle in a 10-month-old patient*, *Med Pediatr Oncol* **34**, 445 (Jun, 2000).
14. G. Bacci *et al.*, *Serum lactate dehydrogenase (LDH) as a tumor marker in Ewing's sarcoma*, *Tumori* **74**, 649 (Dec 31, 1988).
15. N. Weidner, J. Tjoe, *Immunohistochemical profile of monoclonal antibody O13: antibody that recognizes glycoprotein p30/32MIC2 and is useful in diagnosing Ewing's sarcoma and peripheral neuroepithelioma*, *Am J Surg Pathol* **18**, 486 (May, 1994).
16. J. Zucman *et al.*, *Combinatorial generation of variable fusion proteins in the Ewing family of tumours*, *Embo J* **12**, 4481 (Dec, 1993).
17. J. S. Miser *et al.*, *Treatment of metastatic Ewing's sarcoma or primitive neuroectodermal tumor of bone: evaluation of combination ifosfamide and etoposide--a Children's Cancer Group and Pediatric Oncology Group study*, *J Clin Oncol* **22**, 2873 (Jul 15, 2004).
18. S. Burdach, H. Jurgens, *High-dose chemoradiotherapy (HDC) in the Ewing family of tumors (EFT)*, *Crit Rev Oncol Hematol* **41**, 169 (Feb, 2002).
19. D. S. Hawkins *et al.*, *Peripheral blood stem cell support reduces the toxicity of intensive chemotherapy for children and adolescents with metastatic sarcomas*, *Cancer* **95**, 1354 (Sep 15, 2002).
20. J. Dunst, A. Schuck, *Role of radiotherapy in Ewing tumors*, *Pediatr Blood Cancer* **42**, 465 (May, 2004).
21. E. A. Kolb *et al.*, *Long-term event-free survival after intensive chemotherapy for Ewing's family of tumors in children and young adults*, *J Clin Oncol* **21**, 3423 (Sep 15, 2003).
22. K. Tanaka, T. Matsunobu, A. Sakamoto, S. Matsuda, Y. Iwamoto, *High-dose chemotherapy and autologous peripheral blood stem-cell transfusion after conventional chemotherapy for patients with high-risk Ewing's tumors*, *J Orthop Sci* **7**, 477 (2002).
23. H. Jurgens *et al.*, *[The Cooperative Ewing Sarcoma Study CESS 81 of the German Pediatric Oncology Society--analysis after 4 years]*, *Klin Padiatr* **197**, 225 (May-Jun, 1985).

24. C. Rodriguez-Galindo, S. L. Spunt, A. S. Pappo, *Treatment of Ewing sarcoma family of tumors: current status and outlook for the future*, *Med Pediatr Oncol* **40**, 276 (May, 2003).
25. H. Y. Huang *et al.*, *Ewing sarcomas with p53 mutation or p16/p14ARF homozygous deletion: a highly lethal subset associated with poor chemoresponse*, *J Clin Oncol* **23**, 548 (Jan 20, 2005).
26. H. E. Grier, *The Ewing family of tumors. Ewing's sarcoma and primitive neuroectodermal tumors*, *Pediatr Clin North Am* **44**, 991 (Aug, 1997).
27. H. E. Grier *et al.*, *Addition of ifosfamide and etoposide to standard chemotherapy for Ewing's sarcoma and primitive neuroectodermal tumor of bone*, *N Engl J Med* **348**, 694 (Feb 20, 2003).
28. P. A. Meyers *et al.*, *High-dose melphalan, etoposide, total-body irradiation, and autologous stem-cell reconstitution as consolidation therapy for high-risk Ewing's sarcoma does not improve prognosis*, *J Clin Oncol* **19**, 2812 (Jun 1, 2001).
29. B. H. Kushner, P. A. Meyers, *How effective is dose-intensive/myeloablative therapy against Ewing's sarcoma/primitive neuroectodermal tumor metastatic to bone or bone marrow? The Memorial Sloan-Kettering experience and a literature review*, *J Clin Oncol* **19**, 870 (Feb 1, 2001).
30. M. Paulussen *et al.*, *Primary metastatic (stage IV) Ewing tumor: survival analysis of 171 patients from the EICESS studies. European Intergroup Cooperative Ewing Sarcoma Studies*, *Ann Oncol* **9**, 275 (Mar, 1998).
31. E. Hendershot, *Treatment approaches for metastatic Ewing's sarcoma: a review of the literature*, *J Pediatr Oncol Nurs* **22**, 339 (Nov-Dec, 2005).
32. S. Burdach *et al.*, *Allogeneic and autologous stem-cell transplantation in advanced Ewing tumors. An update after long-term follow-up from two centers of the European Intergroup study EICESS. Stem-Cell Transplant Programs at Dusseldorf University Medical Center, Germany and St. Anna Kinderspital, Vienna, Austria*, *Ann Oncol* **11**, 1451 (Nov, 2000).
33. S. Burdach *et al.*, *High-dose therapy for patients with primary multifocal and early relapsed Ewing's tumors: results of two consecutive regimens assessing the role of total-body irradiation*, *J Clin Oncol* **21**, 3072 (Aug 15, 2003).

34. E. Koscielniak *et al.*, *Graft-versus-Ewing sarcoma effect and long-term remission induced by haploidentical stem-cell transplantation in a patient with relapse of metastatic disease*, *J Clin Oncol* **23**, 242 (Jan 1, 2005).
35. C. H. June, *Adoptive T cell therapy for cancer in the clinic*, *J Clin Invest* **117**, 1466 (Jun, 2007).
36. V. Shankaran *et al.*, *IFN γ and lymphocytes prevent primary tumour development and shape tumour immunogenicity*, *Nature* **410**, 1107 (Apr 26, 2001).
37. C. M. Southam, A. Brunschwig, A. G. Levin, Q. S. Dizon, *Effect of leukocytes on transplantability of human cancer*, *Cancer* **19**, 1743 (Nov, 1966).
38. A. M. Leen, C. M. Rooney, A. E. Foster, *Improving T cell therapy for cancer*, *Annu Rev Immunol* **25**, 243 (2007).
39. V. H. Engelhard, T. N. Bullock, T. A. Colella, S. L. Sheasley, D. W. Mullins, *Antigens derived from melanocyte differentiation proteins: self-tolerance, autoimmunity, and use for cancer immunotherapy*, *Immunol Rev* **188**, 136 (Oct, 2002).
40. D. E. Speiser *et al.*, *Self antigens expressed by solid tumors Do not efficiently stimulate naive or activated T cells: implications for immunotherapy*, *J Exp Med* **186**, 645 (Aug 29, 1997).
41. A. F. Ochsenbein *et al.*, *Immune surveillance against a solid tumor fails because of immunological ignorance*, *Proc Natl Acad Sci U S A* **96**, 2233 (Mar 2, 1999).
42. R. M. Teague *et al.*, *Interleukin-15 rescues tolerant CD8 $^+$ T cells for use in adoptive immunotherapy of established tumors*, *Nat Med* **12**, 335 (Mar, 2006).
43. T. M. Clay *et al.*, *Efficient transfer of a tumor antigen-reactive TCR to human peripheral blood lymphocytes confers anti-tumor reactivity*, *J Immunol* **163**, 507 (Jul 1, 1999).
44. P. Hwu *et al.*, *In vivo antitumor activity of T cells redirected with chimeric antibody/T-cell receptor genes*, *Cancer Res* **55**, 3369 (Aug 1, 1995).
45. A. C. Armstrong, D. Eaton, J. C. Ewing, *Science, medicine, and the future: Cellular immunotherapy for cancer*, *Bmj* **323**, 1289 (Dec 1, 2001).

46. J. Banchereau *et al.*, *Immunobiology of dendritic cells*, *Annu Rev Immunol* **18**, 767 (2000).
47. F. Meyer-Wentrup, S. Burdach, *Efficacy of dendritic cell generation for clinical use: recovery and purity of monocytes and mature dendritic cells after immunomagnetic sorting or adherence selection of CD14+ starting populations*, *J Hematother Stem Cell Res* **12**, 289 (Jun, 2003).
48. F. O. Nestle *et al.*, *Vaccination of melanoma patients with peptide- or tumor lysate-pulsed dendritic cells*, *Nat Med* **4**, 328 (Mar, 1998).
49. A. Kugler *et al.*, *Retraction: Regression of human metastatic renal cell carcinoma after vaccination with tumor cell-dendritic cell hybrids*, *Nat Med* **9**, 1221 (Sep, 2003).
50. J. D. Geiger *et al.*, *Vaccination of pediatric solid tumor patients with tumor lysate-pulsed dendritic cells can expand specific T cells and mediate tumor regression*, *Cancer Res* **61**, 8513 (Dec 1, 2001).
51. M. H. Huls, C. M. Rooney, H. E. Heslop, *Adoptive T-cell therapy for Epstein-Barr virus-positive Hodgkin's disease*, *Acta Haematol* **110**, 149 (2003).
52. B. Savoldo *et al.*, *Autologous Epstein-Barr virus (EBV)-specific cytotoxic T cells for the treatment of persistent active EBV infection*, *Blood* **100**, 4059 (Dec 1, 2002).
53. T. Haque *et al.*, *Allogeneic cytotoxic T-cell therapy for EBV-positive posttransplantation lymphoproliferative disease: results of a phase 2 multicenter clinical trial*, *Blood* **110**, 1123 (Aug 15, 2007).
54. S. A. Rosenberg, N. P. Restifo, J. C. Yang, R. A. Morgan, M. E. Dudley, *Adoptive cell transfer: a clinical path to effective cancer immunotherapy*, *Nat Rev Cancer* **8**, 299 (Apr, 2008).
55. F. Jotereau *et al.*, *High-fold expansion of human cytotoxic T-lymphocytes specific for autologous melanoma cells for use in immunotherapy*, *J Immunother (1991)* **10**, 405 (Dec, 1991).
56. C. Yee *et al.*, *Adoptive T cell therapy using antigen-specific CD8+ T cell clones for the treatment of patients with metastatic melanoma: in vivo persistence, migration, and antitumor effect of transferred T cells*, *Proc Natl Acad Sci U S A* **99**, 16168 (Dec 10, 2002).

57. C. Yee *et al.*, *Melanocyte destruction after antigen-specific immunotherapy of melanoma: direct evidence of t cell-mediated vitiligo*, *J Exp Med* **192**, 1637 (Dec 4, 2000).
58. A. Mackensen *et al.*, *Phase I study of adoptive T-cell therapy using antigen-specific CD8+ T cells for the treatment of patients with metastatic melanoma*, *J Clin Oncol* **24**, 5060 (Nov 1, 2006).
59. R. A. Morgan *et al.*, *Cancer regression in patients after transfer of genetically engineered lymphocytes*, *Science* **314**, 126 (Oct 6, 2006).
60. M. E. Dudley *et al.*, *Cancer regression and autoimmunity in patients after clonal repopulation with antitumor lymphocytes*, *Science* **298**, 850 (Oct 25, 2002).
61. W. Jeal, K. L. Goa, *Aldesleukin (recombinant interleukin-2): a review of its pharmacological properties, clinical efficacy and tolerability in patients with renal cell carcinoma*, *BioDrugs* **7**, 285 (Apr, 1997).
62. R. A. Figlin *et al.*, *Multicenter, randomized, phase III trial of CD8(+) tumor-infiltrating lymphocytes in combination with recombinant interleukin-2 in metastatic renal cell carcinoma*, *J Clin Oncol* **17**, 2521 (Aug, 1999).
63. R. Childs *et al.*, *Regression of metastatic renal-cell carcinoma after nonmyeloablative allogeneic peripheral-blood stem-cell transplantation*, *N Engl J Med* **343**, 750 (Sep 14, 2000).
64. T. Mutis *et al.*, *Feasibility of immunotherapy of relapsed leukemia with ex vivo-generated cytotoxic T lymphocytes specific for hematopoietic system-restricted minor histocompatibility antigens*, *Blood* **93**, 2336 (Apr 1, 1999).
65. M. S. Staeger *et al.*, *DNA microarrays reveal relationship of Ewing family tumors to both endothelial and fetal neural crest-derived cells and define novel targets*, *Cancer Res* **64**, 8213 (Nov 15, 2004).
66. F. Meyer-Wentrup, G. Richter, S. Burdach, *Identification of an immunogenic EWS-FLI1-derived HLA-DR-restricted T helper cell epitope*, *Pediatr Hematol Oncol* **22**, 297 (Jun, 2005).
67. H. W. Findley, Jr., M. D. Cooper, T. H. Kim, C. Alvarado, A. H. Ragab, *Two new acute lymphoblastic leukemia cell lines with early B-cell phenotypes*, *Blood* **60**, 1305 (Dec, 1982).

68. J. Tomeczkowski *et al.*, *Absence of G-CSF receptors and absent response to G-CSF in childhood Burkitt's lymphoma and B-ALL cells*, *Br J Haematol* **89**, 771 (Apr, 1995).
69. D. J. Giard *et al.*, *In vitro cultivation of human tumors: establishment of cell lines derived from a series of solid tumors*, *J Natl Cancer Inst* **51**, 1417 (Nov, 1973).
70. K. Kodama *et al.*, *Establishment and characterization of a new Ewing's sarcoma cell line*, *Cancer Genet Cytogenet* **57**, 19 (Nov, 1991).
71. H. R. Schlesinger, J. M. Gerson, P. S. Moorhead, H. Maguire, K. Hummeler, *Establishment and characterization of human neuroblastoma cell lines*, *Cancer Res* **36**, 3094 (Sep, 1976).
72. Y. Gluzman, *SV40-transformed simian cells support the replication of early SV40 mutants*, *Cell* **23**, 175 (Jan, 1981).
73. T. Pietsch, *abstract only*, *Cancer Genet* **38** (1989).
74. T. Pietsch *et al.*, *Characterization of a continuous cell line (MHH-NB-11) derived from advanced neuroblastoma*, *Anticancer Res* **8**, 1329 (Nov-Dec, 1988).
75. R. Hurwitz *et al.*, *Characterization of a leukemic cell line of the pre-B phenotype*, *Int J Cancer* **23**, 174 (Feb, 1979).
76. G. H. Richter *et al.*, *EZH2 is a mediator of EWS/FLI1 driven tumor growth and metastasis blocking endothelial and neuro-ectodermal differentiation*, *Proc Natl Acad Sci U S A* **106**, 5324 (Mar 31, 2009).
77. J. L. Biedler, L. Helson, B. A. Spengler, *Morphology and growth, tumorigenicity, and cytogenetics of human neuroblastoma cells in continuous culture*, *Cancer Res* **33**, 2643 (Nov, 1973).
78. E. T. Bloom, *Further definition by cytotoxicity tests of cell surface antigens of human sarcomas in culture*, *Cancer Res* **32**, 960 (May, 1972).
79. R. D. Salter, D. N. Howell, P. Cresswell, *Genes regulating HLA class I antigen expression in T-B lymphoblast hybrids*, *Immunogenetics* **21**, 235 (1985).
80. J. Whang-Peng *et al.*, *Cytogenetic characterization of selected small round cell tumors of childhood*, *Cancer Genet Cytogenet* **21**, 185 (Apr 1, 1986).

81. Amaxa. (Lonza, 2009), vol. 2009.
82. B. Feuerstein *et al.*, *A method for the production of cryopreserved aliquots of antigen-preloaded, mature dendritic cells ready for clinical use*, *J Immunol Methods* **245**, 15 (Nov 1, 2000).
83. H. Rammensee, J. Bachmann, N. P. Emmerich, O. A. Bachor, S. Stevanovic, *SYFPEITHI: database for MHC ligands and peptide motifs*, *Immunogenetics* **50**, 213 (Nov, 1999).
84. K. C. Parker, M. A. Bednarek, J. E. Coligan, *Scheme for ranking potential HLA-A2 binding peptides based on independent binding of individual peptide side-chains*, *J Immunol* **152**, 163 (Jan 1, 1994).
85. M. V. Larsen *et al.*, *An integrative approach to CTL epitope prediction: a combined algorithm integrating MHC class I binding, TAP transport efficiency, and proteasomal cleavage predictions*, *Eur J Immunol* **35**, 2295 (Aug, 2005).
86. H. W. Nijman *et al.*, *Identification of peptide sequences that potentially trigger HLA-A2.1-restricted cytotoxic T lymphocytes*, *Eur J Immunol* **23**, 1215 (Jun, 1993).
87. G. Stuber *et al.*, *Identification of wild-type and mutant p53 peptides binding to HLA-A2 assessed by a peptide loading-deficient cell line assay and a novel major histocompatibility complex class I peptide binding assay*, *Eur J Immunol* **24**, 765 (Mar, 1994).
88. K. Y. Lee, E. Chun, N. Y. Kim, B. L. Seong, *Characterization of HLA-A2.1-restricted epitopes, conserved in both Hantaan and Sin Nombre viruses, in Hantaan virus-infected patients*, *J Gen Virol* **83**, 1131 (May, 2002).
89. A. Moosmann *et al.*, *B cells immortalized by a mini-Epstein-Barr virus encoding a foreign antigen efficiently reactivate specific cytotoxic T cells*, *Blood* **100**, 1755 (Sep 1, 2002).
90. K. Masuda *et al.*, *Loss or down-regulation of HLA class I expression at the allelic level in freshly isolated leukemic blasts*, *Cancer Sci* **98**, 102 (Jan, 2007).
91. C. H. Chang, J. Hammer, J. E. Loh, W. L. Fodor, R. A. Flavell, *The activation of major histocompatibility complex class I genes by interferon regulatory factor-1 (IRF-1)*, *Immunogenetics* **35**, 378 (1992).

92. Y. Hiraki *et al.*, *Molecular cloning of human chondromodulin-I, a cartilage-derived growth modulating factor, and its expression in Chinese hamster ovary cells*, *Eur J Biochem* **260**, 869 (Mar, 1999).
93. C. Osterhoff, R. Ivell, C. Kirchhoff, *Cloning of a human epididymis-specific mRNA, HE6, encoding a novel member of the seven transmembrane-domain receptor superfamily*, *Dev Biol* **16**, 379 (Apr, 1997).
94. S. Varambally *et al.*, *The polycomb group protein EZH2 is involved in progression of prostate cancer*, *Nature* **419**, 624 (Oct 10, 2002).
95. R. S. Hubert *et al.*, *STEAP: a prostate-specific cell-surface antigen highly expressed in human prostate tumors*, *Proc Natl Acad Sci U S A* **96**, 14523 (Dec 7, 1999).
96. M. Mao *et al.*, *Identification of genes expressed in human CD34(+) hematopoietic stem/progenitor cells by expressed sequence tags and efficient full-length cDNA cloning*, *Proc Natl Acad Sci U S A* **95**, 8175 (Jul 7, 1998).
97. J. L. Foell *et al.*, *Membrane-associated phospholipase A1 beta (LIPI) Is an Ewing tumour-associated cancer/testis antigen*, *Pediatr Blood Cancer* **51**, 228 (Aug, 2008).
98. J. C. Steele *et al.*, *The polycomb group proteins, BMI-1 and EZH2, are tumour-associated antigens*, *Br J Cancer* **95**, 1202 (Nov 6, 2006).
99. P. M. Alves *et al.*, *STEAP, a prostate tumor antigen, is a target of human CD8+ T cells*, *Cancer Immunol Immunother* **55**, 1515 (Dec, 2006).
100. V. Dutoit, P. Guillaume, P. Romero, J. C. Cerottini, D. Valmori, *Functional analysis of HLA-A*0201/Melan-A peptide multimer+ CD8+ T cells isolated from an HLA-A*0201- donor: exploring tumor antigen allorestricted recognition*, *Cancer Immun* **2**, 7 (Jul 12, 2002).
101. T. Mutis, E. Blokland, M. Kester, E. Schrama, E. Goulmy, *Generation of minor histocompatibility antigen HA-1-specific cytotoxic T cells restricted by nonself HLA molecules: a potential strategy to treat relapsed leukemia after HLA-mismatched stem cell transplantation*, *Blood* **100**, 547 (Jul 15, 2002).
102. P. J. Amrolia *et al.*, *Allorestricted cytotoxic T cells specific for human CD45 show potent antileukemic activity*, *Blood* **101**, 1007 (Feb 1, 2003).

103. A. M. Whitelegg *et al.*, *Investigation of peptide involvement in T cell allorecognition using recombinant HLA class I multimers*, *J Immunol* **175**, 1706 (Aug 1, 2005).
104. I. G. Schuster *et al.*, *Allorestricted T cells with specificity for the FMNL1-derived peptide PP2 have potent antitumor activity against hematologic and other malignancies*, *Blood* **110**, 2931 (Oct 15, 2007).
105. P. Sanchez-Velasco, N. S. Karadsheh, A. Garcia-Martin, C. Ruiz de Alegria, F. Leyva-Cobian, *Molecular analysis of HLA allelic frequencies and haplotypes in Jordanians and comparison with other related populations*, *Hum Immunol* **62**, 901 (Sep, 2001).
106. K. Cao *et al.*, *Analysis of the frequencies of HLA-A, B, and C alleles and haplotypes in the five major ethnic groups of the United States reveals high levels of diversity in these loci and contrasting distribution patterns in these populations*, *Hum Immunol* **62**, 1009 (Sep, 2001).
107. D. Middleton, L. Menchaca, H. Rood, R. Komerofsky, *New allele frequency database: <http://www.allelefrequencies.net>*, *Tissue Antigens* **61**, 403 (May, 2003).
108. W. W. Overwijk, *Breaking tolerance in cancer immunotherapy: time to ACT*, *Curr Opin Immunol* **17**, 187 (Apr, 2005).
109. R. H. McMahan, J. E. Slansky, *Mobilizing the low-avidity T cell repertoire to kill tumors*, *Semin Cancer Biol* **17**, 317 (Aug, 2007).
110. D. A. Rodeberg, R. A. Nuss, S. F. Elsawa, E. Celis, *Recognition of six-transmembrane epithelial antigen of the prostate-expressing tumor cells by peptide antigen-induced cytotoxic T lymphocytes*, *Clin Cancer Res* **11**, 4545 (Jun 15, 2005).
111. K. Shafer-Weaver, M. Anderson, A. Malyguine, A. A. Hurwitz, *T cell tolerance to tumors and cancer immunotherapy*, *Adv Exp Med Biol* **601**, 357 (2007).
112. K. Shafer-Weaver *et al.*, *The Granzyme B ELISPOT assay: an alternative to the 51Cr-release assay for monitoring cell-mediated cytotoxicity*, *J Transl Med* **1**, 14 (Dec 29, 2003).
113. R. Staszewski, *Murphy's law of limiting dilution cloning*, *Stat Med* **9**, 457 (Apr, 1990).

114. E. Sadovnikova, H. J. Stauss, *Peptide-specific cytotoxic T lymphocytes restricted by nonself major histocompatibility complex class I molecules: reagents for tumor immunotherapy*, *Proc Natl Acad Sci U S A* **93**, 13114 (Nov 12, 1996).
115. E. Traggiai *et al.*, *Development of a human adaptive immune system in cord blood cell-transplanted mice*, *Science* **304**, 104 (Apr 2, 2004).
116. D. A. Oble, R. Loewe, P. Yu, M. C. Mihm, Jr., *Focus on TILs: prognostic significance of tumor infiltrating lymphocytes in human melanoma*, *Cancer Immun* **9**, 3 (2009).
117. G. Markel *et al.*, *Preclinical evaluation of adoptive cell therapy for patients with metastatic renal cell carcinoma*, *Anticancer Res* **29**, 145 (Jan, 2009).
118. L. Gattinoni *et al.*, *Acquisition of full effector function in vitro paradoxically impairs the in vivo antitumor efficacy of adoptively transferred CD8+ T cells*, *J Clin Invest* **115**, 1616 (Jun, 2005).
119. M. L. Disis, H. Bernhard, E. M. Jaffee, *Use of tumour-responsive T cells as cancer treatment*, *Lancet* **373**, 673 (Feb 21, 2009).
120. R. Perret, F. Ronchese, *Memory T cells in cancer immunotherapy: which CD8 T-cell population provides the best protection against tumours?*, *Tissue Antigens* **72**, 187 (Sep, 2008).
121. J. T. Opferman, B. T. Ober, P. G. Ashton-Rickardt, *Linear differentiation of cytotoxic effectors into memory T lymphocytes*, *Science* **283**, 1745 (Mar 12, 1999).
122. C. S. Hinrichs *et al.*, *IL-2 and IL-21 confer opposing differentiation programs to CD8+ T cells for adoptive immunotherapy*, *Blood* **111**, 5326 (Jun 1, 2008).

10 Abbreviations

aa	Amino acids
APC	Allophycocyanin
β_2 M	β_2 -Microglobulin
COG	Children's oncology group
CTL	Cytotoxic T lymphocyte
DC	Dendritic cell
DEPC	Diethylpyrocarbonate
DLI	Donor Lymphocyte Infusion
dNTP	Deoxyribonucleotide triphosphate
DSMZ	Deutsche Sammlung für Mikroorganismen und Zellkulturen
DTT	Dithiothreitol
E / T	Effector to target (ratio)
EBV	Epstein-Barr-Virus
EFS	Event free survival
EFT	Ewing Family of Tumors
EICESS	European Intergroup Cooperative Ewing's Sarcoma Study
ELISpot	Enzyme linked immune sorbent Spot
ER	Endoplasmatic reticulum
EWS	Ewing's Sarcoma oncogene
FISH	Fluorescence <i>in situ</i> hybridization
FITC	Fluorescein isothiocyanate
FLI1	Friend leukemia integration
FBS	Fetal bovine serum
FCS	Fetal calf serum
FSC	Forward scatter
GB	Granzyme B
GFP	Green fluorescent protein
GvHD	Graft <i>versus</i> Host Disease

GvL	Graft <i>versus</i> Leukemia
GvT	Graft <i>versus</i> Tumor
HLA	Human Leukocyte Antigen
IFN	Interferon
IL	Interleukin
IVP	<i>in vitro</i> priming
LCL	Lymphoblastoid cell line
MART	Melanoma Antigen Recognized by T cells
MHC	Major Histocompatibility complex
MPNT	Malignant peripheral neuroectodermal tumor
NTC	Non template control
OMIM	Online Mendelian Inheritance in Man
PBL	Peripheral blood lymphocyte
PBMC	Peripheral blood mononuclear cell
PBS	phosphate buffered saline
PcG	Polycomb Group
PE	Phycoerythrin
PI	Propidium iodide
PNET	primitive neuroectodermal tumor
RA	Relative (binding) affinity
SSC	Sideward scatter
TAP	transporter associated with antigen processing
TBI	total body irradiation
TIL	Tumor infiltrating lymphocyte
WLI	whole lung irradiation